2017

Human Gut Microbiota and Obesity: How Is Gut Microbiota Associated with Obesity Improvement Induced by Bariatric Surgeries or Low-Calorie Diet Treatment?

Rui Zhang
Louisiana State University and Agricultural and Mechanical College

HUMAN GUT MICROBIOTA AND OBESITY: HOW IS GUT MICROBIOTA ASSOCIATED WITH OBESITY IMPROVEMENT INDUCED BY BARIATRIC SURGERIES OR LOW-CALORIE DIET TREATMENT?

A Dissertation

Submitted to the Graduate Faculty of the
Louisiana State University and
Agricultural and Mechanical College
in partial fulfillment of the
requirements for the degree of
Doctor of Philosophy

in

The Department of Environmental Sciences

by
Rui Zhang
B.S., North China Coal Medical University, 2003
M.S., Huazhong University of Science and Technology, 2008
M.S., Louisiana State University, 2012
May 2017

ACKNOWLEDGMENTS

First and foremost, I would like to thank my advisor Dr. Aixin Hou for her generous direction, inspiration, and support in countless aspects during the process of the study.

I appreciate my dissertation committee, Dr. Vince Wilson, Dr. Edward Laws, and the dean's representative Dr. Jan Hondzinski for their insightful comments and suggestions.

I also thank Dr. Eric Ravussin, Dr. Frank Greenway, Dr. Jizhong Zhou, Dr. Edward Overton and Dr. Jolene Zheng for their open-handed cooperation in the lab collaborative projects.

I also thank Dr. Gary King for his kind enlightening, thoughts, comments and recommendations during the discussion of research topics.

Next, I thank the Dean of the School of the Coast & Environment, Christopher D'Elia, Chair of Department of Environmental Sciences, Dr. Kevin Armbrust, former chair of Department of Environmental Sciences Dr. Lawrence J. Rouse, our department academic coordinator Ms. Charlotte St. Romain, administrative staff Ms. Barbara Porche, Ms. Katherine Grimes, research associate Dr. Roberto Wong, and Mr. Ric Pincomb for their work on my academic files, computer settings, and presentation schedules.

Furthermore, I thank my lab colleagues Lauren Navarre, Kris Ackoury, Corwin Hess, Grace Cagle, and Brian Matherne for their different forms of help.

In addition, I thank Dr. Joy van Nostrand, Dr. Tong Yuan, Dr. Ye Deng, Dr. Daliang Ning, Dr. Jiabao Li, Dr. Liyou Wu, Dr. Zhili He, Dr. Pin Zhang, Dr. Chongqin, Dr. Qichao Tu, Dr. Zhou Shi, Dr. Qingyun Yan, Dr. Kai Xue, Ms. Yujia Qin, Dr. Xishu Zhou, Dr. Jie Deng, and Dr. Aifeng Zhou, for their many forms of guidance and assistance.

Last but not least, I want to thank my family for all their support and encouragement.

Table of Contents

ABSTRACT

An increasing number of studies suggest that the complex microbial community of the human gut may have an important role in human health and disease conditions such as obesity and diabetes. However, the causal relationship among gut microbiota, obesity, weight loss, and the influence of bariatric surgery remains largely unknown. This study investigated the correlation between human gut microbiota and obesity via determining how gut microbiota is associated with obesity improvement induced by bariatric surgeries (BRS) and low-calorie diet (LCD) treatment. Specifically, we investigated the effects of various bariatric surgery (BRS) procedures and a low-calorie diet (LCD) treatment on the diversity, composition, and metabolism of the gut microbiota of obese patients using a combination of robust, high-throughput metagenomic technologies, (Illumina sequencing and HuMiChip microarray), quantitative polymerase chain reaction (qPCR), and gas chromatography.

We discovered that following BRS procedures or LCD treatment the gut microbial community structure significantly altered, along with efficient, persistent obesity improvement after bariatric surgeries and, to a lesser degree, LCD treatment. First, microbial richness and diversity were significantly increased after both treatments. Second, the distribution and composition of microbial community were switched toward a healthier profile. For instance, phylum Actinobacteria was significantly reduced, while phylum Verrucomicrobia was significantly increased at week 52 after BRS. Phylum Firmicutes was significantly reduced, while phylum Bacteroidetes was significantly increased after LCD treatment. Microbial community structure at different taxonomic levels and their connectivity were significantly correlated with obesity-related physiological variables, and high-molecular-weight adiponectin (ADPHMW) seemed to be an important factor that links to the correlation. Third, microbial functional gene profile was significantly altered at week 7 post treatments, with the BRS group showing significantly higher gene richness and diversity than the LCD group. Over half of the gene categories showed significant correlations with obesity-related physiological variables, and the entire gene community significantly correlated with obesity-related hormones (adiponectin [ADP], APHMW and active Ghrelin [GHRA]), with the gene richness and diversity significantly negatively correlated with the active hunger hormone GHRA. In addition, we found that genus *Akkermansia* was significantly correlated with better health condition. It significantly increased after BRS treatment, and its change showed a significantly negative correlation with a change of obesity conditions following the treatments. Moreover, the concentrations of gut microbial metabolites (short-chain fatty acids [SCFAs]) were significantly altered. Total SCFAs and acetate were significantly reduced after both treatments. Following BRS, the proportion of acetate was significantly reduced, while proportions of propionate and butyrate were significantly increased. Correspondingly, the relative abundance of most butyrate-producing genera was significantly increased after BRS, and the gene communities relevant to the metabolism of SCFAs significantly correlated with obesity-related hormones (ADP, ADPHW, peptide tyrosine tyrosine [PYY] and GHRA).

Using a combination of multiple approaches, this research revealed that both taxonomical and functional gut microbial communities significantly correlate with obesity-related variables. The study indicates that weight-loss treatments might induce the alteration of gut microbial community structure toward a healthier profile, which then further fosters the weight loss and better health condition and thus form a positive loop. Obesity-related hormones, including ADPHMW, ADP, glucagon-like peptide-1 (GLP-1), PYY, GHR, and GHRA, in particular,

ADPHMW, might play important roles in linking gut microbiota and obesity. A pathway of gut microbiota-ADPHMW-obesity could be one of the important mechanisms that underlie the substantial and persistent weight loss following bariatric surgeries.

The study suggests several potential therapeutic methods that could be developed for treatment and/or prevention of obesity and obesity-related health conditions, including (1) supplying obese people with prebiotics (materials that boost beneficial microbes) and/or probiotics (beneficial microbes, such as *Akkermansia* and butyrate-producing bacteria) that can improve the healthiness of gut microbial community structure, (2) supplying human subjects with beneficial gut microbial products, such as butyrate and propionate that can increase the level of GLP-1 and PYY which have been proven to signal satiety, and (3) direct use of hormones such as ADPHMW, GLP-1, and PYY with caution of other possible health effects.

CHAPTER ONE: INTRODUCTION

1.1 Obesity

Obesity and type 2 diabetes are a growing epidemic worldwide. Among the adults in the world's population in 2008, around 35% were overweight and 12% were obese, nearly doubled when compared to the obesity rate of 6.5% in 1980 (WHO). In the United States, the prevalence of obesity among adults has increased from 15% to 33% during 1980-2004 and currently more than one in three US adults are obese and the prevalence remains stable (Ogden et al., 2007, Ogden et al., 2014).

Obesity has been shown to be associated with multiple comorbidities, including diabetes mellitus type 2 (Eckel et al., 2011), metabolic abnormalities (Chang et al., 2012), cardiovascular diseases (Nakamura et al., 2014), carcinomas in colon, renal, gallbladder, pancreas, esophageal glands, endometria, bone marrow, and breast, malignant melanoma (Dobbins et al., 2013), hepatic adipose infiltration (Fabbrini et al., 2010), fertility (Pasquali et al., 2007), and psychological well-being (Jorm et al., 2003). Type 2 diabetes accounts for 90-95% of all cases of diabetes. With an estimated over 300 million affected individuals by 2025, the lifetime risk of developing type 2 diabetes will approximate 20% (King et al., 1998). The rapidly growing prevalence of obesity and type 2 diabetes impairs the patients' life quality greatly and places a severe burden on our society's economy. A better understanding of the forming mechanism of obesity is critical to developing efficient preventive and therapeutic approaches.

Obesity is a medical status that surplus body fat has accrued to the degree that it may have negative effects on health, causing increased health problems and/or reduced longevity (Haslam and James, 2005). The degree of obesity is often measured by body mass index (BMI), the weight divided by the height (kg/m^2), due to low cost and simplicity, although BMI cannot tell the body fat percentage. The World Health Organization (WHO) has characterized overweight as having a BMI $\geq$25.0 kg/m^2 and obesity as having a BMI $\geq$30.0 kg/m^2.

Obesity is well-known as an outcome of energy expenditure and intake imbalance; an increased intake of energy-dense foods, especially when combined with reduced physical activity, surely predisposes obesity. However, the existence of complex systems that regulate energy balance requires that this paradigm is considered in a more comprehensive context (Morton et al., 2006). Other involved factors may include personal genetics (Vaisse et al., 1998, Clement et al., 1998) and health status. Moreover, increasing studies have evidenced the links between gut microbiota and adiposity (Backhed et al., 2004, Ley et al., 2005, Turnbaugh et al., 2006, DiBaise et al., 2008, Zhang et al., 2009, de La Serre et al., 2010, Caesar et al., 2010, Sanz et al., 2010, Musso et al., 2011, Tremaroli and Backhed, 2012, Nicholson et al., 2012).

1.1.1 History of Obesity

The term 'obesity' was coined during the 1610s. Its origin is the Latin word *'obesus*', the past participle of '*obdere*', where 'ob' means 'over' and 'edere' means 'eat'.[1] Today obesity is

[1] Dictionary.com Unabridged. Retrieved December 8, 2016 from Dictionary.com website http://www.dictionary.com/browse/obesity

defined as a medical condition associated with a variety of adverse health effects and reduced longevity due to the accumulation of excessive amounts of surplus body fat (Haslam and James, 2005). The degree of obesity is often measured by the body mass index (BMI), the weight divided by the square of the height (kg/m^2) of the individual. Measuring the BMI is simple and inexpensive. However, the BMI does not reveal the percentage of body fat. The World Health Organization (WHO) has associated the condition of being overweight with a BMI of 25–30 and obese with a BMI of 30–35.

Before the Neolithic revolution, which began in the Middle East about 12,000 years ago, people obtained food mainly by hunting and gathering. The Neolithic revolution resulted in a transition in the methods of obtaining food to farming (agriculture of crops and domestication of animals). During that period, however, food production was a limiting factor to the human population, as was the primitive state of medicine and poor living conditions. As a result, being corpulent was difficult and was seen as a sign of health and good fortune. After the Industrial Revolution, Medical Revolution, and Green Revolution in the 19^{th} and 20^{th} centuries, the availability of food increased greatly, and living conditions improved dramatically. One the consequence of these revolutions was the increases in the chances for people to lead a sedentary lifestyle and to live a long life. The result was a dramatic increase in the incidence of obesity in the human population.

Obesity has recently become a growing epidemic worldwide**.** The incidence of being overweight or obese increased markedly worldwide between 1980 and 2013. Among adults in the world's population in 2008, around 35% were overweight, and 12% were obese. The latter percentage was nearly double the corresponding figure of 6.5% in 1980. In the United States, the prevalence of obesity among adults increased from 15% to 33% from 1980 to 2004. Currently, about 35% of US adults are obese, and another 6% are extremely obese (BMI > 40) (Ogden et al., 2007, Ogden et al., 2014). Since 2005, those percentages have been stable.

1.1.2 Causes of Obesity

The storing of adipose tissue (i.e., body fat) in the human body is a result of evolution. During prehistoric times, when people survived by hunting and gathering food in a harsh environment, the food was scarce, and the supply was irregular. Natural selection favored a phenotype that was able to store large amounts of fat from a small supply of food and to release it as frugally as possible over the long run. Thus, those individuals who could store fat easily had an evolutionary advantage. However, with the advancement of science and technology, and in particular with the significant changes in the methods of obtaining food as a result of the Neolithic Revolution and Green Revolution, food became much less of a limiting resource, and those thrifty genes and the function of storing fat made people liable to become obese. Body fat was defined as an organ that contained its own genetics, cellular biology, hormones, and receptors, instead of a place that could only passively store energy (Kershaw and Flier, 2004).

Advances in the understanding of the thermodynamics of food utilization and of the nutritional aspects of the metabolism of food have refined the understanding of obesity. After the introduction of chemical analytical methods at the end of the 18th century, the thermodynamics of the nutrition of the human body was elucidated based on the pioneering studies of respiration, the acquisition of nitrogen required for tissue synthesis, and the association of muscular mechanical work with the generation of heat, concomitant with milestone discoveries related to the physiology of digestion. These advances in understanding began with the studies of William Beaumount on

gastric physiology (Beaumont, 1977, Eknoyan, 2006) and the early studies of hunger, beginning with Walter Cannon's studies of hunger sensation (Cannon and Washburn, 1993, Eknoyan, 2006). This research was followed by studies of gastrointestinal absorption, feelings of satiety, disorders related to nutritional deficiencies, and in particular the effects of vitamin and trace mineral deficiencies (Wilmshurst and Crawley, 1980, Krotkiewski, 1984, Wisen and Hellstrom, 1995, Bottiglieri, 1996, Jovanovic-Peterson and Peterson, 1996, Suchner et al., 1996, Eknoyan, 2006).

Currently, obesity is understood to be the result of an imbalance between energy expenditure and caloric intake. An excessive intake of energy-dense foods (e.g., high-fat and high-sugar foods), especially when combined with a lack of physical activity (e.g., much time spent sitting), predisposes a person to obesity. However, the pathogenesis of obesity is not as simple as that. The existence of complex systems that regulate energy balance requires that this paradigm is considered in a more comprehensive context (Fabricatore and Wadden, 2003). Other relevant factors include the following.

1. Genetic susceptibility (Clement et al., 1998). For example, Prader-Willi syndrome caused by several deleted or unexpressed genes on paternal chromosome 15 (Kishimoto et al., 2015), miR-26b mutation (Xu et al., 2015), or whole genome epigenetic changes (Franks and Ling, 2010);
2. Maternal pre-pregnancy obesity (Daraki et al., 2015);
3. Other diseases, for example, tumor-induced hypothalamic damage (Steele et al., 2013), decreased integration of brain regions for awareness of body and emotional states leading to less successful self-regulation (Paolini et al., 2015), and mental disorders (Fezeu et al., 2015);
4. Short sleep duration was identified as an independent risk factor for overweight and obesity (Beccuti and Pannain, 2011, Knutson, 2012) for children and adults (Rutters et al., 2010, Liu et al., 2012). Short sleep duration may trigger increased food intake to meet the energy needs during the elongated awake time (Hasler et al., 2004), impact hormones regulating appetite, and lead to an increase of the appetite for carbohydrate-rich food (Spiegel et al., 2004). Short sleep duration is also related to reduced glucose tolerance, another risk factor for overweight and obesity (Van Cauter and Knutson, 2008). In addition, habitual sleep variability but not habitual sleep duration was found significantly correlated with abdominal obesity, which may result from elevated caloric intake, especially carbohydrates (He et al., 2005).
5. Medical practices such as the use of steroids (Merritt et al., 1986).
6. Environmental stress. For instance, chemical exposure to di-(2-ethylhexyl) phthalate (DEHP) increases the risk of obesity (Lee et al., 2016).

1.1.2.1 The Microbiota in Human Gut May Have an Important Role in the Regulation of Energy Balance and Weight

Obesity arises as a consequence of alterations in energy balance, i.e., how the body regulates energy intake, expenditure, and storage. An increased intake of energy-dense foods, especially when combined with reduced physical activity, surely contributes to the high prevalence of obesity, however, the existence of complex systems that regulate energy balance requires that this paradigm is considered in a larger context (Morton et al., 2006). There are 10 trillion to 100 trillion microorganisms normally residing within the human gastrointestinal tract, collectively referred to as the gut microbiota. Recent studies suggest that obesity may affect the diversity of the gut microbiota (Ley et al., 2005), which in turn may play a role in the pathogenesis of obesity

by increasing the host's energy-harvesting efficiency (Ley et al., 2005, Ley et al., 2006). A review article by DiBaise and colleagues (DiBaise et al., 2008) examined the evidence supporting these claims; much of it obtained recently using tools such as sequencing of 16S rRNA gene clone libraries, metagenomics, DNA microarrays, microbiota transplant, and gnotobiotic knockout mice. It concluded that the gut microbiota has a role in the regulation of energy balance and weight. The evidence further suggests a role for a gut-derived factor, such as lipopolysaccharide (LPS), in the pathogenesis of obesity-related type 2 diabetes (DiBaise et al., 2008). A study observed a large bacterial population shift in the post-RYGB individuals, with the decreased level of interspecies H_2 transfer between bacterial and archaeal species that is possibly an important mechanism for increasing energy uptake by the human large intestine in the obese patient; it provides another perspective about the link between the gut microbiota and host energy balance (Zhang et al., 2009). Despite these very implicative findings, studies are needed to better understand the causal relationship among gut microbiota, obesity, weight loss, and the influence of various bariatric surgery procedures.

1.1.3 Harmful Effects of Obesity

Attitudes to obesity began to be negative in the 18th century, mainly for esthetic reasons. Since the 18th century, the negative impacts of obesity on a person's quality of life have started to be documented. In the middle of the 18th century, obesity was recognized as a cause of compromised health. Morbidity and mortality related to obesity have been reported from the beginning of the 20th century.

Obesity has been shown to be associated with multiple co-morbidities, including the following:

- diabetes mellitus type 2 (Kahn et al., 2006);
- insulin resistance (Kahn and Flier, 2000);
- metabolic syndrome (MetS)[2];
- immune dysregulation (Rizzo and Sen, 2015);
- chronic kidney disease (CKD) (e.g. glomerular hyperfiltration) (associated with non-diabetic obesity) (Srivastava, 2006, Hsu et al., 2006, Gore et al., 2006, Ogna et al., 2016);
- cardiovascular diseases (CVD) (e.g. Myocardial dysfunction) (Nakamura et al., 2014);
- atherosclerosis (Kim et al., 2015, Gustafson and Smith, 2015);
- non-alcohol fatty liver disease (NAFLD) (Fabbrini et al., 2010);
- malignant melanoma (Morpurgo et al., 2012);
- cancers such carcinomas in the colon (Chen and Huang, 2015), kidneys (Wilson and Cho, 2016), bladder (Sun et al., 2015), pancreas (Wang et al., 2015), esophageal glands (Chen et al., 2012), endometria (Kaaks et al., 2002), and postclimacteric breast tissue (Dobbins et al., 2013) and prostate (Joshu et al., 2011);
- hepatic adipose infiltration (Fabbrini et al., 2010);
- increased fracture risk (Gonnelli et al., 2014);
- gout (Lee et al., 2015);

[2] A cluster of associated metabolic traits that collectively confer unsurpassed risk for development of cardiovascular disease (CVD) and type 2 diabetes compared to any single CVD risk factor CHANG, Y., RYU, S., SUH, B. S., YUN, K. E., KIM, C. W. & CHO, S. I. 2012. Impact of BMI on the incidence of metabolic abnormalities in metabolically healthy men. *Int J Obes (Lond),* 36**,** 1187-94.

- osteoarthritis (OA) (Messier, 2009);
- obstructive sleep apnea (Schwartz et al., 2008);
- asthma (Delgado et al., 2008);
- chronic systemic inflammation (Gogebakan et al., 2015, Todendi et al., 2016);
- increased reproductive disorder such as incipient secondary hypogonadism in middle-aged men (Pasquali et al., 2007) and polycystic ovarian syndrome in women (Sam, 2007);
- malaise (Fabricatore and Wadden, 2003);
- infertility (Pasquali et al., 2007);
- poor pregnancy outcomes, including gestational diabetes, fetal macrosomia, stillbirth, post-term pregnancy, and cesarean delivery (Mission et al., 2015);
- reduced telomere length and accelerated aging (Kim et al., 2009);
- lower back pain (Shiri et al., 2010);
- decreased postural control and aiming performance (Boucher et al., 2015). Aiming tasks of pointing to two different sizes of targets were given to obese and normal-weight children in standing and sitting conditions. The measured hand movement time and mean speed of the pressure center switch were used for evaluating their postural stability during the movement, and obese children showed significantly higher values for both two measurements, which may be caused by longer slowdown period during the aiming performance. It indicated that obesity should have added a postural curb to obese children and lead them to spend longer time to correct their movements owing to their body's higher postural instability during the aiming performance test.
- increased risk of neurodegenerative disorders (e.g. Alzheimer disease (AD)) (Petrov et al., 2016);
- psychiatry disorders (e.g. mood and anxiety disorders) (Vieira et al., 2015);
- and social stigmatization.

Thus, the quality of life of an obese person may be greatly impaired. The numerous monetary costs associated with obesity and its rapidly growing prevalence have led to very significant public health costs. Development of efficient preventive approaches and therapeutic treatments for obesity would, therefore, be highly desirable. However, such developments will require a better understanding of the causes of obesity.

1.1.4 Treatment of Obesity

Limiting calorie intake and increasing energy expenditure are well-known methods of treating obesity. As more components involved in the pathogenesis of obesity are identified, more methods for preventing or treating obesity may become available. For example, identification of the relative deficiencies of various nutrients can provide a basis for medical therapy of obesity with drugs. Now a variety of medicines and dietary supplements are available to help people lose weight. Dietary supplements, for example, include vitamins, trace minerals, fiber, probiotics (beneficial microorganisms), and/or prebiotics (substances that can support the growth of the probiotics). Because the severity of obesity in some groups of people has begun to seriously impact morbidity and mortality, treatments are urgently needed, and surgical intervention has been introduced to help people lose weight because it is more efficacious than other traditional methods such as calorie restriction, exercise, and prescription medication, all of which are limited with respect to their impact on weight. The evolution of methods for treating obesity is reflected in the

changes of the name of the society for obesity management. The National Obesity Society was first established in the 1950s; it was then renamed the National Glandular Society, then the American College of Endocrinology and Nutrition, and finally the American Society of Bariatrics[3] in 1961. The Society subsequently divided into the American Association of Bariatrics Surgery[4] and the American Society of Bariatrics Physicians (Eknoyan, 2006).

1.2 Gut Microbiota

1.2.1 Microbiota

'Microbiota' was coined by American molecular biologist Joshua Lederberg in 2001, by combining 'micro(be)', which means microorganisms, and 'biota', which means life of a region, and was defined as 'the ecological community of commensal, symbiotic and pathogenic microorganisms that literally share our body space' (Lederberg and McCray, 2001). Lederberg also coined the term 'microbiome' and was defined as 'the totality of microorganisms and their collective genetic material present in or on the human body or in another environment', by combining 'micro(be)', which means microorganisms, and 'biome' which means a complex biotic community characterized by distinctive species and maintained under the environmental conditions of a region. The terms were coined to emphasize the importance of the microbial inhabitants of human in human health and disease. The difference between these two terms are that the microbiome includes the genetic material of the microbes, but they have been used as synonymous concepts in most cases.

1.2.2 Human Microbiota

There is indigenous microbiota in skin, eyes, respiratory system, oral cavity, the gastrointestinal tract, the urinary system, and the reproductive system in human (Wilson, 2005). There are a variety of environmental determinants at differential locations of the skin and the main determinants that influence the survival and growth of the microbial inhabitants of the skin are temperature, moisture content, pH, oxygen, and carbon dioxide concentration, light, nutrient availability, interactions with other microbes and host defense systems. Different environmental conditions of the different skin locations (e.g. forehead, ear, hands, arm, leg, foot sole, etc) make their community composition different. There are some diseases caused by members of the skin microbiota, such as acne, wound infection, and erythrasma.

Each location site has its specific anatomy and physiology of the respiratory tract and its specific antimicrobial defense mechanisms, environmental determinants at different regions of that location; Indigenous microbiota of the location (1. key members of that location; 2. ways to the acquisition of the respiratory microbiota, 3. community composition at different sites within the location, 4. Interactions among members, 5. Dissemination of organisms, 6. Effects of antibiotics and other interventions on the location); diseases caused by members of the microbiota.

1.2.3 Human Intestinal Microbiota

[3] Bariatrics reflects the evolution of the methods for treating obesity via appetite control, calorie restriction, and exercise.

[4] Bariatric surgery is the use of surgical intervention to treat obesity.

Human intestinal microbiota is an aggregation of microbes dwelling in human Gastrointestinal (GI) tract, including the mouth, esophagus, stomach, small intestine (duodenum, jejunum and ileum), large intestine (caecum, ascending colon, transverse colon, descending colon and sigmoid colon), rectum and anal canal. Gut microbiota is composed of around 300-1000 species and can be bacteria, archaea, yeast, fungi and protozoa, while 99% of them are made up of 30-40 species, and 1/3 of their components is common among the population. The net weight of the microbial components of human being are around 1.25 kg (1-2 kg; 60% of dry feces.), and their cell numbers are around 10^{14}, which is 10 times of the human being's cell number, and 100 times as many genes as the human genome, most of which confer physiological function.

In the human gastrointestinal (GI) tract there are normally about 100 trillion microorganisms, collectively referred to as the gut microbiota (Dore et al., 2013). The gut flora can be derived via early colonization from the mother during delivery, diet, the environment in which the person lives, and medical practices such as vaccination, administration of antibiotics, and poor hygiene (Guarner and Malagelada, 2003). The gut community is typically dominated by 30–40 bacterial species but is composed of 300–1000 species spanning the kingdoms of bacteria, archaea, yeast, fungi, and protozoa (Sears, 2005, Guarner and Malagelada, 2003). Gut microbes exist in human GI systems as symbionts and may exert either beneficial or harmful effect on human health under different scenarios (Sekirov et al., 2010). On the one hand, some gut species (1) help the host process certain components of the host's diet that would otherwise be indigestible for the host by converting the organic compounds into usable forms (Cummings and Macfarlane, 1997), (2) synthesize vitamins in the B and K groups (Hill, 1997, LeBlanc et al., 2011), (3) metabolize primary bile acids into secondary bile acids (Sayin et al., 2013), (4) inhibit the growth of pathogenic microbes (Kamada et al., 2013), and (5) maintain the homeostasis of the immune system (Arrieta and Finlay, 2012). On the other hand, some species may interfere with the excretion of xenobiotics by causing them to enter an enterohepatic cycle (Bjorkholm et al., 2009), induce inflammatory bowel disease (IBD) (Frank et al., 2007), and even influence brain functions and behavior via neural, endocrine, and immune pathways (Cryan and Dinan, 2012).

1.2.4 The Microbiota in Human Gut May Play an Important Role in Regulating Adiposity

In addition, increasing research results support the functions of gut microbiota in energy balance and fat storage regulation. Some human gut microbes take part in the metabolism of bile acids whose main activity is to facilitate the metabolism of dietary fat, affecting signaling pathways complicated in the metabolism of energy and lipid, and leading to changes in lipid peroxidation, hepatic fatty acid production, and triglyceride deposition (Nicholson et al., 2012). Also, it has been found that gut microbiota in mice increase the process of dietary polysaccharides by microbial glycosylhydrolases, promote increased monosaccharides uptake from the gut to the liver by doubling of the density of capillaries that underlie the small intestinal villus epithelium, increase transactivation of lipogenic enzymes by transcription factors such as ChREBP leading to the enhancement of the hepatic triglyceride production, and suppress Fiaf, a circulating LPL inhibitor gene of intestinal villus epithelial cells promoting LPL-directed incorporation of these extra triglycerides into adipocytes of peripheral tissues (Backhed et al., 2004). Besides, it has been discovered that gut microbiota from obese mice helped the host harvest more energy from the diet compared with the counterpart from lean ones and transplantation of germ-free mice with 'obese microbiota' leaded to a significant boost in total body fat than transplantation with 'lean microbiota', indicating gut microbiota could be a factor contributing to obesity by enhancing the

host's energy-harvesting efficiency (Turnbaugh et al., 2006). Furthermore, gut microbiota changes induced by prebiotics in genetic obese mice significantly reduced fat/lean ratio, lowered plasma triglycerides and muscle lipid content, reduced food intake, reduced fasting glycemia, and advanced glucose tolerance; the mechanisms may involve the increased muscle lipoprotein lipase level (Amandine 2011). Gut microbiota changes induced by the administration of prebiotics such as oligofructose markedly reduced body weight and fat, and improved glucose homeostasis in diet-induced obese, although food intake was not significantly changed; the involved mechanisms may relate to the significantly increased portal plasma glucagon-like peptide-1 (GLP-1) levels and colon proglucagon, as well as the improved sensitivities of leptin in its anorectic, weight-loss, and lipogenesis-reducing effects (Everard et al., 2011). Additionally, a large bacteria population shift was observed in the post-RYGB individuals, with the decreased level of interspecies H_2 transfer between bacterial and archaeal species that is possibly an important mechanism for increasing energy uptake by the human large intestine in the obese patient (Zhang et al., 2009).

1.3 Bariatric Surgeries (BRS)

1.3.1 Bariatric Surgical Treatments Show Extremely Promising Results in Severe Obesity

Although lifestyle intervention programs with or without pharmacotherapy induce weight loss and attenuate insulin resistance, these interventions have limited success, especially in severely obese people. Gastric bypass surgery is currently the most effective treatment for advanced obesity (BMI > 40), and lesser obesity (BMI > 35) if associated with type 2 diabetes, cardiopulmonary insufficiency, sleep apnea, or other comorbidities. Last year alone, there were about 200,000 procedures carried out in the US (Mechanick et al., 2008). A meta-analysis of 135,246 patients from 621 studies over 16 years concluded that after bariatric surgery, overall weight loss was 38.5 kg (55.9% of excess weight lost) and that diabetes was improved or resolved in 86.6% of the patients (Buchwald et al., 2009). The growing pool of patients undergoing bariatric surgery is increasingly recruited to study possible mechanisms underlying the large and sustained weight loss and has led to several useful hypotheses (Korner et al., 2006).

1.3.2 A Comparison between Gastric Bypass, Sleeve Gastrectomy, and Gastric Banding

Although gastric bypass as an open surgical procedure has been practiced since the 1980's, a laparoscopic approach to the procedure was not developed until the mid-1990's (Lonroth et al., 1996). Roux-en-Y gastric bypass (RYGB) is an irreversible procedure which alters the intestine anatomy and has the greatest operative risk when compared to the other two procedures. Also, it requires supplements after the operation. Of all the bariatric procedures, it produces the most effectiveness in terms of safe and sustained weight loss and relieves diabetes effectively, and needs lesser requirement for compliance. A review showed excess weight loss achieved via the laparoscopic gastric bypass was 26% greater than laparoscopic gastric banding one year after treatment (Tice et al., 2008). The laparoscopic gastric bypass is recognized as the standard of care for obesity surgery in the United States and is the predominant surgical procedure that has been carried out currently. Gastric bypass is also recognized as being the superior procedure for reversing type 2 diabetes mellitus. Pories et al. reported that 121 of 146 subjects (83%) with type 2 diabetes and 150 of 152 subjects (99%) with impaired fasting glucose maintained normal levels of glucose, glycosylated hemoglobin, and insulin following the surgery (Pories et al., 1995).

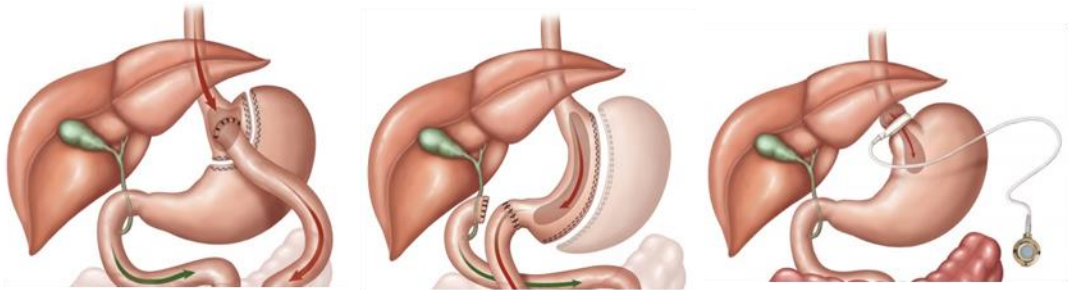

Bypass

- Greatest operative risk
- Alteration of anatomy
- Irreversible
- Faster total weight loss
- Lower need for compliance
- Requirement of supplements

Sleeve

- Less operative risk
- Alteration of anatomy
- Irreversible
- Slower and less weight loss
- Lower need for compliance
- No supplements

Band

- Least operative risk
- Alteration of anatomy
- Irreversible
- Slowest and least total weight loss
- Greater need for compliance
- No supplements

Figure 1.3.2.1 A comparison among gastric bypass, sleeve gastrectomy, and gastric banding.

Sleeve gastrectomy (SGx) is an irreversible procedure which alters the intestinal anatomy and has less operative risk than RYGB and higher operative risk than Gastric banding. It produces slower and less weight loss when compared to RYGB, but faster and more weight loss than the gastric band. It needs lesser requirements for compliance than gastric banding. No supplements are required after its operation. A case series with many sleeve gastrectomy cases reported a 59% excess weight loss after one year and a 62% excess weight loss after two years. A study compared 35 diabetic subjects who had a sleeve gastrectomy procedure with 50 subjects who had a gastric bypass procedure and showed that 4-month after surgery, both groups achieved similar weight losses and comparable improvement of their diabetic condition. Within U.S. academic medical centers, the use of laparoscopic sleeve gastrectomy is significantly increased and has surpassed the adoption of laparoscopic gastric bypass since 2013. Laparoscopic sleeve gastrectomy is now the most commonly performed bariatric surgery nationally in academic centers (Esteban Varela and Nguyen, 2015).

Bands placed by an open approach have been utilized since the 1980's, but the adjustable laparoscopic gastric band was not introduced until 1994 (Belachew et al., 1994). The laparoscopic approach reduced the complication rate of the surgery from 18.5% to 9.5% and has become the procedure of choice for gastric banding (Fried and Peskova, 1995). Gastric banding (GBa) is a reversible procedure which does not alter the intestinal anatomy and has the least operative risk when compared to the other two procedures. It has the slowest and least total weight loss and needs greater compliance after its operation. No supplements are required after its operation. It causes weight loss by restriction of caloric intake but the amount of weight loss is less spectacular and the weight of individuals are more likely to relapse when they do not follow the compliance. Furthermore, in a small study, sleeve gastrectomy was shown to increase PYY levels, a gut hormone associated with satiety, to a similar extent as gastric bypass but reduced ghrelin to a

greater extent than gastric bypass. Sleeve gastrectomy gave a statistically significant greater reduction in excess body weight (70% vs. 60%) at one year.

Some studies showed that although gastric bypass produces greater weight loss within a year, the adjustable gastric band produces slower weight loss over a longer period so that over the long term, its weight loss effect becomes comparable to that of the gastric bypass. Biagini and Karam reported a one-year post surgery of 66.7% excess weight loss increased to 76% after 2 years and 82% after 4 years, and was maintained after 10 years (Biagini and Karam, 2008). A review reported a 56% excess weight loss at five years with the GBa treatment compared to a 59% excess weight loss with the RYGB treatment (O'Brien and Dixon, 2003).

Also, the adjustable laparoscopically-placed gastric band has been shown to reverse type 2 diabetes two years postoperatively in 73% in individuals with type 2 diabetes for two years or less prior to the procedure (Dixon et al., 2008). The adjustable gastric band treatment has also been compared to intensive medical weight loss treatment (a very low-calorie dieting, pharmacologic therapy, and a lifestyle change program). After two years, the laparoscopic adjustable band group lost 22% of body weight and 87% of excess body weight, which is much higher than the intensive medical group (5.5% of initial body weight loss and 22% of excess body weight loss), and reversal of the metabolic syndrome and improvement of the life quality was also greater in the laparoscopic adjustable gastric band group (O'Brien et al., 2006).

1.3.3 Bariatric Surgeries Help Weight Loss

The mechanisms behind the weight-loss effect by bariatric surgery may include restrictive and/or malabsorptive methods (Rubino, 2006). Malabsorptive method bypasses a portion of the small intestine and results in malabsorption by reducing the functional size of the absorptive surface (Tadross and le Roux, 2009). Gastric bypass and sleeve gastrectomy operations involve both restrictive and malabsorptive procedures; they reduce the effective stomach size and/or rearrange small intestine causing incoming food bypassing most parts of the stomach, the entire duodenum, and a section of the jejunum (Tadross and le Roux, 2009), leading to the reduced the amount food that the individual can take and decreased absorption of the food they can consume, and therefore achieve the substantial weight loss. The gastric band operation causes weight loss by the restrictive method; it reduces energy intake mainly by gastric restriction, and the other mechanism underlying these bariatric surgeries may include decreases appetite (Tadross and le Roux, 2009), decreases leptin level (Abbott et al., 2005), and increases fasting and postprandial satiety (Dixon et al., 2005).

In addition, sleeve gastrectomy can cause ghrelin, a hormone secreted from the stomach to stimulate food intake, to drop by two-thirds and this reduction was maintained over the six-month study. It might be caused by the exclusion of the gastric fundus, resulting in the reduced contact between the mucosal cells which secretes ghrelin, and nutrients. Ghrelin is predominantly secreted in stomach and pancreas, and its secretion is stimulated by the empty stomach. Ghrelin stimulates appetite, increase hunger, increase gastric emptying and gastrointestinal motility for preparing for eating, induce the release of growth hormone, and hinders the glucose-stimulated insulin production. Sleeve gastrectomy can also cause increased levels of postprandial glucagon-like peptide-1 (GLP-1) and peptide tyrosine tyrosine (PYY), both of which are beneficial to obesity improvement by increasing the host's feeling of satiety (Dimitriadis et al., 2013). GLP-1 is secreted in L cells in distal ileum and colon and its secretion is stimulated by the nutrients in the gut lumen. It stimulates the production of incretin hormone, promotes the production and release of insulin in

the pancreas, reduces gastric emptying and intestinal motility, and promotes the feeling of satiety. PYY is secreted in L cells in distal small intestine and colon and its secretion is stimulated by nutrients in the gut lumen. It promotes a feeling of satiety, reduces gastric emptying and intestinal motility. That postprandial PYY in obese people was lower than the healthy people and PYY infusion reduced calorie intake have resulted in the hypothesis that obesity is a status of PYY deficiency (Meek et al., 2016).

Both RYGB and sleeve gastrectomy groups showed increased postprandial Cholecystokinin (CCK) levels after treatment when compared to the pre-operative levels, and the sleeve gastrectomy showed a greater increased level of CCK than the RYGB group. CCK is secreted in I cells in duodenal mucosa and its secretion can be induced by fatty acids or amino acids in the duodenum (Meek et al., 2016). It contracts the gallbladder for releasing bile. It induces the secretion of pancreatic enzymes, insulins, glucagon and pancreatic polypeptide (PP). It also slows gastric emptying and promotes the feeling of satiety (Meek et al., 2016).

Patients after gastric bypass are less hungry and prefer healthier food options (le Roux et al., 2006, Miras and le Roux, 2013, Sweeney and Morton, 2014, Behary and Miras, 2015). It may be achieved by the below mechanisms. 1) Increased/more intense taste acuity (Bueter et al., 2011). 2) The appeal of sweet fatty food reduces by a corresponding decrease in activation of the brain reward to high-energy food cues (functional MRI studies). 3) Patients experiencing post-ingestive symptoms with sweet and fatty food develop conditioned aversive behaviors towards the triggers. 4) Elevation of gut hormones and their effect on the appetite centers of the brain: The enhanced nutrient sensing by the L cells of the distal ileum promote the exaggerated release of the gut hormones glucagon-like peptide-1 (GLP-1), peptide tyrosine tyrosine (PYY), and oxyntomodulin in response to a meal, which has been shown to reduce hunger and promote satiety and reduce food intake; they are likely mediators of the beneficial effects of RYGB on appetite, taste functions and food preferences (le Roux et al., 2006, Borg et al., 2006). Also, the reduced postprandial level of gastrin after RYGB was observed after two weeks (Stoeckli et al., 2004) and a year (Dirksen et al., 2013).

Gastrin is produced in enteroendocrine G cells mainly in gastric antrum and duodenum and its secretion is stimulated by gastric distension & food in the stomach. It increases productions of hydrochloric acid, pepsinogen, intrinsic factor, pancreatic secretions and bile, and promotes the feeling of satiety. The fall after RYGB might be caused by that RYGB excluded gastric antrum and duodenum, and so reduced the contact between nutrients and the cells in the gastric antrum and duodenum. The production of hydrochloric acid in the remaining stomach stimulates the secretion of secretin and somatostatin, which further hinder the production of gastrin. Reduced ghrelin level was also observed after RYGB treatment. It might be caused by the exclusion of the gastric fundus, resulting in the reduced contact between the mucosal cells which secretes ghrelin, and nutrients (Meek et al., 2016). Oxyntomodulin showed a significant increase after RYGB treatment. Oxyntomodulin is secreted in L cells in ileum and its secretion is stimulated by nutrients in the gut lumen. It promotes the feeling of satiety, competes for the receptors of GLP-1 and glucagon, and increase energy expenditure. An increase in insulin sensitivity (Falken et al., 2011, Umeda et al., 2011, Jacobsen et al., 2012) and improved beta cell function (Umeda et al., 2011, Jorgensen et al., 2012) after RYGB was observed. A significant decrease in fasting glucose, insulin, and improvements of beta-cells sensitivity was observed one week after RYGB treatment (Jorgensen et al., 2012) and the effects may result from the benefits of GLP-1 (Jorgensen et al., 2013). Improved condition of type-2 diabetes was observed in all these three types of bariatric surgeries (Brethauer et al., 2013). The gastric band operation causes weight loss by the restrictive

method; it reduces energy intake by gastric restriction, decreases appetite (Tadross and le Roux, 2009), decreases leptin level (Dixon et al., 2005), and increases fasting and postprandial satiety (Dixon et al., 2005). However, it is reported that ghrelin was not reduced, but increased after GBa treatment (Fruhbeck et al., 2004).

There could be some other gut hormones and/or mechanisms contributing to the weight loss effect of bariatric surgeries. More studies need to be done to disclose them. Recently, increasing data has supported that gut microbiota composition is altered after bariatric surgeries and the changed gut microbiota might also contribute to the weight loss effect of bariatric surgeries.

1.4 Low-Calorie Diet Treatment (LCD)

During the 1970s it was noted that starvation was the fastest way to lose weight, but had the disadvantage of negative nitrogen balance. Attempts were made to replace the protein lost and to substitute some of that protein with carbohydrate to optimize weight loss while minimizing nitrogen loss. In the mid-1970s, the success of the diets of consuming around 400 kcal per day was reported and people lost an average of 1.5 kg or 1.5% of body weight per week on these regimens (Vertes et al., 1977). Not long after this report, a diet containing a poor quality of protein made from collagen was related with sudden death, and the pathology of the heart are alike the hearts of patients dying of starvation (Sours et al., 1981). Pringle demonstrated that electrocardiographic voltage started to decrease seven weeks after starting starvation, and in the following weeks, a prolonged QT interval (a measure of the time between the beginning of the Q wave and the end of the T wave in the heart's electrical cycle), which is a harbinger of malignant ventricular arrhythmias, was observed (Pringle et al., 1983). Subsequently, it was discovered that not only high-quality protein but also at least 600 kcal per day was necessary to keep the electrocardiographic voltage from falling (Greenway et al., 1994). Diets of between 400 and 800 kcal per day were shown to make the same effect on weight loss and appetite suppression (Foster et al., 1992). Therefore, low-calorie diets are now classified as those that are 800 kcal per day or more, and diets containing less than this or containing poor quality protein are not recommended. As with all rapid weight loss of 1.5 kg or more per week, gallstone is easier to formed (Weinsier and Ullmann, 1993). Ten grams of fat given with one meal per day can induce maximal contraction of the gall bladder and counteracts stasis as a cause of gallstone formation (Stone et al., 1992). Thus, the rate of weight loss seen with obesity surgery could be reproduced safely with a low-calorie diet of 800 kcal per day containing 70 grams of high-quality protein along with 10 grams of fat at one meal per day.

Finally, low-calorie diets (LCD) are still prescribed to those who do not qualify for bariatric surgery with mixed success and poorer weight outcomes at the longer term. An alternative dietary approach is the use of resistant starch, a carbohydrate that is not digested in the lower intestine but is fermented in the colon. This shift in the substrate for the large intestine alters the microbiota profile to one that produces more butyrate and other short-chain fatty acids (Keenan et al., 2006), and increases the production PYY and GLP-1 in rodents (Zhou et al., 2008b) and humans (Greenway et al., 2007). PYY and GLP-1 have both been shown to decrease food intake and reduce body weight while GLP-1 has been shown to increase insulin sensitivity in rodents and human in addition to increasing metabolic rate in rodents (Zhou et al., 2008b).

The low-calorie diet program in this research used the standard of 800 kcal per day by using the meal plan including 5 servings of Health one meal replacement shake with added a tablespoon of canola oil for protection of the gallbladder, following by weight maintenance by prescription of a balanced diet containing 500 kcal/day less than required for body weight

maintenance (measured energy expenditure at week 7–500 kcal/day). The participants needed to have weekly clinic visits with a dietician for the first 7 weeks and monthly thereafter.

1.5 The 'BARIA' Project

The project "*Effect of Bariatric Surgery and Weight Loss on Energy Metabolism and Insulin Sensitivity*" (*BARIA*) is funded by Endo-Surgery, Inc., and compares the four weight loss treatments (RYGB, SGx, GBa, and LCD) on energy expenditure, body composition, insulin sensitivity, and the response of gastrointestinal peptides to a standard meal. This $2.4 million project performs the most comprehensive and in-depth study so far regarding the bariatric procedures and energy metabolism and insulin sensitivity. However, there exists a main scientific knowledge gap in how human gut microbiota is impacted by various bariatric procedures and what the role of the gut microbiota in obesity and the weight loss process after the surgeries is.

The mechanistic observations on the relation of gut microbiota profile change by resistant starch and their effect on the increased release of GLP-1 and PYY, and the association of RYGB with increased GLP-1 and PYY, along with the evidence that suggests the correlation between gut microbiota and host energy balance, bring about our central hypothesis that successful weight loss following gastric bypass surgery may be partially credited to the alteration of gut microbiota after the surgical procedure.

Twenty-four participants seeking bariatric surgery for weight loss in the Baton Rouge area enrolled to the *"BARIA"* project is included in this study. Four groups will be studied before, and 7 and 52 weeks after bariatric surgery (RYGB, SGx, and GBa) or low-calorie diet program (LCD):

1) 5 patients eligible for Roux-en-Y gastric bypass (RYGB)
2) 9 patients eligible for sleeve gastrectomy (SGx)
3) 2 patients eligible for gastric banding (GBa)
4) 8 patients medically eligible for surgery but put on a low-calorie diet program (LCD)

The inclusion criteria include men and women between the ages of 18–65 years, body mass index (BMI) > 40 kg/m^2 or BMI > 35 kg/m^2 with obesity-associated diseases that should improve with weight loss (diabetes, hypertension, dyslipidemia and sleep apnea), medically qualified for obesity surgery by our collaborator group of surgeons Drs LeBlanc or Hausmann (groups 1, 2 and 3 only), and meeting the NIH criteria for bariatric surgery (group 4 only). The exclusion criteria include chronic gastrointestinal disease and chronic medications that have the potential for altering the human gut microbiota.

Our research takes advantages of the *"BARIA"* project at two levels: (a) obtaining stool samples before, 7 weeks and 52 weeks after the four weight loss treatments from the 48 participants seeking weight loss treatments in the Baton Rouge area that complete the *"BARIA"* project, and (b) correlating the microbial data with the physiological data obtained from the physiologic tests done on these participants by the *"BARIA"*. We examine and compare the composition, diversity, and metabolism of the human gut microbial community for difference across the four groups (RYGB, SGx, GBa, and LCD) before, and 7 weeks and 52 weeks after the treatments.

1.6 Hypotheses and Experimental Design

Hypothesis 1: Gut microbial community structure is altered after BRS and LCD treatments
a. Gut microbial diversity is increased.

b. Gut microbial distribution and composition is altered, with increased relative abundance of beneficial microbial groups and reduced harmful microbial groups.

c. The functional gene community involved in metabolic processes of gut microbiota was altered, with increased relative abundance of beneficial microbial genes.

Hypothesis 2: Genus *Akkermansia* is increased after BRS treatment and correlates with obesity improvement.

Hypothesis 3: The amount and constitution of short-chain fatty acids (SCFAs) are altered after treatments, with reduced acetate and increased propionate and butyrate.

Overall experimental design: Stool sample collection for the proposed human gut microbiota study will be carried out in parallel to the "BARIA" project. The overall experimental design of the "BARIA" project is shown in Figure 1. Briefly, following the screening, the study includes both outpatient and inpatient/overnight visits. The major testing periods are conducted at Baseline, at weeks 7 and 52 post-surgery/LCD as described:

1) Baseline (conducted 1–6 weeks prior to surgery or LCD)
2) Week 7 (conducted 6–8 weeks after surgery or LCD)
3) Week 52 (48-56 weeks after surgery or LCD)

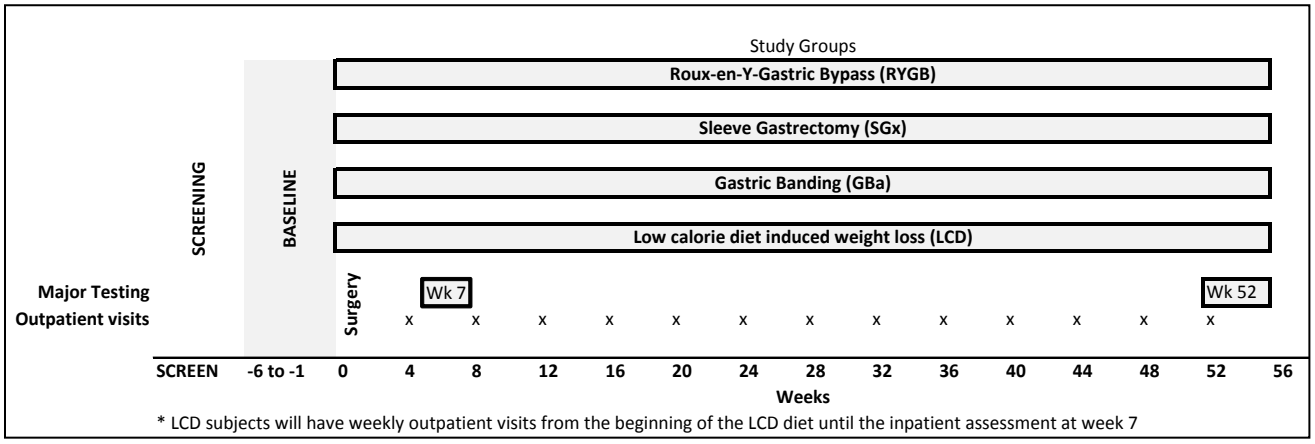

Figure 1.6.1 Experimental design of the BARIA project.

Each testing period includes four outpatient visits and one overnight stay. During each testing period, energy expenditure (24-hour metabolic chamber stay for oxygen consumption and fat oxidation, doubly labeled water study for free-living energy expenditure and accelerometry for activity energy expenditure), body composition (echo magnetic resonance imaging for body fat and lean tissue, multi-slice computerized tomography for visceral fat quantitation, and magnetic resonance spectroscopy for intra-hepatic and intra-myocellular lipid), insulin sensitivity (2-stage euglycemic hyperinsulinemic clamp for insulin sensitivity and hepatic glucose output), and the response of gastrointestinal peptides to a standard meal (glucose, insulin, ghrelin, GLP-1, and PYY) will be measured in all four groups. Changes will be compared across the four groups and between baseline, and 7 and 52 weeks post-operatively. These physiologic data generated by the "BARIA" project will be made available to interpret gut microbial data obtained on these patients in the human gut microbiota research.

After obtaining informed consent, stool samples will be collected in the four groups (RYGB, SGx, GBa, and LCD) at baseline (prior to surgery or LCD) and 7 weeks (after surgery or

LCD) when the "BARIA" project is in its first two major testing periods. Based on previous studies, the people would lose about 11-12% of their body weight (about 12-15kg) over the 7 weeks after surgery or LCD (Greenway et al., 1994, Andrew et al., 2006, Laferrere et al., 2007). This would be sufficient to get the changes in gut microbiota in response to the weight loss as we previously observed in our study of mice fed resistant starch (Bae et al., 2009). A longer duration (week 52, the third testing period of the "BARIA" project) would assess longer term compliance of subjects to the weight loss treatments and the sustainability of changes in gut microbiota.

The DNA extracted from the stool samples collected from the 24 participants at baseline and 7 and 52 weeks after the surgery or LCD, will be used for the following microbial analyses:

1) Community structure change (e.g. diversity) of gut microbiota and the microbial populations changed by the 4 weight loss treatments using Illumina sequencing targeting on the hypervariable V4 regions of the 16S rRNA gene.
2) Change of functional genes involved in the metabolic processes of gut microbiota using HuMiChip.
3) Abundance of microbial groups of interest, which have been previously indicated to associate with obese people and/or to be involved in energy metabolism and the groups that are identified to respond to the 4 weight loss procedures in this research), e.g. Firmicute, and Bacteroidetes, Archaea, the archaeal subgroups, using real-time PCR.
4) Short-chain fatty acids (SCFA) including butyrate, lactate, and acetate, using gas chromatography.

Data integration. Integrated analysis of Illumina sequencing, HuMiChip, and physiologic data (including those generated by the "BARIA" project) represents an immense challenge. We used various statistical approaches to identify relationships within the complexity. First, we used multivariate analyses, such as principal component analysis (PCA), for data reduction. Also, Mantel test was used for variation partition analysis to determine the relative influence of the physiologic variables. These analyses help us to identify any possible overall significant relationships among microbial community structure, physiologic activities, and various metabolic functional processes. In addition, we will examine the relationships between those key genes/populations with gut environmental conditions and host health conditions using the Mantel test, Pearson and/or Spearman correlation analysis and various other statistical approaches.

Expected results. We expect to identify the microbial populations that are responsive (stimulated or inhibited) to the weight loss procedure (surgery or LCD) by comparing changes between baseline and 7 and 52 weeks after the procedures. We also expect the four weight loss procedures (RYGB, SGx, GBa, and LCD) that cure obesity/ diabetes with varying effectiveness to have different effects on the gut microbial community structure and metabolism, and the altered gut microbiota, in turn, to be responsible in part for the greater efficacy in weight loss and improvement in diabetes with gastric bypass and sleeve gastrectomy compared to laparoscopic banding and low-calorie dieting. We anticipate that this research will help better understand metabolic pathways uncovered by bariatric surgery and weight loss in a larger context; it will provide a first step towards intentionally manipulating gut microbial community structure to regulate energy balance in obese/diabetic individuals in future studies.

Overall summary of the research. The synergism of working as a multidisciplinary team (encompassing the areas of microbial ecology, clinical research, gut nutrition and physiology, molecular biology, and molecular analytic techniques) will result in a comprehensive understanding of the role of human gut microbiota in obesity and diabetes. This research may ultimately close the loop in understanding the varying effectiveness of different bariatric surgery

and weight loss procedures and lay the groundwork for the analytic methodologies used in the future human gut microbiome and diseases studies.

CHAPTER TWO: MATERIALS AND METHODS

2.1 Stool Sample Collection

Stool samples were used for studying gut microbiota in this research. The subjects were given stool collection "pilgrim hats" that fit inside the toilet to collect stools. All stools were collected at baseline (bl), week 7 (w7), and week 52 (w52) post treatment. The stools were placed directly into Ziplock® plastic bags and frozen at –80°C immediately after being collected.

In total, 38 prepared samples from the fecal samples of 16 participants obtained before and after bariatric surgeries (Band, Sleeve, and Bypass) and 20 samples from the fecal samples of 8 participants collected before and post low-calorie diet program treatment were processed for Illumina sequencing. Samples from every individual include baseline, and week 7 or week 52 or both week 7 and week 52 post treatments. The participants included 3 males and 21 females, aged from 22 to 62 years old. Two participants had diabetes mellitus (DM); two had pre-DM/insulin resistance; seven had dyslipidemia; 14 suffered from hypertension. None of the patients had a metabolic syndrome.

2.2 DNA Extraction

Genomic DNA was isolated from the stool samples with a fecal DNA extraction kit (MoBio) following the manufacturer's instructions. The extracted DNA was stored at –80°C until the molecular analyses were conducted.

2.3 Illumina Sequencing

16S ribosomal RNA (16S rRNA) is the component of the 30S small submit of a prokaryotic ribosome. 16S rRNA gene is the gene coding for 16S rRNA and its sequence has been widely used for building phylogenetic trees, owing to 1) it is highly conserved in all most all bacteria and archaea species; 2) its slow evolution rate (its function has not changed over time, suggesting that random changes of sequences are a more accurate measurement of time or evolution; and 3) the 1500 bp of its gene sequence is long enough for informatics analysis. (Janda and Abbott, 2007). Now it has been widely accepted that 16s rRNA gene sequence is sufficient to classify microbes, and has greatly saved researcher's s workload when compared to the traditional methods such as culture and microscopy.

Sequencing technology has been greatly advanced since its invention. The first generation of sequencing method (e.g. Sanger sequencing) enabled sequencing of clonal DNA populations. The second generation of sequencing methods is high-throughput by enabling the process of multiple reactions simultaneously (e.g. Illumina sequencing). The third generation of sequencing method is capable of sequencing single DNA molecules (Heather and Chain, 2016).

Previous metagenomic studies of human gut microbiota have mainly relied on the generation of clone libraries of the 16S rRNA genes. First, genomic DNA will be extracted by DNA extraction kit. Then Taq polymerase and universal primers will be used for amplifying a fragment of the microbial 16S rRNA gene sequence of PCR reactions. Then the amplified sequences will often be cloned by using a cloning kit, which contains linearized vector, DNA ligase, DNA ligase buffer, PCR buffer, dNTPs, control DNA template, control PCR primers, sterile water as well as competent cells and corresponding reagents. Since Taq polymerase can add single

deoxyadenosine (A) to the 3' ends of amplified PCR products independent of a template, and the kit-supplied linearized vector has single 3'deoxythymidine (T) residues. This allows the PCR-amplified 16S rRNA gene sequence fragment to ligate with the vector. First, the PCR products are ligated into the supplied linear vector in a commercial clone kit and then transformed into competent *E. coli* cells. Next step is to select colonies and isolate plasmid DNA. After that, analyze plasmid DNA for the presence and orientation of the PCR product by either restriction digestion or sequencing method. Individual recombinant plasmids are required to be analyzed for the confirmation of the right direction because the PCR-amplified 16S rRNA gene sequence can be ligated into the vector in either orientation. The correct recombinant plasmid is then purified for further subcloning for characterization. After that, the traditional sequencing method, Sanger sequencing will be used. Sanger sequencing is developed by Frederick Sanger and his colleagues in 1977, and it is based on the selective incorporation of chain-terminating dideoxynucleotides by DNA polymerase in the process of in vitro DNA replication.

This traditional method can only produce a limited number of bacterial sequences. To our knowledge, none of these human gut microbial diversity surveys that used this methodology has generated more than 20,000 bacterial sequences (Eckburg et al., 2005, Ley et al., 2006, Frank et al., 2007). According to nonparametric estimations and extrapolations from rarefaction curves, however, obtaining a much higher number of sequences may reveal as many as 500-15,000 species (Eckburg et al., 2005, Frank et al., 2007), which include relatively rare members of the microbial community that collectively could have a profound impact on gut health and disease, including obesity (Zhang et al., 2009).

Around a decade ago, several new high-throughput sequencing approaches have been developed. One of the most promising high-throughput 2nd generation sequencing technologies is Illumina sequencing, which is based on the sequence by synthesis approach. It is a highly parallel non-cloning Illumina sequencing system capable of sequencing up to 100 million bases in one four-hour run on a Miseq system. Illumina sequencing has the potential to revolutionize sequencing studies, including characterizing microbial community diversity with a sample tagging approach. Currently, this sequencing method has been successfully used to study the microbial community in animals, humans, soils and oceans.

A recent study analyzing the human gut microbiota with the traditional Sanger and the Illumina pyrosequencing methods revealed that in general, the two methods were in good agreement for the more abundant taxa while the Illumina sequencing could capture the rare taxa missed by Sanger sequencing. Although Illumina sequencing produces relatively short sequences (~250 bp for the Miseq system), recent studies have shown that those short sequences are sufficient to statistically determine significant differences among microbial genomes that reflect the most likely biology occurring in each environment. In addition, multiplexed high-throughput Illumina sequencing of individual genes (e.g., 16S rRNA gene) by tagging or barcoding with short nucleotides has been developed to process many samples simultaneously. Zhou's lab also used a tagged Illumina sequencing approach to characterize several microbial communities.

Many published studies have demonstrated that the Miseq platform (Illumina) may generate tremendous sequencing information and is a powerful tool for studying microbial diversity. Therefore, this study chose Illumina sequencing for studying the effect of bariatric surgery and weight loss on the structure of the human gut microbial community.

Next sequencing techniques will determine the sequences. Then the sequences will be compared with reference sequences in databases and denoted as the same reference sequence if their similarity is greater than 98%. Type strains of 16S rRNA gene sequences of most bacteria

and archaea are available in public databases (e.g. NCBI). However, the quality of the sequences found in these databases is not often validated. Thus, secondary databases that collect only 16SrRNA gene sequences are used widely, and Ribosomal Database Project (RDP) is one of the popular ones.

The problem still exists because, for example, studies on fecal samples found that lots of detected sequences (around 3/4 of the sequences) do not show 98% similarity with any sequences in the reference databases. Their sequences will be deposited into the public database and their classification and identification might be uncovered by the future research.

The PCR primers F515 (GTGCCAGCMGCCGCGGTAA) and 806R (GGACTACHVGGGTWTCTAAT) were selected to target the V4 hypervariable regions of the bacterial 16S rRNA genes. To pool multiple samples for one run of Illumina sequencing, a sample tagging approach was used (Binladen et al., 2007, Hamady et al., 2008). Each tag (12 mer) was added to the 5'-end of both forward and reverse primers, synthesized by Invitrogen (Carlsbad, CA, USA), and then used for the generation of PCR amplicons. PCR amplifications were conducted with Accuprime high-fidelity Taq polymerase. The amplification mix contained 0.1 μl AccuTag polymerase, 2.5 μl reaction buffer II, 1 μl of each primer, and a 2.5–5.0 ng template in a volume of 25 μl. Cycling conditions were an initial denaturation at 94°C for 1 min, 30 cycles of 94°C for 20 s, 53°C for 25 s, 68°C for 45 s, and a final 10-min extension at 68°C. All the amplified PCR products from each tagged primer were pooled and purified by 1% agarose gel electrophoresis, followed by quantification by PicoGreen (Ahn et al., 1996). Finally, amplicons of all samples were pooled in an equimolar concentration for Illumina sequencing. All sequencing reads were initially processed using the Galaxy sequencing pipeline (http://zhoulab5.rccc.ou.edu/). Raw sequences were sorted and distinguished by unique sample tags. All sequences for each sample were aligned by RDP Infernal aligner, a fast secondary-structure aware aligner (Ribosomal Database Project, Michigan State University, East Lansing, MI, USA) (Nawrocki and Eddy, 2007), and then Uclust was used to define operational taxonomic units (OTUs) within a 0.03 difference. A 97% identify was used as the cutoff, and singleton sequence reads were removed. Each OTU contained more than two sequence reads from at least two samples. The sequence reads within an OTU were partitioned into individual samples based on the original sample-tagging information. A total of 3,422,989 V4 regions of 16S rRNA raw sequence reads were generated from the 55 microcosm samples. After removing the undetermined nucleotides and trimming the sequences, a total of 3,413,843 sequences were derived and were clustered into 11,314 unique OTUs without singlet based on 97% sequence similarity. Considering that the sequence numbers of the individual OTUs varied significantly among different samples and the sequence abundance of the sample with the lowest sequence abundance is 13,780, a resampled dataset with a final total of 13,780 sequence abundance of each sample for subsequent analysis (Zhou et al., 2011), was employed to reduce the sampling bias. After resampling, all samples in the baseline, week 7 and week 52 post-treatment samples have a sequence abundance of 13,780. Then assign taxonomy to the representative sequences with the RDP classier (Wang et al., 2007) with a confidence cutoff of 0.5. The lineage of each OTU was summarized with all phylogenetic information.

2.4 HumiChip Analysis

Although the microbial diversity can provide information both on which organisms are present and what metabolic processes are possible in the community, they have limits in giving a full picture of microbial activities and dynamics, especially on a large scale and in a parallel and

high throughput fashion. To overcome such obstacles for studying microbial communities in natural settings, Zhou and He have been dedicated to developing a microarray-based, high-throughput technology, functional gene arrays (FGAs). Over the last decade, many technical difficulties relating to applications of microarray technologies to environmental studies with regard to oligonucleotide probe design, development of computer program, specificity, sensitivity, quantitative capability, and amplification of the target DNA and RNA at the nano-scale were solved (Wu et al., 2001, Rhee et al., 2004, Tiquia et al., 2004, Wu et al., 2004, Zhou et al., 2004, He et al., 2005, Wu et al., 2006, Liebich et al., 2006, Gao et al., 2007, Deng, 2008). With a newly developed computer program, several generations of functional gene arrays or GeoChip have been designed. Comparing with 16S rRNA gene-based microarrays (e.g., PhyloChip), the GeoChip is particularly useful in linking microbial community structure to community function in environmental studies. So far, the GeoChip has been used in a variety of studies such as characterizing marine sediment community structure, characterizing grassland microbial community structure under elevated CO_2, examining the effects of contaminants on microbial communities, assessing spatial scaling of microbial community diversity in a forest soil (Zhou et al., 2008a), and assessing microbial fuel cells (MFC) for hydrogen production. The results from various studies demonstrate that GeoChip works very well with the natural environmental samples, such as soils, marine sediments, and groundwater, and is a powerful tool for profiling microbial community differences in general, and for linking community structure to functions. To our knowledge, this was the first and most comprehensive array currently available for studying various biogeochemical, ecological and environmental processes. With the urgent need for such technique in studying the metabolism of the human gut microbial community, a GeoChip-like technique, HuMiChip has been developed.

Although human gut microbial studies based on 16S rRNA clone libraries or high-throughput next generation sequencing (e.g. Illumina sequencing) technique are very powerful, but they have limited usefulness in determining the metabolic function of the human gut microbiota. Metagenomic analysis among different healthy individuals microbial composition is highly varied but their metabolic pathways and gene content are relatively stable, based on the Human Microbiome Project (Consortium, 2012) and some other related studies (Turnbaugh et al., 2009, Caporaso et al., 2011, Gevers et al., 2012). Using functional gene array-based technologies to characterize human microbiota is a novel and promising tool for human microbiome studies. It is our expectation that the HuMiChip would be a new platform that overcomes the major limitations of many traditional methods (e.g. PCR-based functional gene analysis) currently available for human microbiome studies, and is expected to provide insights into physiologic and ecological mechanisms of human microbiota at the community level. Thus, we applied HuMiChip to determine the effect of bariatric surgery and weight loss on the metabolism of the human gut microbial community.

The current version of HuMiChip (HuMichip2) contains two different types of probes, functional gene probes for identifying functional profiling of human microbiota and strain/species-specific probes for identifying strain or species (Tu et al., 2016). The evaluations of the microarray have been done both computationally and experimentally by using single strains/species and mock communities, as well as pure culture DNA and mock community DNA (Tu et al., 2014, Tu et al., 2016). In total, 2063 sequenced microbial genomes and around 2.5 gigabytes (GB) assembled shotgun metagenome sequences from 14 different human body sites were retrieved from the Human Microbiome Project Data Analysis and Coordination Center (http://hmpdacc.org). The sequenced microbial genomes were employed for designing probes for detection of both microbial

functional gene families and specific strains. The metagenome data were employed for designing probes targeting microbial functional gene families. Another 3327 sequenced microbial genomes and human genome sequences were downloaded from the National Center for Biotechnology Information (NCBI) ftp site, were further employed for specificity check to ensure the specificity of strain-specific probes against non-human microbes and the human genome. For detection of the microbial functional gene profile, it included 94,387 sequence-specific probes, 39,537 group-specific probes, and covers 276,240 coding sequences (CDS) of 157 gene families, which are involved in 11 microbial functional processes that they play important roles in human (Table 2.1).

Table 2.1 Summary of the microbial functional process and the numbers of gene families, sequence-specific probes, group-specific probes, and covered coding sequence on the current version of HuMiChip (HuMiChip2). Gene families targeting human microbiomes are selected from KEGG pathway database, and may participate in multiple pathways (In other words, the overlap of functional genes may occur among different functional processes.). The total number of probes and covered coding sequences is based on non-redundant genes included in all pathways.

Microbial functional process	No. of gene families	No. of sequence-specific probes	No. of group-specific probes	No. of targeted CDS
Antibiotic	18	0	13,567	32,168
Amino acid metabolism	36	24,314	5,723	59,392
Carbohydrate metabolism	27	15,322	4,442	40,173
Energy metabolism	5	7,115	1,878	16,799
Glycan metabolism and biosynthesis	10	6,010	2,560	20,277
Lipid metabolism	5	3,262	1,173	8,984
Non-essential amino acids metabolism	20	14,420	4,040	37,656
Cofactors and vitamins metabolism	16	9,700	2,605	25,854
Terpenoids and polyketides metabolism	5	3,644	861	8,398
Nucleotide metabolism	13	8,523	2,061	20,485
Translation	2	2,077	627	6,054
Sum	157	94,387	39,537	276,240

Target preparation, microarray hybridization, and image processing were carried out as previously described (He et al., 2007). Briefly, about 100 ng of purified DNA from each sample were amplified using whole-community genome amplification (WCGA), labeled with Cy3, and then hybridized with the HuMiChip. Microarray hybridizations were carried out under the stringent condition of 50˚C plus 50% formamide using TECAN Hybridization Station ProHS4800 (TECAN US). After hybridization, microarray image and data processing were carried out as described previously (Rhee et al., 2004, Wu et al., 2006). Briefly, poor or irregular spots were first automatically removed using the software ImaGene® (Biodiscovery, Inc). Second, hybridization spots with a signal-noise ratio (SNR) < 2 (He and Zhou, 2008) were removed from further analysis. In addition, the outlying spots were removed after normalization (Wu et al., 2006). Generally, absolute hybridization signal intensity data are used for statistical analysis.

In total, 27 prepared samples from 10 participants' fecal samples obtained before and post Bariatric surgeries (Band, Sleeve, and Bypass), and 21 samples from 8 participants' fecal samples

collected before and post low-calorie diet program treatment were processed for HumiChip analysis. Samples from every individual include baseline, week 7 or week 52 or both week 7 and week 52 post treatments, except one without a baseline.

2.5 Quantitative Polymerase Chain Reaction (qPCR)

Quantitative PCR is carried out in a thermal cycler with the capacity to illuminate each sample with a beam of light of at least one specified wavelength and detect the fluorescence emitted by the excited fluorophore. The thermal cycler is also able to rapidly heat and chill samples, thereby taking advantage of the physicochemical properties of the nucleic acids and DNA polymerase.

We used non-specific fluorescent reporter detection of PCR products: a double-stranded DNA (dsDNA)-binding dye is used as a reporter. The dye can bind to all dsDNA in the PCR reaction, causing fluorescence of the dye after being excited by a laser. Thus, an increase in DNA product during PCR will produce an increase in measured signal intensity of fluorescence at each cycle. However, dsDNA dyes (e.g. SYBR Green) can bind to all dsDNAs, including non-specific PCR products and/or primer dimers, preventing from obtaining an accurate result of the amount of the anticipated PCR products. For running the real-time PCR experiment using this method, the reaction mix is prepared as that for regular PCR, with the supplement of fluorescent dsDNA dye. Next, the reaction is run in a real-time PCR instrument, and the signal intensity of fluorescence, which is produced when dye binds to the dsDNA, is measured by a detector in real time.

For our experiment, qPCR was performed in a CFX Connect Optics Module real-time PCR detection system from Bio-Rad. A total volume of 600 µl of reaction mixture was made by mixing thoroughly 95 µl of nuclease-free water (NFW), 5 µl each of 100 µM forward and reverse primers, and 500 µl of 2 × concentrated, ready-to-use SsoAdvanced™ Universal SYBR® Green Supermix, which contains antibody-mediated hot start Sso7d-fusion polymerase, dNTPs, $MgCl_2$, SYBR Green I dye, enhancers, stabilizers, and a blend of passive reference dyes, to a final 1 × concentration of SYBR® Green Supermix and 500 µM concentration of primers. Each 6-µl aliquot was dispensed into a well of a 96-well PCR plate, followed by 4 µl of DNA templates (around 0.05 ng/µl) to each well, making each well incorporating 10 µl reaction mixture composed of 5 µl of 2 × SYBR® Green Supermix, 0.05 µl of each primer (100 µM), 4 µl of DNA template, and 0.95 µl of NFW to bring the total volume to 10 µl. Wells with 4 µl of NFW was served as no template controls (NTC). Three replicates of each sample were applied. The thermal cycling conditions were as follows: 3 min at 98 ˚C for enzyme activation/initial DNA denaturation, followed by 40 cycles of 15 s for denaturation at 95 ˚C and 30 s annealing at 60 ˚C for annealing and final melt curve analysis from 65 ˚C to 95 ˚C in 0.5 ˚C increments for 5 ˚C per step. 338f (5'-ACTCCTACG GGAGGCAGCAG-3') and 518r (5 '-ATTACCGCGGCTGCTGG-3') were used as the forward and reverse primers for total bacteria detection (Ovreas et al., 1997, Buckeridge et al., 2013). 5'-ACTCCTACGGGAGGCAGCAGTGGGGAATATTGCACAATGGGCGAAAGCCTGATG CAGCGACGCCGCGTGAGCGAAGAAGTATTTCGGTATGTAAAGCTCTATCAGCAGGG AAGATAATGACGGTACCTGACTAAGAAGCACCGGCTAAATACGTGCCAGCAG CCGCGGTAAT-3', was the DNA sequence used for standard curve construction to quantify total bacteria abundance and the complete, and this sequence fragment was selected by combining the sequence information of the complete genome of *Eubacterium rectale* ATCC 33656 (http://www.ncbi.nlm.nih.gov/nuccore/238922432?report=fasta) with those of forward and reverse primers we applied in this research by the online software Sequence Extractor at

http://www.bioinformatics.org/seqext/ (Guo et al., 2008). The beginning nanograms and copy numbers of the loaded *Eubacterium rectale* standard DNA in each cell are 2×10^{-3}, 2×10^{-4}, 2×10^{-5}, 2×10^{-6}, 2×10^{-7}, and 2×10^{-8} (2.02×10^{7}, 2.02×10^{6}, 2.02×10^{5}, 2.02×10^{4}, 2.02×10^{3}, and 2.02×10^{2}). For designing the primers of detection of the genus *Akkermansia*, first the fragment of *Akkermansia muciniphila* strain ATCC BAA-835 16S ribosomal RNA gene, complete sequence (NR_042817.1, http://www.ncbi.nlm.nih.gov/nuccore/343202494?report=fasta) corresponding to these 42 detected *Akkermansia* sequences were identified, then this fragment sequence was used as reference sequence for aligning all of the 42 16SrRNA sequences of the genus *Akkermansia* detected in our samples by Illumina sequencing and the known *Akkermansia* sequences which have been deposited in the NCBI reference sequence database were aligned and viewed by multiple sequence alignment with the one of the Clustal series of programs (Mview) run on the web server at the EBI (European Bioinformatics Institute) (http://www.ebi.ac.uk/Tools/msa/mview/) (Chenna et al., 2003). Based on this alignment, a 16S rRNA oligonucleotide fragment of the reference sequence which starts from the first segment to the last segment, both of which contains consecutive nucleotides (18 -22 bp) (S. Patricia, 2009) and covers the most highly variable among these sequences, was extracted and used as the reference gene for making the standard curve. The two sequence fragments at the beginning and the end of the sequence were used for designing the primer sequences for real-time PCR amplification to amplify as many of these sequences as possible. Three sets of primers were designed from these two sequence fragments and synthesized by Integrated DNA technologies (IDT), and they are the forward primer for the 1st set of primer (5'-AATCACTGGGCGTAAAGCGT-3'), the reverse primer for the 1nd set of primer (5'-TCTCGCAGTATCATGTGCCG-3'), the forward primer for the 2nd set of primer (GAATCACTGGGCGTAAAGCG), the reverse primer for the 2nd set of primer (TTCCGGTTCCCCCTCCATTA), the forward primer for the 3rd set of primers (TCGGAATCACTGGGCGTAAA), the reverse primer for the 3rd set of primers (CGGTTCCCCCTCCATTACTC). The forward primer 5'-AATCACTGGGCGTAAAGCGT-3' and the reverse primer 5'-TCTCGCAGTATCATGTGCCG-3' were used for the detection of species *Akkermansia Muciniphila*. The specificity of the primers was checked by using the National Center for Biotechnology Information (NCBI) online software primer-baselineAST at http://www.ncbi.nlm.nih.gov/tools/primer-blast/ (Ye et al., 2012) for making sure that the primers would only bind with *Akkermansia*, but not other organisms. The primer-baselineAST result only showed *Akkermansia muciniphila* and several uncultured bacterium clones, the top hit of all of which were *Akkermansia muciniphila* reference sequence (with sequence similarity of equaling to or greater than 98%) after blasting them using standard nucleotide baselineAST against the 16S ribosomal RNA sequences (Bacteria and Archaea) database. 5'-TTCGGAATCACTGGGCGTAAAGCGTGCGTAGGCTGTTTCGTAAGTCGTGTGTGAAAG GCGCGGGCTCAACCCGCGGACGGCACATGATACTGCGAGACTAGAGTAATGGAGGG GGAACCGGAATTC-3', was the DNA sequence used for standard curve construction to quantify *Akkermansia muciniphila* abundance, and this sequence fragment was selected by combining the sequence information of the complete 16S ribosomal RNA (rRNA) gene of *Akkermansia muciniphila ATCC BAA-835* (http://www.ncbi.nlm.nih.gov/nuccore/343202494?report=fasta) with those of forward and reverse primers we applied in this research by the online software Sequence Extractor at http://www.bioinformatics.org/seqext/. The DNA sequences used for standard curve constructions in the real-time PCR assays were double-stranded linear gBlocks® gene fragments synthesized by Integrated DNA technologies (IDT). The beginning

nanograms and copy numbers of the loaded *Akkermansia muciniphila* standard DNA in each cell are 2×10^{-3}, 2×10^{-4}, 2×10^{-5}, 2×10^{-6}, 2×10^{-7}, and 2×10^{-8} (1.17×10^{8}, 1.17×10^{7}, 1.17×10^{6}, 1.17×10^{5}, 1.17×10^{4}, and 1.17×10^{3}).

In addition, the forward primer 5'-TCTCGGTGTAGCAGTGAAATG-3' and the reverse primer 5'-GTGCCTCAGCGTCAGTTAAT-3', the produced top-ranked primers pairs designed by using the sequence fragments of *Akkermansia muciniphila ATCC BAA-835* that fall within the amplification region of the our Illumina sequencing result, and the IDT online software PrimerQuest at https://www.idtdna.com/Primerquest/Home/Index following by the same above-mentioned procedure for specificity double-check, were also used for double-check the result. The DNA sequence used for standard curve construction was identified by the above-mentioned method and its sequence is 5'-TCGTGTGTGAAAGGCGCGGGCTCAACCCGCGGACGGCACATGATACTGCGAGACTA GAGTAATGGAGGGGGAACCGGAATTCTCGGTGTAGCAGTGAAATGCGTAGATATCG AGAGGAACACTCGTGGCGAAGGCGGGTTCCTGGACATTAACTGACGCTGAGGCAC-3'. The beginning nanograms and copy numbers of the loaded *Akkermansia muciniphila* standard DNA in each cell are 2×10^{-3}, 2×10^{-4}, 2×10^{-5}, 2×10^{-6}, 2×10^{-7}, and 2×10^{-8} (1.17×10^{8}, 1.17×10^{7}, 1.17×10^{6}, 1.17×10^{5}, 1.17×10^{4}, and 1.17×10^{3}). The result obtained by using this pair of primers showed the similar pattern as that obtained by using the first set of primer described above. The specificity of the primers for running qPCR was further confirmed by sequencing the qPCR products by the Sanger sequencing, and the sequence results showed that they shared 100% similarity with *Akkermansia muciniphila ATCC BAA-835.*

2.6 Gas Chromatography

Chromatography is a technique used for separating compounds in mixtures. The phase that the sample mixture is dissolved in is called the mobile phase, and the other phase that holds the sample is called the stationary phase. The substances in the mixture are separated owing to that different substances have different solubility in these two different phases, or in other words, each constituent has a different partition coefficient (the ratio of a compound's concentrations in two phases at equilibrium; It measures the difference in solubility of a compound in these two phases). Different components in a mixture have different physical structure's characteristics, making them having different solubility in mobile and stationary phase, so these components move along the mobile phase with different rates and separate from each other gradually.

There are many different types of chromatography technologies existing, based on different methods and techniques. For example, based on the physical states of the mobile phase and stationary phase, it can be classified as homogeneous (e.g. liquid-liquid chromatography) or heterogeneous (e.g. liquid-gas chromatography). Based on the shape of stationary phase, it can be classified as column chromatography (the shape of stationary phase is a column) (e.g. gas chromatography) and planar chromatography (the shape of stationary phases is planar).

Gas chromatography (GC) is a common type of chromatography used in analytical chemistry for the separation and analysis of substances that can be vaporized without decomposition. It has been wildly used to evaluate volatile compounds such as fatty acid, essential oils, etc. Its mobile phase is gas (usually an unreactive gas (e.g. nitrogen) or inert gas (e.g.) helium), and its stationary phase is a microscopic layer of liquid or polymer on an inert solid support, inside a piece of the column which is made of glass or metal. The gaseous sample constituents interact with the walls of the column, which is coated with a stationary phase, causing each constituent to

elute at a different time, which is called the retention time for that constituent. Retention times can be used to calibrate the concentrations of the components in samples by several different methods. For quantitative analysis by GC, 1) the GC system performance should be stable and consistent. 2), a calibration curve for each analyte of interest is needed because, for most GC detectors, they have a different response to different analytes given their different molecular composition and/or size. 3) The range of the concentration of the standard analyte of the calibration curve should include the expected range of the analyte concentration in the samples being measured. The quantitative results for sample analyses that fall outside the calibration range are not trustable, especially when the calibration curve is not linear.

The gas chromatograph is the name of the instrument used to perform gas chromatography. The basic instrument components of gas chromatograph contain the mobile phase gas in a cylinder, the sample injection system, column of gas chromatography, the detector, the computer for recording data, and the thermal chamber for controlling temperature. We used the microFAST™ GC for our experiments. It is a small, fast GC designed to promote analytical efficiency in the laboratory and in the field. It can precisely and efficiently separate different types of compounds in a sample by using real-time microprocessor control of temperatures and pressures. Low thermal mass conduction heater technology is employed by the column heater for precise and fast temperature programming and cool-down of dual, high-resolution separation columns. A trap-based injection system is also used for concentrating and then desorbing the compounds in samples for injection onto the narrow bore capillary columns.

There are several approaches for calibrating the unknown concentrations of an analyte using the calibration curve. The choice depends on many aspects such as the type of the sample and the protocol for sample preparation, the configuration of the instrumentation system, etc. These approaches are 1) external calibration which uses the function of the signal intensity of the detector response versus (vs) analyte's concentration. The external calibration is the most straightforward method and is used most often. 2) internal standard calibration which uses a relative signal intensity of the detector response function of the analyte of interest to another reference substance (it has similar chemical characteristics of the analyte of interest) that is added to the sample prior to any sample preparation and /or analysis. The internal standard calibration method is designed to compensate for the potential sources of errors that may result from sample preparation and inherent variability of the GC system as well as the analysis method. 3) standard addition, which uses the function of the signal intensity of the detector response vs the amount of the concentration of known incremental amounts of the analyte of interest that are added to a sample to calculate the original concentration of the analyte, which has a concentration value of 0 for the added amount of the standard. The standard addition method is like the internal standard calibration method, but it adds different standard concentrations of the analyte of interest to the samples, instead of the reference substance which has similar chemical characteristics as the analyte of interest. This method is developed to overcome inaccurate quantification caused by the baseline noise (The signal intensity may not be inaccurate if the unknown concentration is close to the limit of the detection because that region has great noise) and/or attenuated or magnified response resulting from sample matrix (sample matrix inhibits linear activity).

Calibration curves can be a linear, non-linear, or mixed (e.g. linear in the low concentration region, while curved in the higher concentration). A linear function can be expressed using the form 'y = ax+b', where 'y' is the signal intensity of the response of the detector, 'x' is the concentration of the analyte, 'a' is the slope of the linear line and 'b' is the intercept of the linear line on y-axis given x equals to 0. The calibration curve can be made based on the retention time

and concentrations of a series known different concentrations of the solution for each component. The concentration of the compounds in each sample can be calculated based on the corresponding standard curve.

In most cases, the relationship between the signal intensity and analyte concentration is linear. Then, the values of a and b can be derived by using several pairs of the known concentrations of the standard compounds for each analyte of interest and their corresponding signal intensity under the same running condition as that for running the real samples which contain analytes of interest with unknown concentrations waiting to be determined. Although two sets of data are enough to draw a line, researchers cannot see whether the relationship is curved or not. Thus, at least three sets of standard concentrations are needed to develop a usable calibration curve; one standard concentration should be close to the limit of determination, one should be the high limit of the concentration estimated for the samples, and others is supposed to be spread evenly across the calibration range. More numbers of standard concentrations, more accurate standard curve can be derived. Sometimes, the detected signal intensity for the analyte of interest falls outside of the range of the signal intensity derived from the standard concentrations. Then another standard concentration or several other standard concentrations may need to be added to let the detected signal intensity for the analytes with unknown concentrations fall within the range of the calibration curve.

2.6.1 Instrumentation

A model microFAST™ GC from Analytical Specialists, Inc was used in all experiments and equipped with dual flame ionization detectors (FID). The separation columns were 2 meters in length by 100 µ ID fused silica capillaries coated with 0.4 µ of DB-5 and DB-1701 liquid phases. Sample volumes of 1 µl were injected with a 10-µl glass syringe. The injected analytes were trapped on a Tenax GR absorbent microtrap maintained at 40°C and desorbed at ~240°C.

2.6.2 GC condition

The ready and desorb temperature for concentrator were set at 40 °C and 240 °C and the pre-heat, cleanout and prepurge time were set as 18 s, 50 s, and 10 s. The initial and final column temperatures were set at 35°C and 200°C, and the temperature program heated the capillary columns at a rate 3°C per second, with initial and final hold time for 3 s and 5 s, giving a total run time of 60 s. The initial pressure, final pressure, and pressure programming rate were set at 15 psi, 33 psi, and 0.4 psi per second; with initial and final hold time for 30 s, and 10 s. The Liquid/SPME mode was used for injection with an inject time of 1500 ms and the injector temperature was maintained at 150°C. The detector temperature, fuel pressure, and data acquisition were set at 150°C, 35 psi, and 60s.

2.6.3 Reagents

Acetonitrile (99.8+%, 250 ml), propionic acid (99% 500 ml) and butyric acid (99%+, 100 ml) were obtained from Alfa Aesar, acetic acid (ACS grade, 500 ml) from Amresco, valeric acid (99%, 100 ml) from ACROS ORGANICS MS, and diethyl ether (ACS Grade, 1L) were obtained from BDH SOLVENTS - B&J.

2.6.4 Sample Preparation

After thawing and homogenization of the fecal samples, 0.5 gram of each sample was measured and put into a 2-ml plastic vial. Then 1 ml of DNAase-free water was added to each vial containing the measured biological samples, followed by 2-minute inversion mix for reaching a homogenous state. Next, the vials were centrifuged at 2500 x g at 10 °C for 5 minutes. Then the top layer was transferred to a 1.5-dram (16 x 50 mm) VWR®, borosilicate glass vials with phenolic screw cap from VWR International, using a 100-µl micropipette and stored in the -20 °C freezer till the next step. 1 ml of diethyl ether was added to each vial, followed by 30-second vortex and 2-minute centrifuge at 2000 x g. The upper organic layer was then transferred to a new glass vial with caution for avoiding any lower aqueous material. The procedure was repeated for another four times for elevating the extraction efficiency. The vials containing organic extracts were placed in a chemical hood overnight for allowing the ether to evaporate, followed by storage in the 4 °C refrigerator.

2.6.5 Standard Solution Preparation

2 ml VWR® 9-425 screw thread glass vials with borosilicate glass and a maximum fill volume of 1.8 ml and 9-425 polypropylene cap with ivory PTFE/red rubber septa from VWR International, were used to contain standard solutions. The stock solution of 4000 mg/l of short-chain fatty acids acetic acid, propionic acid, and butyric acid were all prepared in acetonitrile. Standards with lower concentrations 0.25, 0.5, 1, 5, 10, 25, 50, 100, 150, 200, 500, 1000, 1500, 2000, 2500, 3000, and 3500 ppm for experiments were obtained by series dilution starting from the 4000 mg/l stock. All standard solutions were stored at -20 °C.

2.7 Obesity-related Physiological Variables

Measured obesity-related physiological variables contain 1) obesity indicators including weight, fat mass, lean mass, fat%, 24-hour energy expenditure (24HourEE), body mass index (BMI), and subcutaneous fat size (SubcutMeanSize); 2) insulin resistance indicators, fasting glucose (GLU), fasting insulin (INS), and glucose disposal rate (GDR1/Weight and GDR2/Weight); 3) lipid profile, including triglyceride (TRIG), low-density lipoprotein (LDL), high-density lipoprotein (HDL), and cholesterol (CHOL); 4) hormones, including adiponectin (ADP), high-molecular-weight adiponectin (ADPHMW), ghrelin (GHR), active ghrelin (GHRA), glucagon-like peptide 1 (GLP-1), peptide tyrosine tyrosine (PYY), and leptin (LEP); and 5) inflammation indicator, high-sensitivity C-reactive protein (hsCRP).

Height was measured with a wall-mounted stadiometer and metabolic weight with a digital scale. Body mass index was equated to weight in kilograms divided by height in meters. Excess weight losses (% EWL) were estimated as follows:

$$\mathrm{EWL}_{\mathrm{Wk7}} = \frac{\mathrm{W}_{\mathrm{BL}} - \mathrm{W}_{\mathrm{Wk7}}}{\mathrm{W}_{\mathrm{BL}} - \mathrm{IBW}_{\mathrm{BL}}} \times 100\%$$

$$\mathrm{EWL}_{\mathrm{Wk52}} = \frac{\mathrm{W}_{\mathrm{BL}} - \mathrm{W}_{\mathrm{Wk52}}}{\mathrm{W}_{\mathrm{BL}} - \mathrm{IBW}_{\mathrm{BL}}} \times 100\%$$

where EWL_{Wk7} and EWL_{Wk52} are the excess weight losses at week 7 and week 52, respectively, and $IBW_{baseline}$ is the ideal body weight at the baseline. Whole-body percent body fat was measured by Dual Energy X-ray absorptiometry (DXA) (Hologics QDR 4500A; Hologics, Bedford, MA). The mass of fat tissue and lean tissue (kg) were obtained by QuickScan. Twenty-four-hour energy expenditure (24HourEE) (kcal/d) was measured with a metabolic chamber. Plasma glucose (mg/dl) was analyzed with a Yellow Springs Instruments 2300 STAT Glucose Analyzer (Yellow Springs Instruments Inc., Yellow Springs, OH). Plasma insulin (μU/dl) was measured by chemiluminescent immunoassays on an Immulite 2000 Analyzer (Diagnostic Products). Total fasting cholesterol (CHOL) (mg/dl) and fasting high-density lipoprotein (HDL) (mg/dl) concentrations were measured with a Beckman Coulter Synchron DXC 600 Pro. Fasting low-density lipoprotein (LDL) (mg/dl) was determined with a Friedewald calculation. Fasting triglyceride concentrations (TRIG) (mg/dl) were measured by computed tomography and magnetic resonance spectroscopy. Fasting high-sensitivity C-reactive protein (hsCRP) (mg/dl) was determined by a chemiluminescent immunoassay (Immulite 2000^{TM}, Siemens Healthcare Diagnostics, Deerfield, IL, USA). In vivo insulin sensitivity was measured with a two-step hyperinsulinemic-euglycemic clamp (low insulin, 20 mU/m^2/min for 180 min; high insulin, 80 mU/m^2/min for 120 min), and the glucose disposal rate (GDR) (mg/kg/min) was calculated. The units for adiponectin (ADP) and high molecular weight ADP (ADPHMW) are mg/dl, and the units for Ghrelin (GHR), active Ghrelin (GHRA), glucagon-like peptide-1 (GLP-1), and peptide tyrosine tyrosine (PYY) are mg/l. The unit for subcutaneous adipocyte size is μl and the unit for leptin is ng/ml. IDXA weight, IDXA fat mass, and IDXA lean mass were measured directly or calculated indirectly from dual-energy X-ray absorptiometry methods. Values and descriptions of physiological variables and patient information were provided in the supplemental data.

2.8 Statistical Methods

Multivariate analyses, including Detrended correspondence analysis (DCA) and canonical correlation analysis (CCA), were used to determine the differences in overall microbial community structure among different groups. Mantel test was based on Euclidean dissimilarity and was also performed by R version 3.3.2 for examining the correlation between microbial community and environmental factors. BioEnv was used to identify the most significant environmental factors important to microbial community structure. Alpha diversity as measured by Shannon index and inversed Simpson index was calculated by the Mothur package. Beta diversity was calculated based on Jaccard's incidence-based dissimilarity matrices and Bray-Curtis's abundance-based dissimilarity matrices and were compared with three complementary dissimilarity tests, including permutational multivariate analysis of variance (Adonis), multiresponse permutation procedure (MRPP) and analysis of similarity (ANOSIM), and performed by the Vegan package in R 3.3.2 (http://www.r-project.org/). Shapiro-Wilk test performed in R was used for the normality test of the data distribution. Non-parametric Wilcoxon rank sum test and parametric unpaired student's t-test were used for analysis of variance between unpaired groups, and non-parametric Wilcoxon signed rank test and parametric paired student's t-test were carried out in R version 3.3.2 for analysis of variance between paired groups. Non-parametric Spearman rank correlation test, spearman rank partial correlation test, parametric Pearson correlation test and Pearson partial correlation test were carried out in R version 3.3.2 to determine the correlation between variables. Statistical significance was set as $\alpha = 0.1$.

CHAPTER THREE: STATISTICAL METHODS IN ECOLOGY STUDIES

3.1 Analysis of Variance

3.1.1 Abstract

When investigating whether there is a difference between two groups of data, it is important to employ statistical tests to check whether the result is statistically meaningful. Various statistical methods, for example, analysis of variance (ANOVA), have been used in microbiological research to determine whether the mean of one group is significantly different from another one. However, data do not always satisfy the assumptions that underlie these tests. In other words, these tests may not always be appropriate for the targeted datasets. Specific tests need to be chosen with sufficient caution, and the results of the analysis need to be explained reasonably for validating the explanation of the data pattern. However, it has been observed that many published studies used inappropriate ANOVA tests for their data sets and explained their test result with limited description. In this writing, we compared the premises for different types of paired or unpaired and parametric or non-parametric tests for determining whether two populations were significantly different and compared their analysis results. The result showed that there are some differences which were detected by all tests, but each test detected the differences that other test did not, based on its specialized underlying theory. We concluded that employing different statistical methods can disclose more facts of the actual data and discover more meaningful differences from distinct angles of viewpoints. We suggest that researchers should take caution in choosing which specific ANOVA test they are going to use and give a more detailed explanation of the corresponding results related to the specific test.

3.1.2 Introduction

The variance of X, $V(X)$, is technically defined to be the expected value of the difference $V(X) = E((X - E(X))^2)$, where X is a group of observations and E is the expectation value. The expectation value is supposed to be obtained by the following steps: 1) repeat the experiment infinite number of times, 2) calculate the expression every time, and then 3) take the average of that. The expression $S^2 = \frac{\sum (X - \bar{X})^2}{N - 1}$ calculates an estimate of the variance of X. It represents the average of the squared deviations of a group of observations from their respective mean. The division by N – 1 rather than N corrects for the bias created by using the average of X rather than E(X) in the expression. It measures how much a set of data deviate from their mean. Analysis of variance (ANOVA) is a group of statistical methods used to analyze the differences between group means and their associated procedures.

3.1.2.1 Parametric versus Non-parametric ANOVA Tests

1) Parametric statistical tests assume that the measured parameters of the population are normally distributed, while non-parametric tests do not. However, parametric tests can perform well with continuous data that are not normally distributed if the sample size satisfies the

guidelines (Frost, 2015). For example, a one-sample *t*-test needs a sample size greater than 20, and a two-sample *t*-test needs each group to have a sample size greater than 15.

2) Parametric statistical tests assume that the variance of the measurement is homogeneous, while non-parametric tests do not.

3) Parametric tests are typically used to test continuous (ratio or interval) data. However, non-parametric statistical tests are designed for analysis of ordinal, ranked, or nominal data. The existence of outliers can greatly affect the results of parametric tests, but not in the case of non-parametric tests.

4) The best measure of the central tendency of data is not always the mathematical mean. The center of a skewed distribution can be better represented by the median. Half of the data are below the median, and half of the data are above the median. If several extremely large or small data points are added to a sample, the mathematical mean would be impacted strongly, even though most of the typical data do not change, whereas such additions have relatively little effect on the median, which is a metric of the center of the distribution. Thus, in this case, even if parametric tests result in a significant difference between the two groups and non-parametric test do not, the non-parametric test would be more suitable to choose to analyze and explain the difference between these two groups.

Decisions on choosing parametric or non-parametric tests are often made based on whether the mean or median more accurately represents the center of the data distribution. 1) If the mean can more accurately represent the center of the distribution and the sample size is large enough, then a parametric test should be valid and preferred because parametric tests are more powerful. 2) If the median can represent the center of the distribution, no matter whether the sample size is large or small, the non-parametric test should be considered. 3) If the sample size is very small, then a non-parametric test should be considered. Considering that when sample size is small, the distribution of the data is difficult to ascertain because the distribution test does not have sufficient power to give meaningful results (Frost, 2015), and non-parametric test tend to make a test weak, the chance of detecting a significant difference when these two conditions coexist would be very low. This explains why collecting as many data as possible is important and can make a big difference to the result of the analysis, considering that 15 or 20 samples are the threshold for validating the parametric tests, and only a few more samples need to be collected to satisfy this requirement if the sample number is below 15 or 20.

Table 3.1 Comparisons between parametric and non-parametric ANOVA tests.

	Parametric	Non-parametric
Assumed data distribution	Normal	Any
Assumed variance	Homogeneous	Any
Data type	Continuous	Ordinal or ranked or nominal
Dataset relationships	Independent	Any
Measure of central tendency	Mean	Median
Advantages	More conclusions; more statistical powerful	Simple conclusions; less statistical powerful; Less impacted by outliers

The foregoing points are general differences between parametric and non-parametric analysis of variance statistical tests. However, different analysis of variance statistical tests have specific assumptions, and they need to be checked before using the corresponding test.

3.1.2.2 Wilcoxon Signed Rank Test

It is a paired non-parametric test. It is usually used for comparing observations that can be grouped in pairs.

Assumptions: 1) Data are paired and come from the same continuous population. 2) Each pair is independent. 3) The values of x_i and y_i are logically paired, so the comparisons (greater than, less than or equal to) are meaningful.

Hypotheses: Designate x and y to be the paired observations and (x_i, y_i) to be a random pair. Null hypothesis (H_0) states that difference between the pairs follows a symmetric distribution around 0. This distribution has an expected mean value of 0 and a variance of $\frac{n(n+1)(2n+1)}{6}$. The alternative hypothesis (H_1) states that the difference between the pairs does not follow a symmetric distribution around 0.

Method: The method involves calculating the difference between the paired datasets (x_i, y_i) and ordering them based on their absolute value from the smallest to the largest value. Pairs with no difference are removed. Then rank the pairs, with the starting number being 1. For ties, when the absolute values of the differences are equal, the ranks equal the average of the ranks (e.g., if they rank as 5^{th} and 6^{th}, then they will get the rank of (5+6)/2 = 5.5 for each). Then calculate the test statistic *W*, which is the sum of the sign of the difference multiplied by the rank. The calculated *W* will be compared with the critical values in a reference table. If |*W*| is greater than or equal to the critical value, and then H_0 would be rejected (the two-sided test) (Wilcoxon, 1946).

3.1.2.3 Wilcoxon Rank Sum Test

This is an unpaired non-parametric test and is also called a Mann-Whitney U test.

Assumptions: 1) All the observations from both groups are independent of each other. 2) Data can be ordinal.

Hypotheses: The null hypothesis H_0 states that the probability of an observation from the population group x being greater than an observation from the second population group y equals the probability of an observation from the group y being greater than an observation from the x group (Fay and Proschan, 2010).

In the two-sided test, the alternative hypothesis (H_1) states that the probability of an observation from the population group x being greater than an observation from the second population group y is different from the probability of an observation from the group y being greater than an observation from the group x. In the left-tail or right-tail one-sided test, the H_1 states that the probability of an observation from the population group x being greater than an observation from the second population group y is greater (or less) than the probability of an observation from the group y being greater than an observation from the group x (Mann and Whitney, 1947).

Method 1: For each measurement in one group, count the number of times the first value is greater than any measurements in the other group and count 0.5 for any ties. Then the sum of

the counts is the statistic *U* for the first dataset. Its converse is the *U* for the second data set. If the calculated *U* is greater than the value of *U* in the reference table, then the H_0 is rejected.

Method 2: Rank all observations in the two groups with the starting number 1 for the smallest value. Ties will be ranked with the average of the ranks they span. Then calculate the sum of the ranks for the observations in group 1 and designate it as R_1. Then $U_1 = R_1 - n_1(n_1 + 1)/2$ (Zar, 1998). If U_1 is greater than the *U*-value in the reference table, then the H_0 is rejected.

3.1.2.4 Sign Test

This test is a type of paired non-parametric test. It is usually used for testing for consistent differences between pairs of observations, for example, the abundance of a genus before and after bariatric surgeries. The consistent difference means one group is consistently greater or smaller than the other group.

Hypotheses: Designate x and y to be the paired observations and (x_i, y_i) to be a random pair. Null hypothesis (H_0) states that the probability for x_i being greater than y_i equals 0.5 (p = Pr(X > Y) = 0.5). 1) For the left tail one-sided test, the alternative hypothesis (H_1) states that the x measurements tend to be higher than y measurements ($p < 0.5$). 2) For the right-tailed one-sided test, H_1 states that the x measurements tend to be lower than y measurements ($p > 0.5$). 3) For a two-sided test, the H_1 states that there is a difference between x measurements and y measurements. It means x measurements may be either greater than or less than y measurements. The p-value is twice as the smaller tail value.

Assumptions: 1) the differences w_i ($w_i = y_i - x_i$) are supposed to be independent. 2) Each w_i is from the same continuous population. 3) The values of x_i and y_i are paired logically, so the comparisons (greater than, less than or equal to) are meaningful.

Method: The differences of the paired datasets (x_i, y_i) are calculated and labeled as positive '+' or negative '–' sign. Pairs with no difference are removed. Assuming H_0 is true, then w follows a binomial distribution. Suppose there are 10 (n) pairs of x and y. The probability of the conditions that there are k (0, 1, 2, 3, 4, 5, 6, 7, 8, 9, and 10) numbers of x greater than y is $\Pr = \binom{n}{k} p^k (1-p)^{n-k}$. If the difference w is binomially distributed, p is 0.5. The probability of 9 or more cases of one variable being greater than the other variable is Pr(0)+Pr(1)+Pr(9)+Pr(10) = 0.0215. In this case, the result shows that the difference is significant (Whitley and Ball, 2002).

3.1.2.5 Independent (Unpaired) Two-sample *T* Test

Hypotheses: The null hypothesis (H_0) states that the means of the two populations are equal. The alternative (H_1) states that the means of the two populations are unequal.

Assumptions: 1) Each of the two sets of data should follow a normal distribution. 2) If using the original definition of the Student's *t*-test, the two populations being compared should have the same variance, no matter the two sample sizes are equal or not. If the variances are unequal, the original Student's *t*-test is robust enough in case the sample sizes are equal. If the variances are unequal, no matter the sample sizes are unequal or not, Welch's *t*-test is a better alternative. 3) The data from the two populations should be sampled independently.

Methods: For equal and unequal variance conditions, no matter whether the sample sizes are equal or unequal, the value of the test statistic *t* will be calculated by the below two different formulas. Then the calculated *t* value will be compared with the critical value for Student's *t*-distribution, which can be calculated by the software, such as MATLAB, automatically or be found

in a traditional reference table. If the calculated *t* value is not as large as the critical *t* value, then H_0 is not rejected. Otherwise, H_0 is rejected (Student, 1908).

a) Equal variance

$$t = \frac{X_1 - X_2}{S_{X_1X_2} \cdot \sqrt{\frac{1}{n_1} + \frac{1}{n_2}}} \text{ where } S_{X_1X_2} = \sqrt{\frac{(n_1 - 1)S_{X1}{}^2 + (n_2 - 1)S_{X2}{}^2}{n_1 + n_2 - 2}}$$

n_1 - 1 and n_2 - 1 are the numbers of the degrees of freedom for these two groups and $n_1 + n_2 - 2$ is the total number of degrees of freedom.

b) Unequal variance

$$t = \frac{\overline{X}_1 - \overline{X}_2}{S_{\overline{X}_1 - \overline{X}_2}} \quad \text{where } S_{\overline{X}_1 - \overline{X}_2} = \sqrt{\frac{s_{X1}{}^2}{n_1} + \frac{s_{X2}{}^2}{n_2}}$$

$$df = \frac{(s_1{}^2 / n_1 + s_2{}^2 / n_2)^2}{(s_1{}^2 / n_1)^2 / (n_1 - 1) + (s_2{}^2 / n_2)^2 / (n_2 - 1)}$$

3.1.2.6 Dependent (Paired) *T*-test for Paired Samples

Hypotheses: H_0: the mean of the differences between the paired populations is equal to a specific value μ_0. H_1: the mean of the differences between the paired populations is unequal to a specific value μ_0 (Student, 1908).

Assumptions: 1) Each of the two data populations should follow a normal distribution. 2) The data from the two populations should be sampled independently.

Method: The differences between pairs of the datasets are calculated. Then the test statistic *t* will be calculated by the formula below. Then the calculated *t* value will be compared with the critical value for Student's *t*-distribution. If the calculated *t* value is not as large as the critical *t* value, then H_0 is not rejected. Otherwise, H_0 is rejected.

$t = \frac{\overline{X_D} - \mu_0}{\frac{S_D}{\sqrt{n}}}$ where $\overline{X_D}$ is the average of the differences, μ_0 is a constant that the user wants to check whether the average of the differences is significantly different from, and S_D is the standard deviation of those differences.

3.1.2.7 Randomization Test on Two Dependent Samples (Paired)

Hypotheses: H_0: there is no difference between treatments for any subject. H_1: there is a difference between treatments for at least one subject.

Assumptions: This test makes no assumptions because we have not randomly sampled from any population. With respect to this point, this test is very different from standard parametric tests (e.g. Student's *t* test), for which it is assumed that the data are randomly sampled from populations. With no random sampling, there is no basis for making inferences about the

corresponding parameters, so the test only answers the question whether there is an effect of the treatment, instead of whether the means of the two populations are different.

Method: Pick a test statistic (e.g., the difference of sample averages) and calculate the observed value. Then create all possible rearrangements of the data between the two groups, keeping the pairs of observations together. Then calculate the test statistic for each rearrangement and construct the distribution using all these test statistics. Then compare the observed test statistic to the distribution just created by assuming H_0 is true (The assignments are randomly distributed, in which case the probability distribution function is the histogram of all the values from all possible ways that the observations could have been randomly assigned to groups, keeping pairs of observations together.). The *p*-value will be the proportion of test statistics in the randomization distribution that are as much or more extreme than the observed test statistic. If the *p*-value is smaller than the threshold α value (e.g. 0.05), then the H_0 is rejected (Dwass, 1957, Verbyla and Litvaitis, 1989, Nichols and Holmes, 2002).

3.1.2.8 Randomization Test on Two Independent Samples (Unpaired)

Hypotheses: H_0: there is no difference between treatments for any subject. H_1: there is a difference between treatments for at least one subject. H_1 can be true in several different ways. A) One treatment results in a fixed additive change in response for all subjects; B) one treatment results in a greater mean of the responses across subjects; C) one treatment results in a greater variance in response across subjects and D) one treatment results in more skewness in response across subjects.

Assumptions: There are no assumptions because we have not randomly sampled from any population. With respect to this point, the assumption is very different from standard parametric tests (e.g. Student's *t* test), for which it is assumed that the data are randomly sampled from populations. With no random sampling, there is no basis for making inferences about the corresponding parameters, so the test only answers the question whether there is an effect of the treatment, instead of whether the means of the two populations are different.

Method: Pick a test statistic (e.g., the difference in sample averages) and calculate the observed value. Then compare the observed test statistic to the randomization distribution of the test statistic obtained by assuming H_0 is true (The probability distribution function is the histogram of all the values from all possible ways that the observations could have been randomly assigned to groups.). The *p*-value will be the proportion of test statistics in the randomization distribution that are as extreme as or more extreme than the observed test statistic. If the *p*-value is smaller than the threshold α value (e.g. 0.05), then the H_0 is rejected (Dwass, 1957, Verbyla and Litvaitis, 1989, Nichols and Holmes, 2002).

3.1.3 Materials and Methods

The abundance of genera (a taxonomic level in microbiology) detected by Illumina sequencing (Illumina Miseq platform) from the genomic DNA samples extracted from fecal samples obtained at baseline before bariatric surgeries and fecal samples obtained at week 52 post bariatric surgeries were used. There were 11 bariatric surgery participants included, and 11 pairs of relative abundance data for each genus. In total, 247 genera were detected.

Non-parametric tests including Wilcoxon signed rank test, Wilcoxon rank sum test and sign test, as well as parametric tests including paired *t*-test, unpaired *t*-test, randomization test, and

unpaired randomization test in MATLAB (R2013b), were employed for checking whether each genus was significantly different between baseline and week 52 samples.

3.1.4 Results and Discussions

Below tables showed the genera whose abundances were identified as different between baseline and week 52 by Wilcoxon signed rank test, Wilcoxon rank sum test, sign test, paired *t*-test, unpaired *t*-test, paired randomization test, and unpaired randomization test.

A paired *t*-test requires that the difference between the two samples to be compared must be normally distributed. The unpaired *t*-test requires that both variables be normally distributed. The data were therefore first checked for normality by using Kolmogorov-Smirnov, Lilliefors or Jarque-Bera test. For the *t*-tests, several genera that showed the significant difference after the power 1/5 transformation were still not normally distributed based on a Kolmogorov-Smirnov test after data transformation. However, the transformed data were judged to be normal based on either a Lilliefors test or a Jarque-Bera test. In these cases, the conservative approach was to look for differences using non-parametric tests, which showed that the differences were significant.

Randomized test circumvents the normality issue and allows one to do parametric tests in cases where it would not be allowed otherwise. The randomization tests were done in two ways. For the paired randomization test, the baseline and week 52 results were scrambled randomly but for each patient separately. The program just calculated the number of times in the original data that baseline exceeded week 52 and that week 52 exceeded baseline. Baseline got +1 if it exceeded week 52, and week 52 got +1 if it exceeded baseline. If there were ties, both baseline and week 52 got 0.5. Whichever got the highest score, baseline or week 52, that score became the criterion. Then the baseline and week 52 numbers for each patient were randomly scrambled, and the statistic was calculated. If the statistic equaled or exceeded the criterion 10% of the time or less, the original result was considered significant.

For the unpaired randomization test, the baseline and week 52 data for all the patients combined were scrambled. The criterion was the greater of the number of counts in the baseline or week 52 data. Take *Arsenicicoccus* as an example. It showed up a total of 7 times in the baseline patients and zero times in the week 52 patients. So, the criterion would be 7. Then the assignments of baseline and week 52 were randomly scrambled for each of the patients. Each time the larger of the total counts in the baseline and week 52 patients was determined, and that number was compared to 7. If the number equaled or exceeded 7 10% of the time or less, the result with the original data was significant. In this case, there is no way the number could have exceeded 7, but it could have equaled 7 some of the time.

Table 3.2 Wilcoxon signed rank test detected 16 genera, the abundance of which was shown to be significantly different between baseline and week 52 samples ($p < 0.1$). The genera were ordered from the smallest to the largest *p*-value.

Genus	Wilcoxon signed rank (p)
Ruminococcus	0.051
Sporobacter	0.051
Anaerosporobacter	0.0513
Arsenicicoccus	0.0654
Desulfovibrio	0.066
Parasutterella	0.073
Lactonifactor	0.073
Anaerofustis	0.074
Bifidobacterium	0.0742
Anaerotruncus	0.082
Oscillibacter	0.083
Subdoligranulum	0.083
Eubacterium	0.0858
Clostridium IV	0.0862
Parabacteroides	0.098
Bilophila	0.0985

Table 3.3 Wilcoxon rank sum test detected 18 genera, the abundance of which was found to be significantly different between baseline and week 52 samples ($p < 0.1$). The genera were ordered from the smallest p-value to the largest one.

Genus	Wilcoxon rank sum (p)
Pseudomonas	0.001
Clostridium XII	0.001
Anaerofustis	0.002
Desulfovibrio	0.0029
Arsenicicoccus	0.003
Acinetobacter	0.0117
Rudaea	0.0293
Alloscardovia	0.034
Anaerosporobacter	0.0388
Robinsoniella	0.0483
Lactonifactor	0.057
Sporobacter	0.0654
Ruminococcus	0.0658
Akkermansia	0.0674
Acetanaerobacterium	0.0674
Anaerotruncus	0.073
Eubacterium	0.073
Bilophila	0.098

Table 3.4 Sign test detected 11 genera, the abundance of which was shown to be significantly different between baseline and week 52 samples ($p < 0.1$). The genera were ordered from the smallest *p*-value to the largest one.

Genus	Sign (*p*)
Bilophila	0.0039
Desulfovibrio	0.0039
Anaerosporobacter	0.005
Subdoligranulum	0.026
Lactonifactor	0.0295
Sporobacter	0.0382
Akkermansia	0.0702
Eubacterium	0.076
Ruminococcus	0.085
Anaerotruncus	0.085
Arsenicicoccus	0.099

Table 3.5 The paired *t* test detected 15 genera, the abundance of which was shown to be significantly different between baseline and week 52 samples ($p < 0.1$). The data were raised to the power 1/5 to produce numbers that passed the normality test. The genera were ordered from the smallest *p*-value to the largest one.

Genus	Paired t (*p*)
Hydrogenoanaerobacterium	0.0152
Rudaea	0.016
Anaerofustis	0.033
Bifidobacterium	0.046
Eubacterium	0.047
Arsenicicoccus	0.0625
Alloscardovia	0.0625
Anaerosporobacter	0.0781
Oscillibacter	0.0784
Lactonifactor	0.084
Sporobacter	0.091
Subdoligranulum	0.098
Clostridium IV	0.0989
Desulfovibrio	0.0999
Anaerovorax	0.1

Table 3.6 The unpaired *t* test detected 16 genera, the abundance of which was shown to be significantly different between baseline and week 52 samples. The data were raised to the power 1/5 to produce numbers that passed the normality test. The genera were ordered from the smallest *p*-value to the largest one.

Genus	Unpaired t (*p*)
Anaerovorax	0.0107
Anaerosporobacter	0.0117
Clostridium IV	0.0195
Desulfovibrio	0.021
Alloscardovia	0.0323
Eubacterium	0.0348
Arsenicicoccus	0.037
Rudaea	0.037
Acinetobacter	0.0414
Oscillibacter	0.0438
Anaerofustis	0.046
Lactonifactor	0.047
Subdoligranulum	0.048
Caulobacter	0.0592
Sporobacter	0.0654
Bifidobacterium	0.1

Table 3.7 Paired randomization test detected 17 genera, the abundance of which was shown to be significantly altered in week 52 samples when compared to the baseline samples ($p < 0.1$). The genera were ordered from the smallest *p*-value to the largest one.

Genus	Paired randomization (*p*)
Parabacteroides	0.017
Anaerostipes	0.0251
Anaerotruncus	0.0268
Parasutterella	0.031
Oscillibacter	0.0348
Subdoligranulum	0.0379
Bifidobacterium	0.041
Clostridium IV	0.041
Clostridium sensu stricto	0.062
Desulfovibrio	0.0671
Lactonifactor	0.0774
Sporobacter	0.0816
Anaerosporobacter	0.0816
Methanobrevibacter	0.084
Eubacterium	0.084
Arsenicicoccus	0.084
Bilophila	0.09

Table 3.8 Unpaired randomization test detected 16 genera, the abundance of which was significantly different between baseline and week 52 samples ($p < 0.1$). The genera were ordered from the smallest *p*-value to the largest one.

Genus	Unpaired randomization (*p*)
Caulobacter	0.028
Bifidobacterium	0.0313
Clostridium sensu stricto	0.0313
Clostridium IV	0.0317
Lactonifactor	0.033
Acinetobacter	0.0377
Anaerosporobacter	0.039
Arsenicicoccus	0.042
Rhizobium	0.0552
Paracoccus	0.067
Alloscardovia	0.0736
Oscillibacter	0.079
Eubacterium	0.079
Desulfovibrio	0.08
Sporobacter	0.083
Subdoligranulum	0.0885
Anaerofustis	0.0938
Azoarcus	0.0964

All these analyses were looking at the data in different ways. The genera that were found to be significantly different based on one metric might not be screened out based on another. Only 5 genera (*Sporobacter*, *Eubacterium*, *Lactonifactor*, *Desulfovibrio,* and *Anaerosporobacter*) were judged to be significantly different based all these tests, while each specific test detected several cases that the other tests missed.

We found that the paired tests tended to identify fewer significant differences than the unpaired tests in this study. Also, the genera identified in the paired tests were not always just a subset of the genera identified in the unpaired tests. The Wilcoxon signed rank test, for example, identified several genera that were not flagged by the Wilcoxon rank sum test, *Parasutterella, Bifidobacterium, Oscillibacter, Subdoligranulum, Clostridium IV* and *Parabacteroides*. However, the Wilcoxon rank sum test identified the abundance of *Clostridium XII, Pseudomonas,* Acinetobacter, *Rudaea, Alloscardovia, Robinsoniella, Acetanaerobacterium* and *Akkermansia* as being different between baseline and week 52. The reason was that a few large differences counted heavily in an unpaired test, but their magnitude was ignored, for example, in a simple sign test; however, if one dataset was consistently higher or lower than another but by a small amount each time, that counted heavily in the case of a paired test but tended to get lost in the noise of an unpaired test. In this study, the chance of the existence of a few large differences might be a little higher than the chance of the existence of consistently higher or lower differences, the result being that the unpaired tests detected more differences. The trend that unpaired tests detected more differences was not fixed, and it could become opposite in other studies.

To determine whether a paired or unpaired test was reasonable, other possible factors that could impact the results should be considered. For instance, if 11 individuals were employed as replicates in the study because the variance among them had negligible effects on the research

target (gut microbiota in our case), then both unpaired and paired tests would be reasonable to use. Otherwise, paired tests would be more reasonable than unpaired tests.

Table 3.9 The number of genera the abundance of which was found to be significantly different between baseline and week 52 samples by different types of analysis of variance tests.

	Non-parametric		Parametric	
Paired	Wilcoxon signed rank	Sign	Paired t	Paired randomization
	16	11	15	17
Unpaired	Wilcoxon rank sum		Unpaired t	Unpaired randomization
	18		16	18

If we just counted the number of genera found to be significantly different, I would get the same results (18) with the unpaired Wilcoxon rank sum and unpaired randomization tests. However, the genera found to be different were not entirely the same. If we look at the actual data, we can see why some genera were found to be different by some tests and not by others.

For example, there were more *Akkermansia* at week 52 than at baseline for 9 of the 11 patients. The probability of 9 or more patients having more *Akkermansia* at week 52 than at baseline was only 0.0325. If there was no difference between baseline and week 52, that result was significant at $p = 0.065$ by a two-sided test. Thus, the non-parametric test, e.g. Wilcoxon rank sum and sign tests, detected the difference. However, the two unusual cases had a lot more *Akkermansia* at baseline than week 52, so if the test was based on the actual data, the difference was not significant, as concluded by the parametric Student's *t* and randomization tests.

The results of different types of non-parametric tests could also be different, and some genera that were found to be significantly different by one test but not by another test. For example, the genus *Akkermansia* was more abundant at week 52 in 9 of the 11 patients. That was significant at $p = 0.0654$ by a simple two-sided sign test. The reason the Wilcoxon signed test did not pick it up was that the two exceptions were very different—they were the second and third largest differences in magnitude. Thus, although the Wilcoxon signed rank test was nominally a non-parametric test, it was looking at ranks, whereas the sign test just looked at pluses and minuses and paid no attention to the magnitude of the numbers.

Another example is the genus *bifidobacterium*, which was identified as having changed only by the Wilcoxon signed rank test, but not the Wilcoxon rank sum and sign tests. It actually decreased in 7 of the 11 patients between baseline and week 52. In 3 other cases, there was either no change or a change of only 1. There was only one case of it increasing by more than 1 (1225). The sign test did not detect a difference because the sign test ignored the magnitude of the decrease in those 7 patients. The Wilcoxon rank sum test did not detect a difference because it tests counted the number of times the first value in one group was greater than any measurements in the other group and counted 0.5 for any ties. Considering that before treatment the levels of this genus were variable and this test neglected the initial variance among these 11 patients and that the data in these two groups were not completely independent, this test is not the most reasonable and powerful test in this scenario.

The results of different types of parametric tests could also be different, and some genera that were found to be significantly different by one test might not be detected by another test. The

traditional parametric test such as Student's *t*-test could be greatly influenced by outliers when compared to the randomization tests, although both tests are based on actual data. For example, the genus *Parabacteroides* was only detected by paired randomization test among all above-mentioned parametric tests. Actually, its abundance in 8 patients increased, but its levels in three other patients were reduced by some small amounts. A small outlier could have a great influence on the significance of the traditional parametric tests.

For the ANOVA analyses in microbial studies, the researchers should first take enough carefulness in choosing which ANOVA test is more reasonable or appropriate to use. Then, when explaining their test results, more details of the statistical test results relating to the corresponding tests should be researched, described, and explained by. In this way, more detailed, reasonable and trustable information or discoveries could be disclosed, and the understandings of their conclusions made based on these tests could be more accurate and thorough.

3.2 Analysis of Covariance

3.2.1 Abstract

Because data on human subjects in the field of medical research are limited by ethical and practical considerations, data from every human subject are valuable, and the inclusion of any valid human subject in a medical study enhances the probability of making important discoveries. Hence there is an incentive to make the best use of available information by combining data from different groups of human subjects if possible. Analysis of covariance (ANCOVA) has been widely used as a statistical tool to determine whether data from two or more groups of subjects can be combined. However, typical ANCOVA software programs test only the null hypothesis that the regression slopes of different groups are homogeneous. However, if the slopes appear to be homogeneous, it is appropriate to ask whether there is a difference among the groups in the elevations of the relationships. Typical ANCOVA software programs do not address this question. Failure to do so could result in an inappropriate combining of datasets. Here we report the use of an improved ANCOVA program that tests for the homogeneity of regression elevations if the slopes of regression lines are judged to be homogeneous. Use of this program allows decisions about combining datasets to be made in a more informed way and in particular, lowers the probability that different datasets may be inappropriately combined.

3.2.2 Introduction

Analysis of covariance (ANCOVA) is a general linear model that integrates analysis of variance and regression. It has been used to assess whether mean of a population of a dependent variable is equal across all levels of a categorical independent variable (e.g., a treatment) while statistically controlling for the effects of other continuous variables (covariates) that are not of primary interest. It can be employed to increase statistical power and to adjust for preexisting differences between unequal groups. But its application in the latter case requires that the regression slopes be homogeneous. This application aims at correcting for initial differences (prior to group assignments) that exist among several groups of the dependent variable. Categorical variables are used to adjust scores to make them more similar than was the case without taking account of the categorical variable.

Some research groups have used only before-treatment baseline data to perform correlation tests to check whether there are significant correlations between the relative abundance

of specific microbial component such as the genus *Akkermansia* and physiological variables such as the fasting glucose level (Ding et al., 2010, Collado et al., 2010, Marlene et al., 2013, Everard et al., 2013, Everard et al., 2014, Damms-Machado and Mitra, 2015, Zhang et al., 2015, Schneeberger et al., 2015, Dao et al., 2016, Louis et al., 2016). This method is rather conservative and does not make good use of all the available information, such as post-treatment datasets. Some other groups have done the correlations by combining all of the before-and-after treatment data points without even bothering to test if the before-and-after treatment datasets are statistically different from one another (In other words, the linear relationships within the groups have slopes and elevations that are not significantly different) by using the analysis of covariance test (Marlene et al., 2013). The same concern applies to regression tests.

Most software, for example, SAS, performs analysis of covariance by only checking to determine if there is a significant difference between or among the slopes of different lines fit to each data set. These tests do not determine if the intercepts or elevations are significantly different or not. Thus, by using this software, when the ANCOVA test finds no significant difference for the slopes among different groups, then the researchers may combine the two different datasets because they suppose that the ANCOVA results showed that these different datasets are from the same population and can be combined. However, that is not always the case. When the intercepts or the elevations of the different linear relationships (lines) are different, even though they have the same slope, the implication is that these different datasets are not from the same population, so it is not reasonable to combine these different datasets and carry out statistical analyses such as correlation and regression tests.

We created a MATLAB program for the ANCOVA test that includes the steps of testing both the slopes and elevations of the linear relations belonging to different datasets. This program added an additional step that was designed for checking the difference of the elevations of the lines, on the basis of the original ANCOVA test, which only checks for significant differences in the slopes of the lines for different datasets. In short, to check if the two different datasets are from the same dataset, this new program checks 1) whether the slopes of the two datasets are parallel. (Hypothesis 1: whether they are separate or parallel lines). 2) if the slopes are parallel, then whether their elevations are the same (Hypothesis 2: whether there is only one line).

3.2.3 Materials and Methods

The abundances of genera (a taxonomic level in microbiology) detected by Illumina sequencing (Illumina Miseq platform) from the genomic DNA samples extracted from fecal samples obtained at baseline before bariatric surgeries (procedures used to alter the anatomy of the human digestive system, to limit the food amount that can be taken in and digested for obesity reduction) and fecal samples obtained at week 52 post bariatric surgeries were used. There were 11 bariatric surgery participants included, and 11 pairs of relative abundance data for each genus. In total, 247 genera were detected. All statistical analyses and programming were carried out using MATLAB R2016a software.

3.2.4 Results and Discussions

To illustrate how to perform the analysis step by step, we used the before-treatment baseline and week 52 post bariatric surgery data for the relative abundance of the genus *Akkermansia* and the corresponding host's body weight as an example. For instance, the issue we

are trying to investigate is whether there is a significant correlation between the relative abundance of the genus *Akkermansia* in the gut and body weight. Instead of using only baseline data or combining all the baseline and week 52 datasets, I used the following program to determine whether the two datasets seemed to come from the same population. If the answer is yes, then I can go ahead and combine all the baseline and week 52 data to determine the significance of the correlation. This method can help make the best use of all the data I have (i.e., not waste any data).

Table 3.2.4.1 The relative abundance of the genus *Akkermansia* in the gut microbiota and the weights of 11 participants before and after bariatric surgeries.

	Baseline		Week 52	
BRS participants	*Akkermansia* (X1)	Weight (kg) (Y1)	*Akkermansia* (X2)	Weight (kg) (Y2)
P1	0	124.2	1.59E-02	99.8
P2	1.07E-02	110.5	4.85E-02	60.3
P3	0	126.1	2.18E-04	88.2
P4	1.35E-02	126.6	5.30E-02	89.1
P5	0	123	4.14E-03	80.3
P6	0	151	3.03E-02	111
P7	1.09E-03	159.1	3.16E-02	90.1
P8	7.26E-05	152.9	2.83E-03	103.4
P9	0	140.4	6.50E-02	94.8
P10	4.33E-02	102.4	7.26E-05	81.1
P11	6.48E-02	140.7	8.56E-03	82.2

The analysis can be divided into three steps. 1) The first step is to determine the equation of a best-fit line using linear regression for each dataset (i.e., a separate regression line for each dataset). Specifically, the slope and intercept for each dataset is calculated to determine the equation ($Y = A + BX$) for each dataset. The equation for calculating the slope of the regression line is

$$B = \frac{\sum (x - \bar{x})(y - \bar{y})}{\sum (x - \bar{x})^2}$$

where $\bar{x}$ and $\bar{y}$ are the averages of the x and y values, respectively. Using the data in Table 3.2.4.1, I found that $B_1 = (-1.0487)/0.0048 = -220.8$, and $B_2 = (-0.2238)/0.0055 = -40.6$, where the subscripts 1 and 2 refer to the baseline data and week 52 data, respectively. The equation for calculating the corresponding intercept is $A = \bar{y} - B\bar{x}$. Using the data in Table 3.2.4.1, I found that $A_1 = 135.1$, and $A_2 = 90.1$. Thus, the equations of these two lines are $Y_1 = 135.1 - 220.8X_1$, and $Y_2 = 90.1 - 40.6X_2$. 2) The second step is to determine whether the null hypothesis that the slopes of the two straight lines for the two datasets (e.g., the baseline and week 52 groups) are the same should be accepted or rejected based on an F-test. The alternative hypothesis states that the slopes of the two straight lines for the two datasets are not the same. To carry out the analysis, two parallel

lines are fit to the two datasets. Their common slope was calculated using the equation B = (–1.0487 – 0.2238) / (0.0048 + 0.0055) = –123.5. Then the intercept for each straight line was calculated using the equation $A = \bar{y} - B\bar{x}$, so $A_1 = \bar{y}_1 - (-123.5)\bar{x}_1$ = 132.4 + (123.5) × (0.0121) = 133.9, and $A_2 = \bar{y}_2 - (-123.5)\bar{x}_2$ = 89.1 + (123.5) × (0.0236) = 92. Thus, the equations for these two lines are $Y_{p1} = 133.9 - 123.5X_1$ and $Y_{p2} = 92 - 123.5X_2$. To test if the difference of the slopes of the two lines is significant, an F test was used, and for this step I first calculated the normalized difference of the sums of squares between the baseline and week 52 groups when the two lines were parallel and the sums of squares between the two groups when the two lines were separate, $(SS_p - SS_{sep}) / (df_p - df_{sep})$. This normalized difference is then compared with the normalized sum of squares of the two groups when the two lines are separate (SS_{sep}/df_s). The F-value is calculated using the equation

$$F = \frac{(SS_p - SS_{sep}) / (df_p - df_{sep})}{SS_{sep} / df_{sep}} = F_{df_p - df_{sep}, df_{sep}} \quad (3.2.1)$$

In equation 4.1,

$$SS_p = \sum (y_1 - \hat{y}_{p1})^2 + \sum (y_2 - \hat{y}_{p2})^2 = 3034 + 1880 = 4914 \quad (3.2.2)$$

$$SS_{sep} = \sum (y_1 - \hat{y}_{s1})^2 + \sum (y_2 - \hat{y}_{s2})^2 = 2989 + 1842 = 4831 \quad (3.2.3)$$

In equations 4.1, 4.2 and 4.3, y is the measured value of y given a value of x (y_1 indicates the baseline dataset and y_2 the week 52 dataset), $\hat{y}_p$ is the calculated or predicted value of y given a value of x using the equations obtained from forcing the two lines to be parallel in the second step (y_{p1} indicates the baseline dataset and y_{p2} the week 52 data), and $\hat{y}_s$ represents the predicted value of y calculated by using the equations obtained from the separate lines obtained in the 1st step ($\hat{y}_{s1}$ indicates the baseline dataset and $\hat{y}_{s2}$ the week 52 dataset). SS stands for the sum of the squares of the deviations: SS_{sep} stands for the SS value when the two lines are separate, and SS_p is the SS value when the two lines are parallel. The degrees of freedom are equal to the number of data points minus the number of coefficients in the linear model. For example, there is a total of 22 data points, and 2 intercepts and 2 slopes for the separate lines, so $df_{sep} = 22 - 2 - 2 = 18$. There are 2 intercepts and 1 slope for the parallel lines, so $df_p = 22 - 2 - 1 = 19$. Therefore,

$$F = \frac{(SS_p - SS_{sep}) / (df_p - df_{sep})}{SS_{sep} / df_{sep}} = \frac{(4914 - 4831) / (19 - 18)}{4831 / 18} = 0.309$$

This F-value is to be compared with the threshold value of $F_{(1,18)} = 4.41$ for $\alpha = 0.05$. If the F-value is greater than the threshold F-values for the relevant degrees of freedoms in the reference table, then the null hypothesis is rejected. In that case, the implication would be that the slopes of the two regression lines were different, and it would be illogical to go forward to the next step (i.e., it would be illogical to ask if the two lines were one line because they clearly would not). If the F-value is less than the threshold F-value, then the null hypothesis is accepted. The implication is that the slopes of the two regression lines are not significantly different. In this case, the next step would be needed, so it is necessary to go ahead to test the second hypothesis. 3) The

third step is to determine if the two parallel lines are the same line. In other words, the test is to determine if the intercepts (or elevations) of the two parallel lines are the same. To test if the difference between the elevations of the two lines is significant, an F test is used, and for this step one calculates the normalized difference of the sums of squared deviations of the baseline and week 52 groups when the two lines are one line, and the sums of squared deviations of the baseline and week 52 when the two lines are parallel $(SS_1 - SS_p) / (df_1 - df_p)$. This difference is then compared with the normalized sums of squares when the two lines are parallel (SS_p/df_p). In the equation, SS_1 represents the SS value calculated when fitting one line to all the data. The value of F is calculated with the equation

$$F = \frac{(SS_1 - SS_p)/(df_1 - df_p)}{(SS_p/df_p)}$$

$SS_1 = \sum(y_1 - \hat{y}_{11})^2 + \sum(y_2 - \hat{y}_{12})^2$. To get the equation to calculate the values of y_{11} and y_{12}, which are the predicted y values given the x values on the assumption that the two lines are one line (y_{11} is for the baseline dataset, and y_{12} is for the week 52 dataset.), the slope and the intercept of the regression line for the dataset obtained by combining the data in both the baseline and week 52 groups need to be calculated first. B = –365.6, $A = \bar{y} - B\bar{x}$ = 117.3, so the equation for the combined dataset is Y = 117.3 – 365.6X; $SS_1 = \sum(y_1 - \hat{y}_{11})^2 + \sum(y_2 - \hat{y}_{12})^2$ = 13,929. When there is only one line, there are only two coefficients (one slope and one intercept), so the corresponding degrees of freedom, represented as df_1, is 22 – 1 – 1 = 20. F = ((13929 – 4914)/(20 –19))/(4914/19) = 34.9, which is greater than the threshold value for $F_{(9\text{-}8,19)} = F_{(1,19)} = 4.38$ for $\alpha = 0.05$. The implication is that the null hypothesis should be rejected because the intercepts of the two parallel lines are different. It is, therefore, unreasonable to combine these two datasets for further statistical analyses. If the F-value were smaller than the threshold value, then the null hypothesis would be accepted because the intercepts of the two lines would not appear to be different. Thus, it would be reasonable to combine the two datasets for further analyses. Further analysis using each dataset separately would be unnecessary. For our datasets, the results of the analysis of covariance showed that the baseline and week 52 data should not be combined for further statistical analysis because it is very likely that the data came from different populations. Below is a plot produced by an analysis of covariance program written in Matlab (Figure 3.2.4.1). For the 1st null hypothesis, the F-value is 0.3096, and the *p*-value is 0.5848. For the 2nd null hypothesis, the F-value is 34.854, and the *p*-value is 1.1×10^{-5}. The relevant computer programs are attached in the supplemental data.

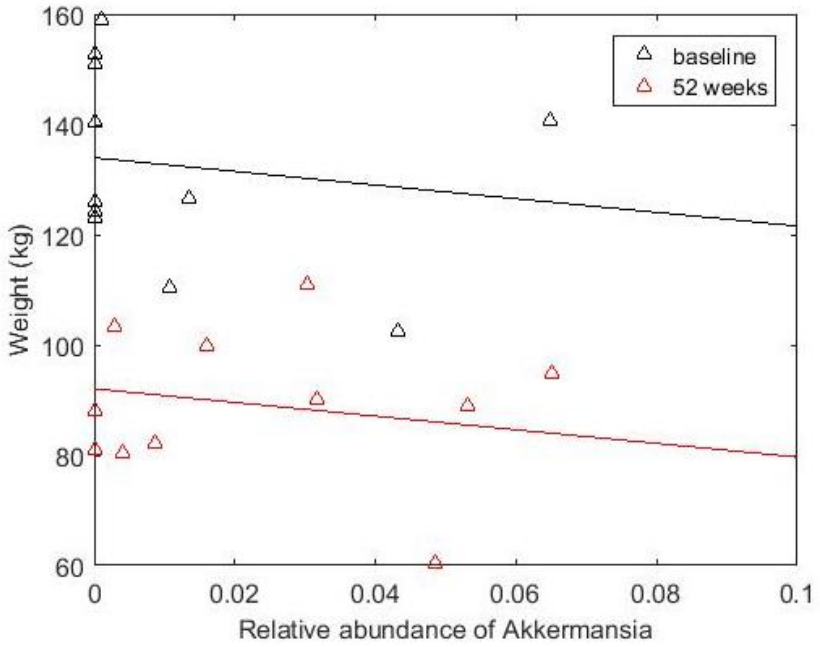

Figure 3.2.4.1 The parallel regression lines for the relative abundance of the genus *Akkermansia* vs weight at baseline (black) and week 52 (red).

The equation

$$E(\Sigma(y - \hat{y})^2) = V(y|x)df + \Sigma(E(y - \hat{y}))^2 \qquad (3.2.4)$$

follows from the definition of the variance of the variable y. In Eq. (4.4), df is the degrees of freedom, $\hat{y}$ is the value of y estimated using an analytical equation that contains parameters that were chosen to give the best fit to the data, and V(y|x) is the variance of y given x. Because the parameters in the model were deliberately chosen to minimize $\Sigma(y - \hat{y})^2$, the expectation value of that sum is less than would be the case if the true parameter values (which are never known) were used to calculate $\hat{y}$. The result is that V(y|x) in Eq. (4.4) must be multiplied by the df, which is equal to N, the number of data, minus the number of parameters in the model.

Equation (4.4) follows from the formal definition of the variance of a variable y:

$$V(y) = E(y - E(y))^2 = E(y^2) - (E(y))^2 \qquad (3.2.5)$$

which can be rearranged to give

$$E(y^2) = V(y) + (E(y))^2 \qquad (3.2.6)$$

When applying this expression to a dataset that contains finite data points (x_k, y_k), this equation

$$\begin{aligned} NV\ y|x &= E(\Sigma(y_k - \hat{y}_k - E(y_k - \hat{y}_k))^2) \\ &= \Sigma E((y_k - \hat{y}_k)^2) - \Sigma(E(y_k - \hat{y}_k))^2 \\ &= \Sigma E((y_k - \alpha - \beta x_k)^2) - \Sigma(E(y_k - \alpha - \beta x_k))^2 \end{aligned} \quad (3.2.7)$$

biased estimate because A and B were chosen to minimize the sum of the squared differences $\hat{y}_k - A - Bx_K$. Alpha and beta are the expectation values of A and B if A and B are unbiased estimates of α and β. A and B must be used because we do not know the values of α and β. The problem with A and B is that they were calculated to minimize the sum of the squared deviations every time we do the experiment, so we are getting a smaller expression for the sum of the squared deviations than we would if we used the values of α and β. The correction for this bias is to multiply V(y|x) by df rather than N in Eq. 4.7, where df represents the degrees of freedom. In other words, an unbiased estimate of V(y|x) is the right-hand side of Eq. 4.7 divided by df. After modification, the above expression becomes the following one:

$$\begin{aligned} dfV\ y|x &= E(\Sigma(y_k - \hat{y}_k - E(y_k - \hat{y}_k))^2) \\ &= \Sigma E((y_k - \hat{y}_k)^2) - \Sigma(E(y_k - \hat{y}_k))^2 \\ &= \Sigma E((y_k - A - Bx_k)^2) - \Sigma(E(y_k - A - Bx_k))^2 \end{aligned} \quad (3.2.8)$$

Rearranging Eq. 4.8 gives

$$dfV(y|x) = \Sigma E((y_k - A - Bx_k)^2) + \Sigma(E(y_k - A - Bx_k))^2 \quad (3.2.9)$$

In ANCOVA, an important question is whether

$$E(y_k - \hat{y}_k) = 0 \quad (3.2.10)$$

For the condition of two separate lines, Eq. 4.10 can be expressed as

$$E(\sum(y - \hat{y}_s)^2) = V(y|x)df_s + \sum(E(y - \hat{y}_s))^2$$

For the condition of two parallel lines, the equation can be expressed as

$$E(\sum(y - \hat{y}_p)^2) = V(y|x)df_p + \sum(E(y - \hat{y}_p))^2$$

For the condition of one single line, the equation can be expressed as

$$E(\sum(y - \hat{y}_1)^2) = V(y|x)df_1 + \sum(E(y - \hat{y}_1))^2$$

For testing if the two lines are parallel or not

$$E\ SS_p - SS_S = V\ y|x\ \ df_p - df_s + \sum(E(y - \hat{y}_p))^2 - \sum(E(y - \hat{y}_s))^2 \quad (3.2.11)$$

and

$$F = \frac{(SS_p - SS_s)/(df_p - df_s)}{SS_s / df_s}$$

If the lines are parallel, then

both

$$\sum(E(y-\hat{y}_p))^2$$

and

$$\sum(E(y-\hat{y}_s))^2$$

are zero.

In that case, both the numerator and denominator of the quotient used to calculate F are unbiased estimates of V(y|x), and the calculated F-value would be expected to be less than or equal to the critical F-value 95% of the time and greater than the critical F-value 5% of the time.
If the lines are separate (i.e., not parallel), then

$$\sum(E(y-\hat{y}_p))^2$$

would be greater than 0, but

$$\sum(E(y-\hat{y}_s))^2$$

would still be 0, so $\sum(E(y-\hat{y}_p))^2-\sum(E(y-\hat{y}_s))^2$ would be greater than 0. In that case, the numerator of the quotient used to calculate the F ratio would be an overestimate of V(y|x), and the calculated F-value would be expected to be greater than the critical F-value more than 5% of the time. That is the reason why the null hypothesis would be rejected when the calculated F-value is greater than the critical F if the type I error rate is 5%.
For testing whether the two lines are one single line or not,

$$E(SS_1-SS_p)=V(y\mid x)(df_1-df_p)+\sum(E(y-\hat{y}_1))^2-\sum(E(y-\hat{y}_p))^2$$

and

$$F=\frac{(SS_1-SS_p)/(df_1-df_p)}{SS_p/df_p}$$

If the two parallel lines are in fact one single line, then both

$$\sum(E(y-\hat{y}_1))^2$$

and

$$\sum(E(y-\hat{y}_p))^2$$

are 0. In that case, both the numerator and denominator of the quotient used to calculate F are unbiased estimates of V(y|x), and the calculated F-value would be expected to be less than or equal to the critical F-value 95% of the time and greater than the critical F-value 5% of the time.
If the lines are not the same line, then

$$\sum(E(y-\hat{y}_1))^2$$

would be greater than 0, but

$$\sum(E(y-\hat{y}_p))^2$$

would still be zero, so $\sum(E(y-\hat{y}_1))^2-\sum(E(y-\hat{y}_p))^2$ would be greater than zero, and the numerator of the quotient used to calculate the F ratio would be an overestimate of V(y|x). The calculated F-value would, therefore, be expected to be greater than the critical F-value more than 5% of the time. That is the reason why the null hypothesis would be rejected when the calculated F-value is greater than the critical F if the type I error rate is 5%.

In this case, if we use the current ANCOVA program would lead to the conclusion that it is valid to combine the data from the data from baseline and week 52 post treatment to do other intended tests (e.g. correlation tests). However, based on the test results of our program, it is not reasonable to combine these two data sets. Therefore, it is meaningful to employ this ANCOVA program for examining homogeneity of the regression intercepts for the validity of data combination and we suggest that it could be used in other related research for reducing the chances of making error conclusions and/or increasing the chances of making more discoveries.

3.3 Principal Component Analysis

3.3.1 Abstract

It is important to investigate the differences between the ecological communities in different experimental samples (e.g., samples before and after specific treatments) because those differences provide information about the relationships between environment factors and community ecology. This information can be used to guide manipulations of environmental factors to maintain or control ecological communities in a desirable way. Principal component analysis (PCA) analysis is one of the commonly used methods for analyzing and visualizing ecology distance. However, no programs have been created to test whether the ecological distance between samples or groups represented in a PCA plot is statistically significant or not. To address this issue, a program to determine the statistical significance of the ecological distances between groups represented in a PCA plot was developed. Another issue in applying PCA to the field of microbial ecology is that PCA cannot include all variables (e.g., all species) in the analyses when the variable size (the number of variables) is greater than the sample size (the number of samples) because in that case for n data points there can only be (n-1) principal components (no remaining variation can be assigned to the extra principal components). This issue can be addressed by employing dissimilarity tests, which can be used to compare the ecological distances between different sample groups, including all microbial components. Use of the program to examine whether two microbial community structures were significantly different showed that both the program and the dissimilarity test detected statistically significant differences between microbial community structure of samples before and after treatment. We conclude that both the dissimilarity tests and PCA analyses with a significance test for ecological distances are useful for determining the significance of the ecological distance between two communities.

3.3.2 Introduction

Principal component analysis (PCA) is one of the oldest ordination methods used as a tool in exploratory data analysis and for making predictive models. It has been used, for example, to calculate so-called ecological distances in the context of microbial composition and abundance. Ecology can be defined as the study of all processes that influence the distributions, abundances, and interactions of organisms with one another and with their environment (Begon, 2006). Differences in microbial composition and abundance are reflected in the ecological distance between samples. PCA analysis is one way to calculate ecological distances, and a scatter diagram of the PCA scores on the first two principal components is one way to visualize ecological distances. The scores are basically the representation of the centered, normalized matrix of observations (rows) and variables (columns) in principal component space. The distance between a pair of points on this graph is a measure of the ecological distance between the pair of observations. If the variables are patients and the observations are the numbers of specific kinds of flora in their guts, then patients that are close together on the graph are interpreted as having gut flora that are similar in composition, whereas patients that are far apart on the graph are interpreted as having gut flora that is different in composition. However, currently no published tests to determine whether the ecological distances are significantly different from zero in a statistical sense.

3.3.3 Materials and Methods

The abundance of genera detected by Illumina sequencing (Illumina Miseq platform) of the genomic DNA samples extracted from human feces at baseline before bariatric surgery and at week 52 post bariatric surgery was used. Eleven bariatric surgery patients participated in the study, and 11 pairs of relative abundance data for each of 247 genera were analyzed.

PCA analyses and the tests for significance of the ecological distances were performed using MATLAB (R2013b). Three complementary non-parametric dissimilarity tests, including MRPP (multiresponse permutation procedure) (Sickle, 1997), ANOSIM (analysis of similarity) (Clarke, 1993) and Adonis (permutational multivariate analysis of variance) (Anderson, 2001) were performed using the Vegan package in R 3.1.2 (http://www.r-project.org/) based on the Bray-Curtis or Jaccard similarity distance matrices.

3.3.4 Results and Discussions

A PCA analysis can be carried out only when the number of columns (e.g., genera) is less than or equal to the number of rows (e.g., patients). Otherwise, the matrix that must be inverted to carry out the PCA is singular (i.e., has a determinant of zero) and cannot be inverted. Therefore, microbial study researchers usually include only the microbial components that are found to be significantly different among patients. Since 247 genera were detected in all baseline and week 52 samples obtained from the 11 participants, these genera could not all be included in the PCA analysis. Thus, we chose to include only the 16 genera for which the abundances were judged to be significantly different between baseline and week 52 samples by a Wilcoxon signed rank test. The relevant matrix, therefore, contained 16 columns and 22 rows (11 baseline patients and 11 week 52 patients). The PCA plot below showed that the baseline samples were more clustered together than the week 52 samples, the indication being that the relative abundances of these 16 genera were more similar among the baseline samples than among the week 52 samples, in other

words, the difference between the baseline and week 52 groups was greater than the difference between the baseline or within the week 52 group, the indication being that the relative abundances of the 16 genera in the baseline and week 52 groups were different.

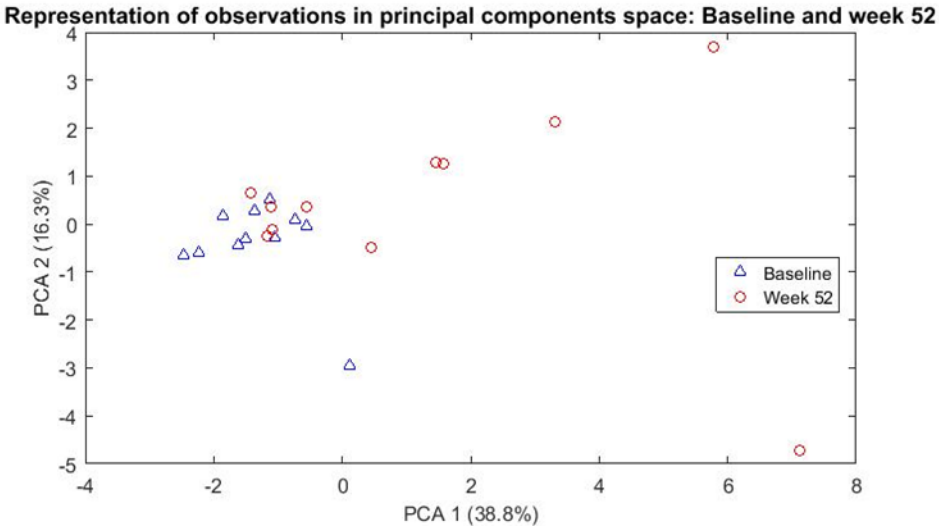

Figure 3.3.4.1 PCA plot of the 16 genera that were determined to be significantly different (p < 0.1) between the baseline and week 52 groups based on Wilcoxon signed rank test. Principal component 1 explained 38.8% of the total variance and principal component 2 explained 16.3% of the total variance.

3.3.5 The Significance of the PCA Result

The observation that the distance between the baseline and week 52 groups was larger than the distance within the baseline group and within the week 52 group indicated that the relative abundances of the genera in the baseline and week 52 samples were different, but whether the difference between the relative abundance of the genera in the baseline and week 52 samples is statistically significant was not investigated or reported by researchers.

To solve this problem, we coded a Matlab program (supplemental data) that scrambled the genera data randomly between baseline and week 52 and determined in what percentage of the cases the distance between baseline and week 52 was as large as or larger than the observed distance in the score analysis. The 16 genera that were judged to be significantly different by a Wilcoxon signed rank test were chosen for this analysis. Because there were only 11 patients, when the data were scrambled between baseline and week 52, there were only 2^{11} = 2048 possibilities. Systematic consideration of these possibilities revealed that only two of the possible permutations produced a distance equal to or greater than the observed distance. One was the observed assignment of weeks, and the other corresponded to reversing the baseline and week 52 assignments for all the genera. The type I error rate was therefore 2/2048 = 0.00098. It's unnecessary to write a program that went through all those possibilities in a systematic way. Instead, the baseline and week 52 data for each patient were scrambled 4000 times. This undoubtedly produced many repeat scenarios. However, it was enough to get good convergence on the type I error rate, which was about 7.5E−04. We need to know what the type I error rate would have to be if we did 18 independent tests and came up with an overall type I error rate of 1%. To be correct 99% of the time after making 18 tests, we would need (1-p)^18 = 0.99, where p

is the type I error rate for an individual test. Then $p = 0.00056$. The p-value of 7.5E−04 we obtained was smaller than 0.00056, so it indicated that the result of the test was statistically significant. In other words, it meant that for the community of the genera whose abundance was significantly altered between the baseline and week 52 groups, their difference was statistically significant. The null hypothesis that the relative abundance of the 16 bacterial genera was the same for the baseline and week 52 samples can, therefore, be rejected with a high degree of confidence.

In detail, to test whether the difference between the two treatment groups (baseline and week 52) was significantly different, we first calculated the distance between these two groups by using the mean value on axis PC1 and the mean value on axis PC2 (DISTANCE = sqrt((xb-x7)^2+(yb-y7)^2)).

Then we permuted the two sets of data (baseline and week 52 groups in this case) in each column in matrix X randomly to make a new matrix and obtained the corresponding PC scores and calculated the distance between these two groups again, by using the code 'distance = sqrt((xb-x7)^2+(yb-y7)^2)' and ran this procedure for 4000 times. The ratio of the probability of times to get the distance which is greater or equal to the distance that we obtained from our PCA solution to the total times we permutated will be calculated and displayed.

The above PCA analysis answered the question of whether there was a significant difference in the relative abundances of the 16 genera between baseline and week 52. However, the gut flora consisted of 247 genera, not just 16 genera. It was obviously of interest to determine whether the entire microbial community was significantly different between baseline and week 52 samples.

3.3.6 Limitation of PCA Analysis

PCA analysis usually cannot give much meaningful information for the analysis of the OTU table because usually, the number of variables (microbes) is greater than the number of samples (patients). To overcome this problem, the microbes can be clustered at specific taxonomic levels (e.g., using HCluster in R) and then one chosen from each cluster and the PCA performed on the representatives from the different clusters. Also, as in the example above, an ANOVA can be used to identify OTUs that are different between baseline and week 52. The PCA can then be carried out using the samples and the variables identified from the ANOVA. A PCA plot can then be made, but the plot cannot reveal whether the baseline and week 52 groups are different or not. Eventually, the *p* values from a statistical analysis will be needed to reach a conclusion.

3.3.7 Dissimilarity Tests

To determine whether there was a significant difference between the entire microbial community at baseline and week 52, a distance matrix was produced based on either the Bray-Curtis dissimilarity index or the Jaccard similarity index, followed by application of three non-parametric dissimilarity tests, including analysis of variance (Adonis), analysis of similarity (ANOSIM), and a multiresponse permutation procedure (MRPP). The Jaccard index includes only presence or absence information, while Bray-Curtis index includes both presence/absence and abundance information. The results showed that there was a significant difference between baseline and week 52 based on all three dissimilarity tests using the matrix based on the Jaccard similarity index (Table 3.3.7.1).

Table 3.3.7.1 The results of the dissimilarity tests to determine whether the ecological distance associated with the gut bacterial genera at baseline and week 52 were significantly different.

BRS_BL vs W52	MRPP		ANOSIM		Adonis	
Genus	Delta	*p*	R	*p*	F	*p*
Jaccard	0.602	0.079	0.073	0.064	1.344	0.055
Bray-Curtis	0.551	0.164	0.059	0.159	1.572	0.154

Two different programs, Jaccard and Bray-Curtis, were used to make the distance matrix, and three different programs, MRPP, Anosim, and Adonis, were used to test the statistical significance of the distance.

The Jaccard index, which can also be called the Jaccard similarity coefficient, measures the similarity between sample groups, and it can be used to compare the similarity of data sets (Jaccard, 1901). It is calculated by calculating the size of the intersection divided by the size of the union of the sample sets. The letters A and B stand for two datasets. J stands for the Jaccard index.

$$J(A,B)=\frac{|A\cap B|}{|A\cup B|}=\frac{|A\cap B|}{|A|+|B|-|A\cap B|}$$

The Jaccard distance measures the dissimilarity between sample groups. It is obtained by subtracting the Jaccard coefficient from 1, that is, the difference of the sizes of the union and the intersection of the two datasets divided by the size of their union. d_J stands for the Jaccard distance.

$$d_J(A,B)=1-J(A,B)=\frac{|A\cup B|-|A\cap B|}{|A\cup B|}$$

The Bray-Curtis dissimilarity index is a statistic used to quantify the compositional dissimilarity between two different sites, based on the counts at each site.

$$BC_{ij}=1-\frac{2C_{ij}}{S_i+S_j}$$

C_{ij} is the sum of the lesser values for the units of interest, which is a genus in this case, in common between the baseline and week 52 groups. S_i and S_j are the number of genera in these two datasets, respectively (Bray and Curtis 1957).

3.3.8 Conclusion

PCA is a useful way to determine whether groups have different microbial components, when the number of the microbial components is less than the number of samples or, alternatively, when using only the significantly different microbial components. It can provide a way to visualize the difference directly. Dissimilarity tests must be used to investigate the differences when the number of microbial components exceeds the number of samples and if all microbial components are to be taken into consideration.

3.4 Measurement of Biodiversity

3.4.1 Abstract

There are many types of diversity indices used to describe the diversity in the ecology studies, and usually, researchers choose the most popular ones, for example, Shannon diversity or Simpson diversity to use. However, these different diversity indices were all developed from true diversity index with different selected. Choosing the different value of the parameters in the true diversity equation could make the produced diversity index have specific stresses on a specific group of the interested entities. Thus, by using this methodology the true diversity index can be customized by the users to meet their specific emphasis and make more discoveries. This paper reviewed the true diversity and the group that it emphasizes when the different parameter is chosen. We conclude that researchers can tailor the true diversity index by applying different parameters to make more discoveries on the diversity with the emphasis on some specific group of the entities that they are interested in.

3.4.2 Introduction

In the field of ecology, three different types of diversity, alpha diversity (α diversity), beta diversity (β diversity) and gamma diversity (γ diversity) were developed for describing species diversity. Gamma diversity was defined as the total species diversity in a geological area, and it is determined by alpha diversity and beta diversity. Alpha diversity was referred as the diversity in a particular local ecosystem or habitat, or the mean of the diversity in particular local sites and beta diversity is the distinction or diversity among those different habitats.
When diversity indices are used in ecology, the types of interest are usually species, but they can also be other categories, such as other taxonomic levels including classes, orders, families, and genera. The interested entities are usually individual plants, animals, and microbes, and the measure of abundance can be, for example, the number of individuals.

Researchers often use diversity indices to measure alpha diversity. A diversity index is a quantitative measure that considers both species richness (the number of different types) and their evenness. For example, the Shannon index or the Simpson index are most commonly used. However, it might be more reasonable to use true diversity, which is the effective number species, as the measurement of species diversity because this method can weight abundant and rare species in differential means (weight more on abundant species, weight more on rare species or weight abundant and rare species equally), and its implication can be understood intuitively easier. The Shannon index and the Simpson index, are simple transformations of true diversity, which is the effective number of types, but different diversity indices can explain the diversity from different angles. True diversity is the effective number of species, which is the number of equally distributed types required to obtain the equal average relative abundance of types as that observed in the investigated dataset in which the abundance of all types may not be equally abundant.
Suppose species diversity is the effective number of species. Alpha diversity is the mean species diversity per subunit and can be calculated by first taking the weighted generalized mean Mq-1 of the proportional abundances within subunits, and then taking its inverse. The equation is ${}^{q}D = \frac{1}{M_{q-1}} = \frac{1}{\sqrt[q-1]{\sum_{i=1}^{R} p_i p_i^{q-1}}} = (\sum_{i=1}^{R} p_i^q)^{1/(1-q)}$ (Tuomisto, 2010). In the equation, the denominator Mq-1 equals the average proportional abundance of the types in the dataset as calculated with the weighted generalized mean with exponent q-1. R is richness, the total number of types that were

contained in the dataset of interest, and pi is the proportional abundance of the ith type. The nominal weights are the proportional abundances.

The form $^{q}D = (\sum_{i=1}^{R} p_i^q)^{1/(1-q)}$ is usually written as the general expression of true diversity (Hill, 1973, Jost, 2006). The term q is usually referred to as the order of the diversity. By changing its value the measurement of the true diversity can adjust the weight put on abundant or rare types, to customize its sensitivity to abundant or rare species. In general, a higher q value leads to the higher effective weight given to the most abundant types, and thus result in a greater M_{q-1} value and a smaller true diversity value. When q = 1, the weighted geometric mean of the pi values is used, and each type is exactly weighted by its proportional abundance. When q > 1, more weight was given to abundant types, and when q < 1, more weight was given to rare types. Some prevalent diversity indices such as Shannon index and Simpson index are transformations of the true diversity with different q values (Jost, 2006).

As q equals 1, the weighted geometric mean of the pi values is used, and each type is exactly weighted by its proportional abundance. Although the equation of true diversity is undefined when q = 1, it can be defined as q approaches to 1 infinitely. Below is its equation.

$$H' = -\sum_{i=1}^{R} p_i \ln p_i = -\sum_{i=1}^{R} \ln p_i^{p_i}$$

$$= -(\ln p_1^{p_1} + \ln p_2^{p_2} + \ln p_3^{p_3} + \ldots + \ln p_R^{p_R})$$

$$= -\ln p_1^{p_1} p_2^{p_2} p_3^{p_3} \ldots p_R^{p_R}$$

$$= \ln\left(\frac{1}{p_1^{p_1} p_2^{p_2} p_3^{p_3} \ldots p_R^{p_R}}\right)$$

$$= \ln\left(\frac{1}{\prod_{i=1}^{R} p_i^{p_i}}\right)$$

Shannon index quantifies the uncertainty in predicting the identity of an entity that is taken at random from the dataset (Shannon 1948). In the field of ecology, pi in the equation stands for the proportion abundance of the ith type in the dataset of interest. The sum of the pi values equals unit by definition, so the denominator equals the weighted geometric mean of the pi values, with the pi values themselves being used as the weights. The term inside of the parentheses is true diversity ^{1}D, so H' = ln(^{1}D) (Hill, 1973, Tuomisto, 2010).

When the proportional abundance of each type in the dataset is equal, all pi equals to 1/R, the Shannon index equals ln(R). The more different types there are, the more equal their proportional abundances in the dataset of interest. As the proportional abundance becomes more even, the smaller the weighted geometric mean of the pi value is, and the greater the Shannon index is. Conversely, the more uneven proportional abundance becomes, the greater the weighted geometric mean of the pi value is, and the smaller the Shannon index is. As the degree of the extent for the proportional abundance becomes uneven increases, the intensity becomes more focused on one type, and the Shannon index approaches to 0. When there is only one type, the Shannon index equal to 0, suggesting that there should be no indeterminacy in predicting the identity of the following type taken from the dataset at random.

Moreover, the Renyi entropy is a generalization of the Shannon index to other q values. Its expression is ${}^{q}H = \frac{1}{1-q}\ln(\sum_{i=1}^{R} p_i^q) = \ln(\frac{1}{\sqrt[q-1]{\sum_{i=1}^{R} p_i p_i^{q-1}}}) = \ln({}^{q}D)$ (Beck and Schlögl, 1993), and it is the logarithm of true diversity with any values of q.

On the contrary to the the Shannon index, which measures the probability to get a different type of the next draw when taking the individuals randomly from the dataset with replacement, the Simpson index (λ) measures the probability that two entities chosen from the interested dataset randomly belong to the same type instead (Simpson 1049). Its equation is $\lambda = \sum_{i=1}^{R} p_i^2$. It equals the weighted arithmetic mean of the proportional abundances of the types in the dataset of the interest, with the proportional abundances themselves as the weights.

However, the above formula needs to do some modification when the size of the dataset is small. This is because when the size of the dataset is large enough, the calculated result using the above equation could be the same. However, for small size dataset, the result of calculation using the above equation could be very different. In this case, the formula was modified to $l = \frac{\sum_{i=1}^{R} n_i(n_i - 1)}{N(N-1)}$. In the equation, ni is the number of entities for the ith type and N is the total number of entities in the dataset. In the field of microbiology, the Hunter–Gaston index is another name for this form of Simpson index.

Based on the measurement of Simpson index (λ), the diversity index increases when the diversity reduces. It counteracts with the human intuitive, leading to inversed Simpson index (1/λ) or Gini-Simpson index (1- λ), whose value increases with increasing diversity, was used more popularly (Hill 1973; Jost 2006). The inversed Simpson index is $1/\lambda = \frac{1}{\sum_{i=1}^{R} p_i^2} = {}^{2}D$, which is equated with the true diversity with q = 2. For example, the effective number of types that is obtained when the weighted arithmetic mean is used to quantify the average proportional abundance of types in the dataset of interest. Gini–Simpson index, which was written as 1 – λ, measures the probability that the two entities are taken from a dataset represent different types. Its equation is $1-\lambda = 1-\sum_{i=1}^{R} p_i^2 = 1-1/{}^{2}D$ and it can be expressed as a transformation of true diversity with q = 2.

3.4.3 Materials and Methods

The abundances of genera (a taxonomic level in microbiology) detected by Illumina sequencing (Illumina Miseq platform) from the genomic DNA samples extracted from fecal samples obtained at baseline before bariatric surgeries and fecal samples obtained at week 52 post bariatric surgeries were used. There were 11 bariatric surgery participants included, and 11 pairs of relative abundance data for each genus. In total, 247 genera were detected.

3.4.4 Results and Discussions

To illustrate the values and differences of these different diversity indices, we used the genus data for the baseline and week 52 post bariatric surgery treatment as an example to calculate them and make comparisons among them. The true diversity is calculated by the formula ${}^{q}D = (\sum_{i=1}^{R} p_i^q)^{1/(1-q)}$. If choosing q = 1 to not give more weight to either abundant or rare type, and then the true diversity equals to the Shannon index, that is, ${}^{1}D = -\sum_{i=1}^{R} p_i \ln p_i$. If choosing a q value greater than 1, then the true diversity becomes more sensitive to abundant types and more weight will be given to abundant types. For example, when choosing q = 2, the true diversity is the inversed Simpson index in this case and equals to ${}^{2}D = \frac{1}{(\sum_{i=1}^{R} p_i^2)}$. If choosing a q value less than 1, and then the true diversity becomes more sensitive to rare types, and more weight will be given to rare types. For instance, when choosing q = 0.5, the true diversity will be equal to ${}^{0.5}D = (\sum_{i=1}^{R} \sqrt{p_i})^2$. Below are the results of the calculations for the diversity indices in the above-mentioned conditions.

Table 3.4.4.1 The richness of genus for each baseline and week 52 post bariatric surgery sample. The means sand standard deviations for the genus richness of these two groups were listed at the bottom.

BRS	Genus richness	
Participant ID	BL	W52
Band0186	61	83
Bypass0610	54	63
Bypass9968	67	90
Sleeve1517	82	79
Sleeve2069	65	80
Sleeve2104	56	69
Sleeve3036	66	81
Sleeve3289	83	85
Sleeve5155	58	47
Sleeve7603	32	61
Sleeve8684	59	75
Mean	62.09	73.91
Std	13.85	12.70

Table 3.4.4.2 The result of tests for comparing whether the difference between the genus richness in baseline and week 52 post bariatric surgery samples are statistically significant.

Genus richness_BL vs W52	*p*
Paired t test	0.008
Paired u test	0.018

The result showed that the mean genus richness of the week 52 samples was higher than the mean genus richness of the baseline samples (Table 3.4.4.1), and both paired t-test and paired u test results showed that the increase was statistically significant (Table 3.4.4.2). In other words, the genus richness at baseline was significantly lower when compared to the week 52 samples, and the genus richness at week 52 post-treatment was significantly higher when compared to the baseline samples.

Table 3.4.4.3 The values of the true diversities of the genus community in baseline and week 52 post bariatric surgery samples, when calculated with different q values, were listed. The means and standard deviations of the true diversities for the genus community in the baseline and week 52 groups were listed at the bottom of the table.

BRS	Genus diversity at BL			Genus diversity at W52		
Participant ID	q = 1	q = 2	q = 0.5	q = 1	q = 2	q = 0.5
Band0186	1.728	3.297	12.286	2.602	8.474	25.526
Bypass0610	2.150	6.250	13.729	2.720	10.742	24.089
Bypass9968	2.183	4.749	17.655	2.548	7.247	25.479
Sleeve1517	2.626	8.417	26.184	2.957	12.224	30.432
Sleeve2069	2.418	5.762	20.633	2.212	4.381	21.413
Sleeve2104	2.129	4.295	16.511	2.738	9.710	24.699
Sleeve3036	1.801	3.924	12.999	1.957	3.964	17.471
Sleeve3289	2.178	4.738	19.729	2.270	5.084	21.835
Sleeve5155	2.609	9.858	20.501	2.093	5.757	12.764
Sleeve7603	1.368	2.385	7.640	1.522	2.529	11.350
Sleeve8684	1.765	3.366	13.429	1.960	3.718	17.599
Mean	2.087	5.186	16.482	2.325	6.712	21.151
Std	0.391	2.263	5.141	0.428	3.194	5.817

Table 3.4.4.4 The test results for comparing whether there is a statistically significant difference between the true diversities for the genus community in the baseline and week 52 post bariatric surgery samples when calculated with different q values, were listed.

BRS_BL vs W52	*p*		
True diversity of genus	q = 1	q = 2	q = 0.5
Paried t test	0.067	0.123	0.019
Paired u test	0.083	0.083	0.019

The results showed that the average of the true diversity was increased at week 52 when compared to the baseline level (Table 3.4.4.3). In addition, both paired t-test and paired u test results showed that when choosing smaller q values, the difference of the true diversity between baseline and week 52 samples become more statistically significant. For example, when q was set as 0.5 to emphasize the rarer genera, the baseline diversity was significantly lower than the week 52 diversity ($p = 0.019$), while when q was set as 2 to emphasize the abundant genera, the p-value, which is equal to 0.083, was not as significant as the p-value calculated when q was set as 0.5 (Table 3.4.4.4). It indicates that the difference for the rare genera between before and after treatment was more significant when compared to the difference for the abundant genera. In other words, it indicates that the changes in the gut flora have been mainly in the comparatively rare genera.

Therefore, we conclude that it would be meaningful for researchers to employ different types of diversity indices or the true diversity with different q values when comparing the diversities between different groups. This methodology can help the researchers to dig out more detailed information, for example, whether the difference in diversities is more concentrated on abundant types or rare types in the dataset we are interested in.

CHAPTER FOUR: OBESITY IMPROVEMENT WAS EFFICIENT AND PERSISTENT AFTER BRS AND IT WAS LESS EFFICIENT AND PERSISTENT AFTER LCD

4.1 Obesity Improvement after BRS Was Efficient and Persistent

We observed that almost all physiological variables were significantly improved at week 7 and week 52 after BRS. Weight, fat mass, lean mass, fat%, BMI, 24HourEE, SubcutMeanSize, GLU, INS, GHRA, ADP, ADPHMW, and hsCRP were all significantly improved at week 7 and week 52 post BRS, and CHOL and GHR were significantly improved at week 7 post BRS, GDR1/Weight, GDR2/Weight, TRIG, HDL, were significantly improved at week 52 post BRS.

More specifically, weight was significantly reduced from mean of 128.36 kg (std = 4.94 kg) at baseline to mean of 111.99 kg (std = 4.14 kg) at week 7 to mean of 85.62 kg (std =3.34 kg) at week 52 post BRS (p =3.05E−05 for baseline and week 7; p =1.22E−04 for baseline and week 52; p = 0.0001 for week 7 and week 52). Similarly, IDXA weight was significantly reduced from baseline mean of 129.6 kg (std =20.6 kg) to week 7 mean of 115.0 kg (std =17.19 kg) to week 52 mean of 86.92 kg (std =13.72 kg) (p = 4.37E−04 for baseline & week 7, p = 4.38E−04 for baseline & week 52 and week 7 & week 52). Fat mass was significantly reduced from mean of 69.56 kg (std = 11.86 kg) at baseline to mean of 60.48 kg (std = 10.70 kg) at week 7 (p = 1.22E−04), and from mean of 67.48 kg (std = 14.30 kg) at baseline to mean of 37.02 kg (std = 9.44 kg) at week 52 (p = 0.0156), and from mean of 59.69 kg (std = 13.78 kg) at week 7 to mean of 37.02 kg (std = 9.44 kg) at week 52 (p = 0.0156). IDXA fat mass was significantly reduced from baseline mean of 67.36 kg (std = 13.17 kg) to week 7 mean of 58.15 kg (std = 11.43 kg) (p = 6.10E−05), from baseline mean of 67.36 kg (std = 13.17 kg) to week 52 mean of 33.93 kg (std = 10.42 kg) (p = 6.10E−05), and from week 7 mean of 57.28 kg (std = 11.57 kg) to week 52 mean of 33.22 kg (std = 10.46 kg) (p = 4.38E−04). Lean mass was also significantly reduced from mean of 54.13 kg (std = 13.02 kg) at baseline to mean of 48.65 kg (std = 10.25 kg) at week 7 (p = 1.22E−04), from baseline mean of 50.72 kg (std = 16.46 kg) to week 52 mean of 44.52 kg (std = 11.63 kg) (p = 0.0156). IDXA lean mass was significantly reduced from baseline mean of 57.49 kg (std = 8.53 kg) to week 7 mean of 52.86 kg (std = 7.45 kg) (p = 6.10E−05), from baseline mean of 57.66 kg (std = 8.82 kg) to week 52 mean of 50.32 kg (std = 6.08 kg) (p = 2.44E−04), and from week 7 mean of 54.67 kg (std = 9.87 kg) to week 52 mean of 52.07 kg (std = 8.96 kg) (p =0.0054). Fat% was significantly reduced from baseline mean of 53.81 (std = 4.67) to week 7 mean of 52.21 (std = 4.90) (p = 0.0054), from baseline mean of 53.81 (std = 4.67) to week 52 mean of 39.80 (std = 7.59) (p = 6.10E−05), and from week 7 mean of 51.02 (std = 6.71) to week 52 mean of 38.61 (std = 8.73) (p = 4.38E−04). 24HourEE was significantly reduced from baseline mean of 2453.56 kcal/day (std = 418.48 kcal/day) to week 7 mean of 2085.5 kcal/day (std = 261.66 kcal/day) (p = 4.38E−04), from baseline mean of 2451.4 kcal/day (std = 433.08 kcal/day) to week 52 mean of 1918.13 kcal/day (std = 304.80 kcal/day) (p = 6.10E−05), and from week 7 mean of 2087 kcal/day (std = 270.78 kcal/day) to week 52 mean of 1918.13 kcal/day (std = 304.80 kcal/day) (p = 0.0014). BMI was significantly reduced from baseline mean of 45.83 kg/m^2 (std = 6.56 kg/m^2) to week 7 mean of 40.02 kg/m^2 (std = 5.77 kg/m^2) to week 52 mean of 30.57 kg/m^2 (std = 4.44 kg/m^2) (p = 4.38E−04) for baseline & week 7, baseline & week 52, and week 7 & week 52). Subcutaneous fat size was significantly reduced from baseline mean of 1.52 µl (std = 0.657 µl) to week 7 mean of 1.203 µl (std = 0.23 µl) (p = 0.064), from week 7 mean of 1.251 µl (std = 0.222 µl) to week 52 mean of 0.829 µl (std = 0.230 µl) (p = 0.0098), from baseline mean of 1.543 µl (std = 0.718 µl) to

week 52 mean of 0.829 µl (std = 0.230 µl) (p = 0.0039). It indicated that after BRS, obesity was significantly improved.

Fasting glucose was significantly reduced from baseline mean of 100.59 mg/dl (std = 11.40 mg/dl) to week 7 mean of 91.19 mg/dl (std = 13.48 mg/dl) to week 52 mean of 86.09 mg/dl (std = 8.38 mg/dl) (p = 0.0034 for baseline & week 7; p = 6.10E−05 for baseline & week 52). INS was significantly reduced from baseline mean of 13.24 uU/dl (std = 8.57 uU/dl) to week 7 mean of 5.77 uU/dl (std = 3.03 uU/dl) to week 52 mean of 5.34 uU/dl (std = 6.80 uU/dl) (p = 9.35E−04 for baseline & week 7; p = 7.76E−04 for baseline & week 52; p = 0.0494 for week 7 & week 52). GDR1/Weight was not significantly altered during baseline and week 7, but was significantly increased from week 7 mean of 2.49 mg/kg/min (std = 0.83 mg/kg/min) to week 52 mean of 4.91 mg/kg/min (std = 1.13 mg/kg/min) (p = 4.37E−04) and from baseline mean of 2.57 mg/kg/min (std = 0.84 mg/kg/min) to week 52 mean of 4.91 mg/kg/min (std = 1.13 mg/kg/min) (p = 4.38E−04). Similarly, GDR2/Weight was not significantly altered during baseline and week 7, but was significantly increased from week 7 mean of 7.11 mg/kg/min (std = 1.88 mg/kg/min) to week 52 mean of 12.93 mg/kg/min (std = 1.58 mg/kg/min) (p = 4.38E−04) and from baseline mean of 7.29 mg/kg/min (std = 2.27 mg/kg/min) to week 52 mean of 12.93 mg/kg/min (std = 1.58 mg/kg/min) (p = 4.38E−04). It indicated that after BRS, the insulin resistance was significantly improved.

Triglycerides were significantly reduced from baseline mean of 143.47 mg/dl (std = 86.11 mg/dl), to week 7 mean of 96.67 mg/dl (std = 37.04 mg/dl) (p = 0.0291), from baseline mean of 140.06 mg/dl (std = 84.29 mg/dl), to week 52 mean of 75.63 mg/dl (std = 35.62 mg/dl) (p = 0.0023), and from week 7 mean of 96.67 mg/dl (std = 37.04 mg/dl) to week 52 mean of 78 mg/dl (std = 35.53 mg/dl) (p = 0.0946). HDL was significantly reduced from baseline mean of 51.43 mg/dl (std = 10.32 mg/dl) to week 7 mean of 44.58 mg/dl (std = 10.66 mg/dl) (p = 0.174), but was significantly increased from baseline mean of 51.43 mg/dl (std = 10.32 mg/dl) to week 52 mean of 61.89 mg/dl (std = 10.90 mg/dl) (p = 0.0025), and from week 7 mean of 44.58 mg/dl (std = 10.66 mg/dl) to week 52 mean of 61.89 mg/dl (std = 10.90 mg/dl) (p = 4.38E−04). Cholesterol was significantly reduced from baseline mean of 173.88 mg/dl (std = 47.19 mg/dl) to week 7 mean of 148.56 mg/dl (std = 37.36 mg/dl) (p = 0.014), but was significantly increased from week 7 mean of 148.56 mg/dl (std = 37.36 mg/dl) to week 52 mean of 170.69 mg/dl (std = 32.54 mg/dl) (p = 0.0057), but it was still less than the baseline mean and there was no statistically significant difference between baseline and week 52 levels. No significant alteration of LDL was observed during the three periods. It indicated that after BRS, the lipid profile became significantly improved.

Hormone adiponectin (ADP) was significantly increased from baseline mean of 8.19 mg/dl (std = 5.09 mg/dl) to week 52 mean of 16.45 mg/dl (std = 11.60 mg/dl) (p = 0.037), and from week 7 mean of 10.13 mg/dl (std = 5.69 mg/dl) to week 52 mean of 16.76 mg/dl (std = 11.27 mg/dl) (p = 6.42E−04). The normal range of adiponectin for individuals with BMI > 30 kg/m^2 is 2-20 mg/dl for males and 4-22 for females (Mayo medical laboratories 2017). The patients who had over 10 years of diabetic mellitus type 2 showed abnormally higher level of ADP, and after excluding it from the analysis, ADP showed significant increased at week 7 (mean = 9.7 mg/dl, std = 5.62 mg/dl), when comparing to baseline (mean = 8.19 mg/dl, std = 5.09 mg/dl) (p = 0.037). Meanwhile, this patient also showed least lean mass (but not IDXA lean mass), biggest SubcutMeanSize, highest GLU, lowest INS, highest ADPHMW, and lowest LEP. Similarly, the active form of ADP, high-molecular-weight adiponectin (ADPHMW) was significantly increased from mean week 7 mean of 5435.73 mg/dl (std = 3343.05 mg/dl) to week 52 mean of 9780 mg/dl (std = 6893.75

mg/dl) (p = 0.0072), and from baseline mean of 5795.56 mg/dl (std =7138.77 mg/dl) to week 52 mean of 10029 mg/dl (std = 6734.06 mg/dl) (p = 4.38E−04), and after excluding the patient with greater than 10-year diabetics, ADPHMW was significantly increased from at week 7 (mean = 5435.73 mg/dl, std = 3343.05 mg/dl), when comparing with baseline (mean = 4162.07 mg/dl, std = 2976.53 mg/dl) (p = 0.0012). GHR was significantly reduced from baseline mean of 550.44 mg/dl (std = 129.68 mg/dl) to week 7 mean of 407.81 mg/dl (std = 182.06) to week 52 mean of 479.88 mg/dl (std = 240.29 mg/dl) (p = 0.0027 for baseline & week 7; p = 0.098 for baseline & week 52). GHRA was significantly reduced from baseline mean of 119.67 mg/dl (std = 60.11 mg/dl) to week 7 mean of 61.6 mg/dl (std = 16.78 mg/dl) (p = 9.16E−04), but was significantly increased from week 7 mean of 59.03 mg/dl (std = 19.19 mg/dl) to week 52 mean of 85.88 mg/dl (std = 41.54 mg/dl) (p = 0.0067); However, the week 52 level was still lower than the baseline level. There were many GLP-1 values were below 2 mg/dl, making the comparison between baseline, week 7 and week 52 inaccurate, so it was not reported. No significant alteration of PYY levels were observed among the three periods. Leptin was significantly reduced from baseline mean of 53.76 mg/dl (std = 20.76 mg/dl) to week 7 mean of 32.88 mg/dl (std = 13.34 mg/dl) to week 52 mean of 21.56 mg/dl (std = 13.33 mg/dl) (p = 9.35E−04 for baseline & week 7; p = 5.30E−04 for baseline & week 52; p = 0.0032 for week 7 & week 52). It indicated the significant improvement of obesity-related hormones after BRS.

HsCRP was significantly reduced from baseline mean of 10.01 mg/l (std = 8.86 mg/l) to week 7 mean of 7.31 mg/l (std = 5.59 mg/l) (p = 0.098), from baseline mean of 10.46 mg/l (std = 8.97 mg/l) to week 52 mean of 2.97 mg/l (std = 3.17 mg/l) (p = 6.10E−05), and from week 7 mean of 7.27 mg/l (std = 5.79 mg/l) to week 52 mean of 3.14 mg/l (std = 3.21 mg/l) (p = 6.10E−05). HsCRP measures general inflammation levels, and the normal range of hsCRP in healthy human beings is below 10 mg/l. At week 52 post BRS, all patients showed hsCRP levels less than 10 mg/l, except one patient showed hsCRP level equaling to 10 mg/l. Considering that obesity is usually linked with increased inflammation levels and the significant reduction of hsCRP further supported the signinificant improvement of obesity condition.

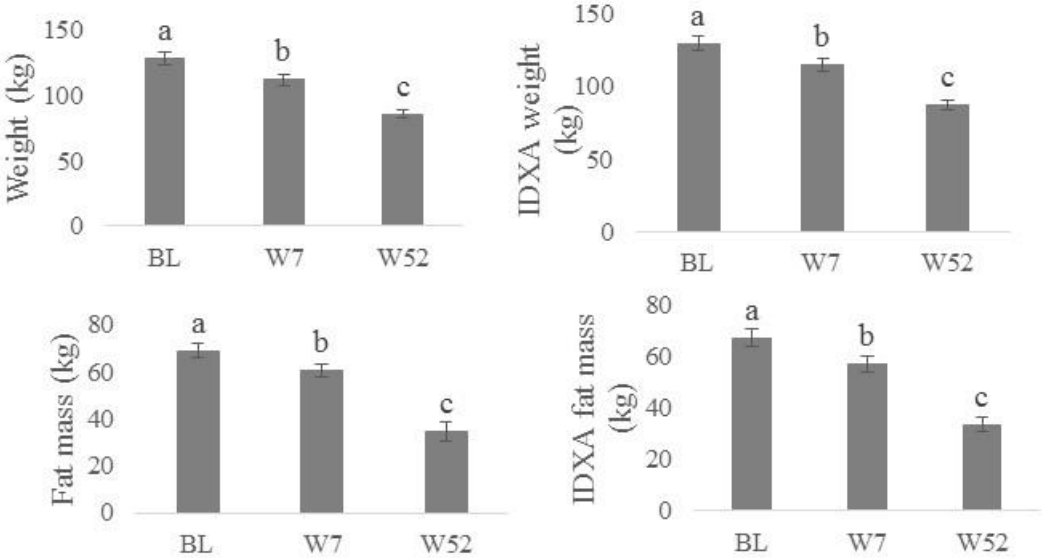

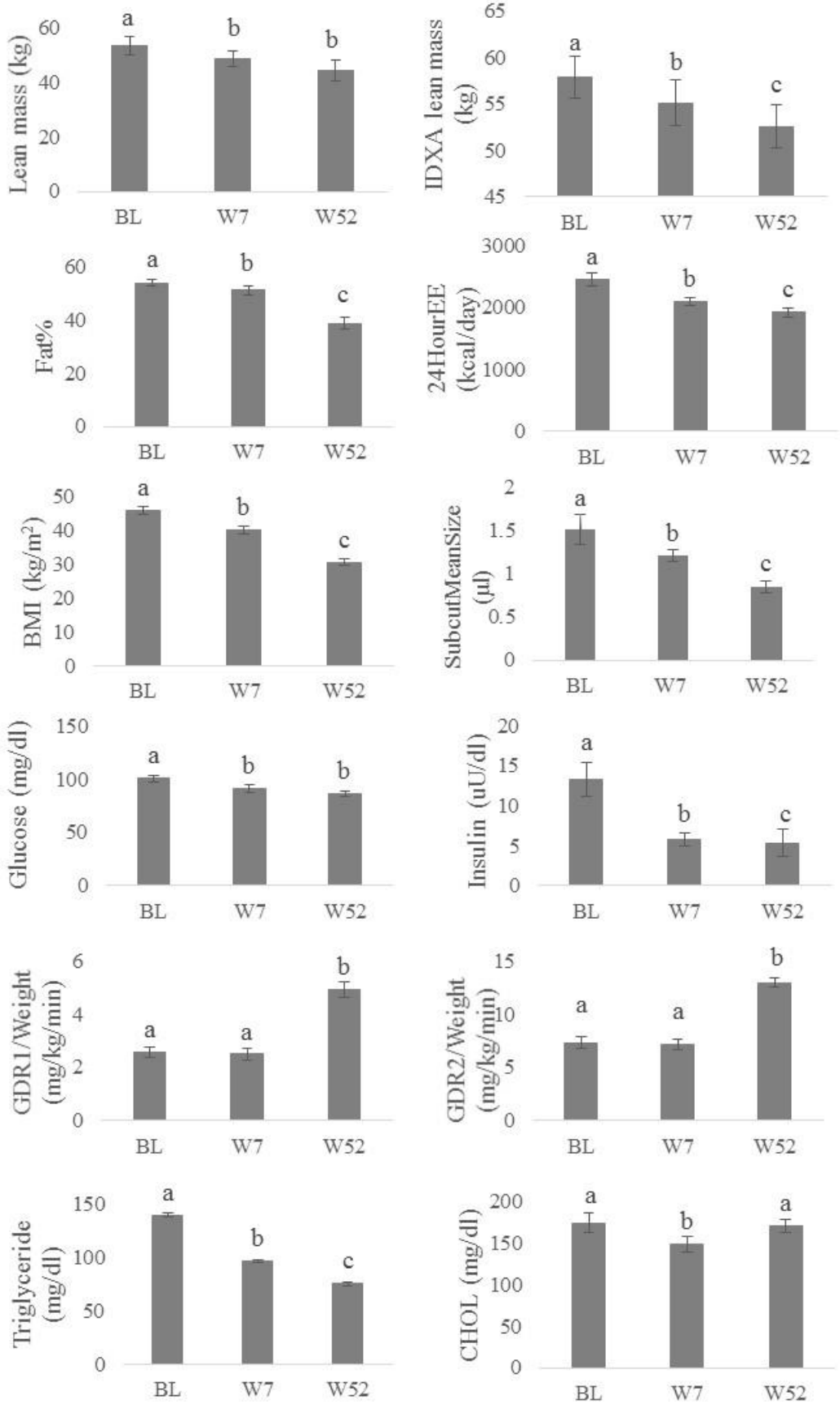
Lean mass (kg)
60
40
20
0
a
b
b
BL
W7
W52
IDXA lean mass (kg)
65
60
55
50
45
a
b
c
BL
W7
W52
Fat%
60
40
20
0
a
b
c
BL
W7
W52
24HourEE (kcal/day)
3000
2000
1000
0
a
b
c
BL
W7
W52
BMI (kg/m²)
50
40
30
20
10
0
a
b
c
BL
W7
W52
SubcutMeanSize (µl)
2
1.5
1
0.5
0
a
b
c
BL
W7
W52
Glucose (mg/dl)
150
100
50
0
a
b
b
BL
W7
W52
Insulin (uU/dl)
20
15
10
5
0
a
b
c
BL
W7
W52
GDR1/Weight (mg/kg/min)
6
4
2
0
a
a
b
BL
W7
W52
GDR2/Weight (mg/kg/min)
15
10
5
0
a
a
b
BL
W7
W52
Triglyceride (mg/dl)
150
100
50
0
a
b
c
BL
W7
W52
CHOL (mg/dl)
200
150
100
50
0
a
b
a
BL
W7
W52

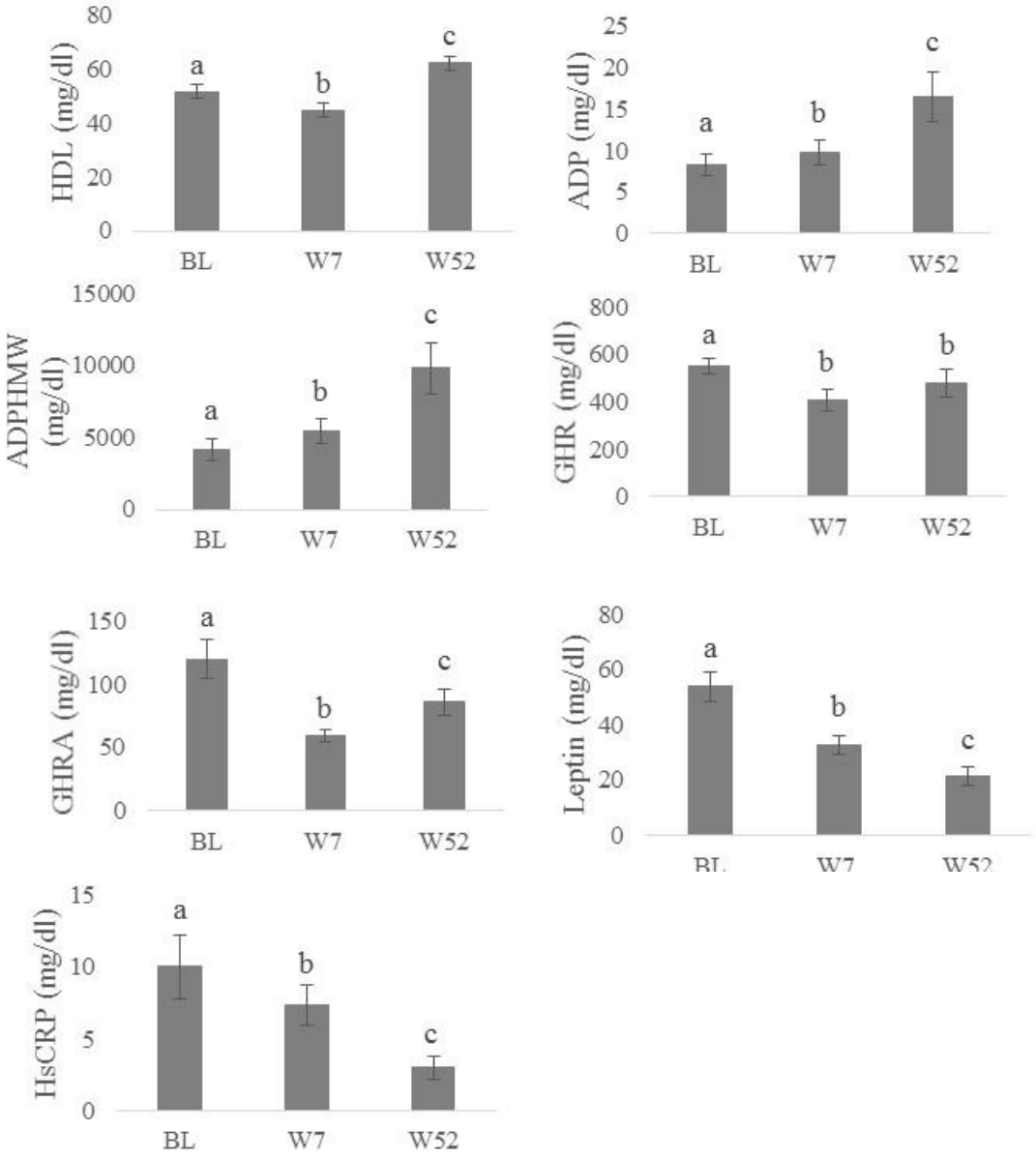

Figure 4.1.1 Changing patterns of obesity-related physiological variables in the BRS group. Different letters (a, b, and c) stand for statistical significance.

4.2 Obesity Improvement after LCD Was Less Efficient and Persistent

For the LCD group, we also observed significant improvement of obesity-related physiological variables, but the number of significantly improved variables and the degree of their improvements were much less than the BRS group. Weight, fat mass, lean mass, and ADP were all significantly improved at week 7 and week 52 post LCD treatment, and BMI, 24HourEE, GLU, INS, and CHOL were significantly reduced at week 7 post LCD, and SubcutMeanSize and hsCRP were significantly reduced at week 52 post LCD.

More specifically, weight was significantly reduced from baseline mean of 130.01 kg (std = 30.59 kg) (p = 0.0078). IDXA weight was significantly reduced from baseline mean of 129.91 kg (std = 30.19 kg) to week 7 mean of 122.94 kg (std = 31.92 kg) to week 52 mean of 125.05 kg (std = 30.13 kg) (p = 0.0078 for baseline & week 7 and p = 0.0781 for baseline & week 52). Fat mass was significantly reduced from baseline mean of 70.17 kg (std = 19.98 kg) to week 7 mean of 65.32 kg (std = 20.56 kg) (p = 0.0078), and from baseline mean of 74.35 kg (std = 21.78 kg) to week 52 mean of 68.9 kg (std = 21.33 kg) (p =0.0625). IDXA fat mass was significantly reduced from baseline mean of 57.51 kg (std = 8.97 kg) to week 7 mean of 53.70 kg (std = 7.71 kg) (p = 0.0625), but was significantly increased from week 7 mean of 56.32 kg (std = 9.43 kg) to week 52 mean of 59.37 kg (std = 10.02 kg) (p = 0.0313). Lean mass was significantly reduced from baseline mean of 52.61 kg (std = 11.87 kg) to week 7 mean of 49.97 kg (std = 10.84 kg) (p = 0.0078), and from baseline mean of 54.98 kg (std = 12.78 kg) to week 52 mean of 51.53 kg (std = 12.79 kg) (p = 0.0313). IDXA lean mass was significantly reduced from baseline mean of 51.22 kg (std = 3.06 kg) to week 7 mean of 47.38 kg (std = 3.77 kg) (p = 0.0625). No significant alteration of fat% or SubcutMeanSize was observed after LCD. 24HourEE was significantly reduced from baseline mean of 2365.13 kcal/day (std = 363.84 kcal/day) to week 7 mean of 2160.25 kg (std = 351.60 kg) (p = 0.0156). BMI was significantly reduced from baseline mean of 47.19 kg/m^2 (std = 8.76 kg/m^2) to week 7 mean of 44.11 kg/m^2 (std = 9.41 kg/m^2) (p = 0.0078). It indicated that obesity was significantly improved after LCD treatment.

GLU was significantly reduced from baseline mean of 98 mg/dl (std = 9.25 mg/dl) to week 7 mean of 92.69 mg/dl (std = 9.12 mg/dl) (p = 0.0234). INS was significantly reduced from baseline mean of 14.18 uU/dl (std = 9.06 uU/dl) to week 7 mean of 9.35 uU/dl (std = 6.83 uU/dl) (p = 0.0391). No significant alteration of GDR1/weight or GDR2/Weight was observed after LCD. It indicated during LCD treatment, the insulin resistance was significantly improved, but the improvement disappeared after the cease of the LCD treatment.

No significant alteration of TRIG or LDL was observed. HDL was significantly reduced from baseline mean of 51.28 mg/dl (std = 5.80 mg/dl) to week 7 mean of 45.6 mg/dl (std = 5.67 mg/dl) (p = 0.0781), but was significantly increased from week 7 mean of 45.6 mg/dl (std = 5.67 mg/dl) to week 52 mean of 50.48 mg/dl (std = 8.53 mg/dl) (p = 0.0547); no significant difference between baseline and week 52 levels. CHOL was significantly increased from week 7 mean of 165.13 mg/dl (std = 26.14 mg/dl) to week 52 mean of 189.63 mg/dl (std = 42.48 mg/dl) (p = 0.0858), but no significant difference between baseline and week 52 levels. It indicated that lipid profile was not significantly altered after LCD.

ADP was significantly increased from baseline mean of 9.06 mg/dl (std = 4.61 mg/dl) to week 7 mean of 11.2 mg/dl (std = 6.08 mg/dl) (p = 0.0313). LEP was significantly reduced from baseline mean of 67.16 mg/dl (std = 27.27 mg/dl) to week 7 mean of 49.21 mg/dl (std = 8.58 mg/dl) (p = 0.0391), but was significantly increased from week 7 mean of 49.21 mg/dl (std = 8.58 mg/dl) to week 52 mean of 68.01 mg/dl (std = 19.25 mg/dl) (p = 0.0156); no significant difference of LEP between baseline and week 52 post LCD. No significant alteration of ADPHMW, GHR, GHRA, GLP-1, or PYY was observed. It indicated the significant improvement of obesity-related hormone during LCD treatment, but the significant improvement was short-term, considering that it was disappeared after the cease of LCD treatment.

No significant alteration of the hsCRP level was observed after LCD.

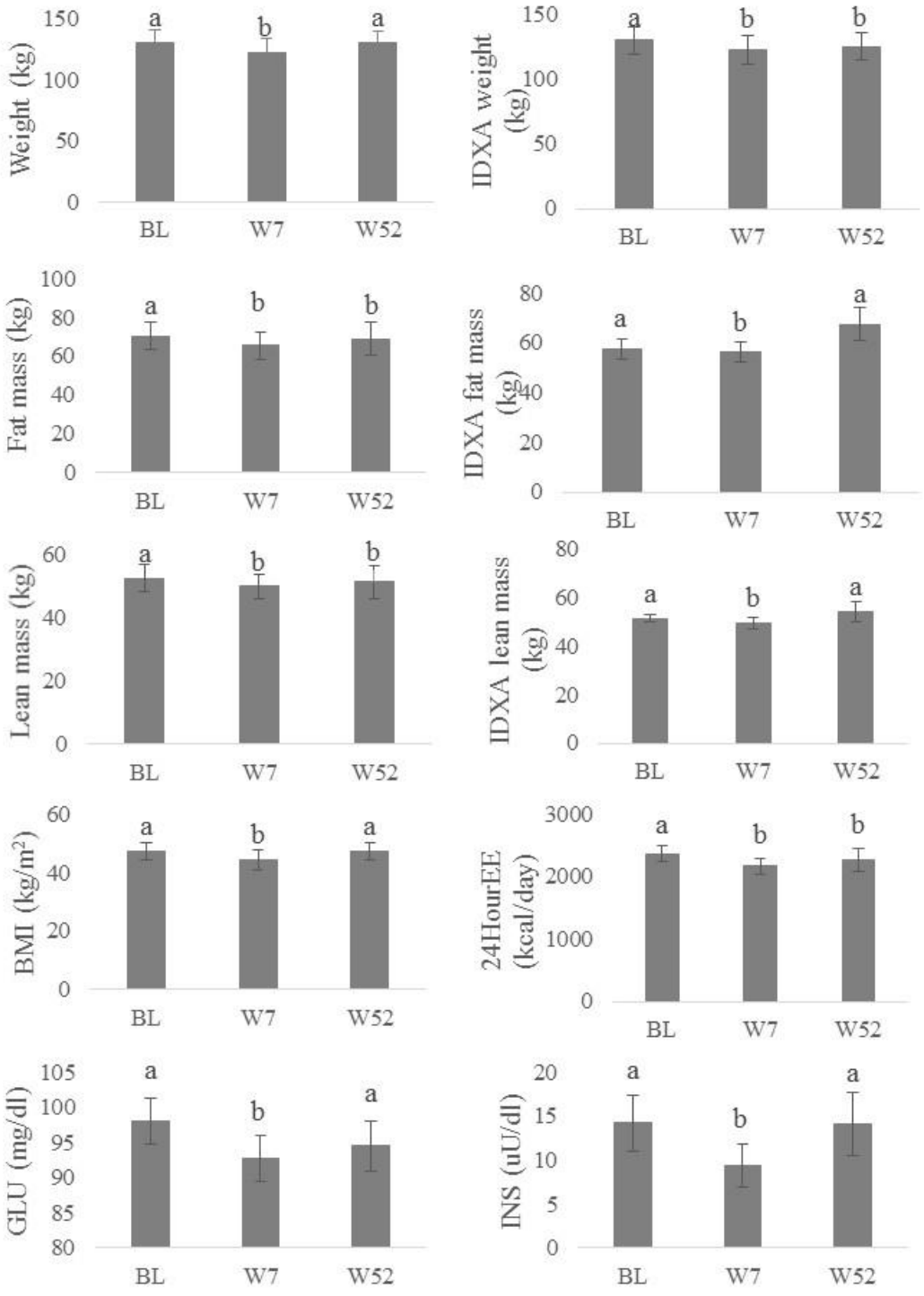
Weight (kg)
150
100
50
0
a
b
a
BL
W7
W52
IDXA weight (kg)
150
100
50
0
a
b
b
BL
W7
W52
Fat mass (kg)
100
80
60
40
20
0
a
b
b
BL
W7
W52
IDXA fat mass (kg)
80
60
40
20
0
a
b
a
BL
W7
W52
Lean mass (kg)
60
40
20
0
a
b
b
BL
W7
W52
IDXA lean mass (kg)
80
60
40
20
0
a
b
a
BL
W7
W52
BMI (kg/m2)
60
40
20
0
a
b
a
BL
W7
W52
24HourEE (kcal/day)
3000
2000
1000
0
a
b
b
BL
W7
W52
GLU (mg/dl)
105
100
95
90
85
80
a
b
a
BL
W7
W52
INS (uU/dl)
20
15
10
5
0
a
b
a
BL
W7
W52

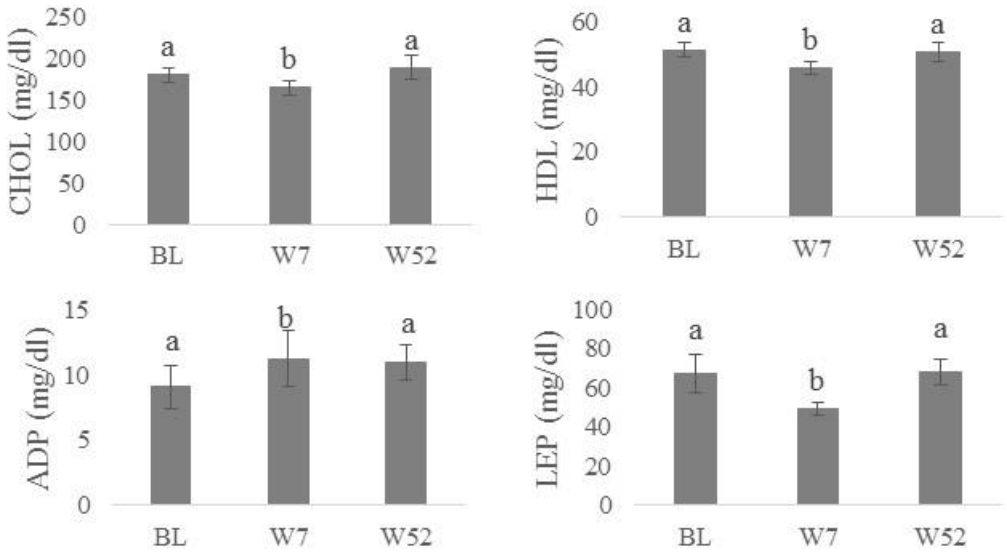

Figure 4.2.1 Changing patterns of obesity-related physiological variables in the LCD group. Different letters (a, b, and c) stand for statistical significance.

CHAPTER FIVE: MICROBIAL COMMUNITY STRUCTURE WAS SIGNIFICANTLY ALTERED AFTER TREATMENTS

5.1 Gut Microbial Richness and Diversity Was Significantly Increased

Richness measures how many different types of categories existing in the sample, and it increases as the number of different category type increases. The genus richness was significantly from around 60 to 80, and OTU richness was significantly increased from around 800 to 100. Diversity considers both richness and evenness, and it increases as richness and evenness increase. Alpha-diversity measures local diversity, and here it was measured by Shannon index and inversed Simpson index, both of which showed significantly increase at genus and OTU level. Combining them together, it indicated that microbial richness and diversity were significantly increased at genus and OTU levels.

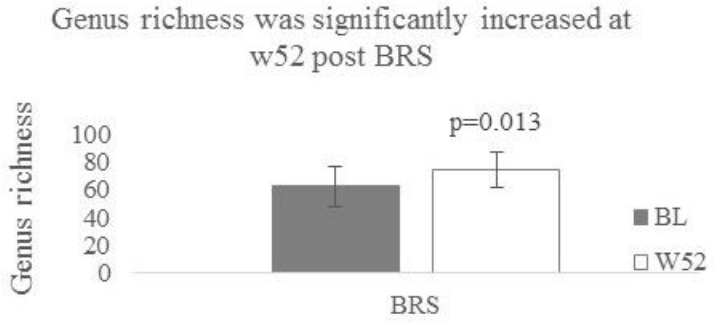

Figure 5.1.1 Genus richness was significantly increased at week 52 after BRS treatment.

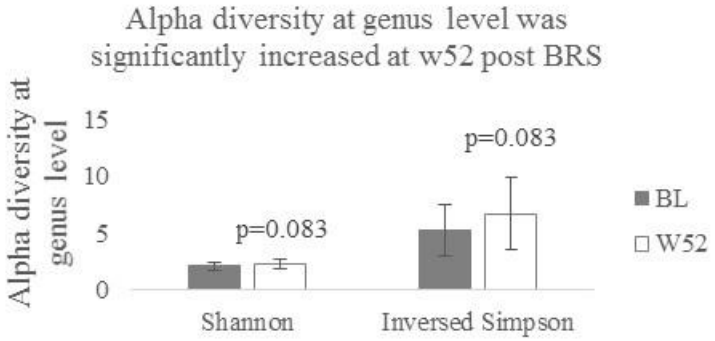

Figure 5.1.2 Genus alpha diversity was significantly increased at week 52 after BRS treatment.

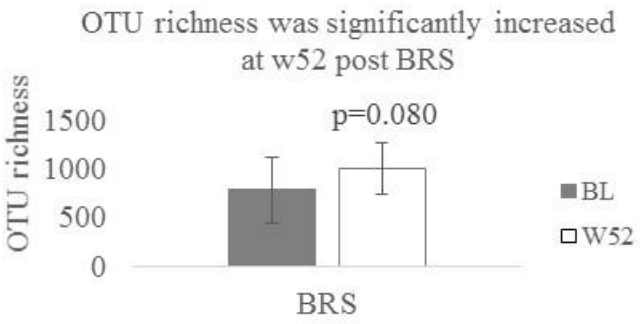

Figure 5.1.3 OTU richness was significantly increased at week 52 after BRS treatment.

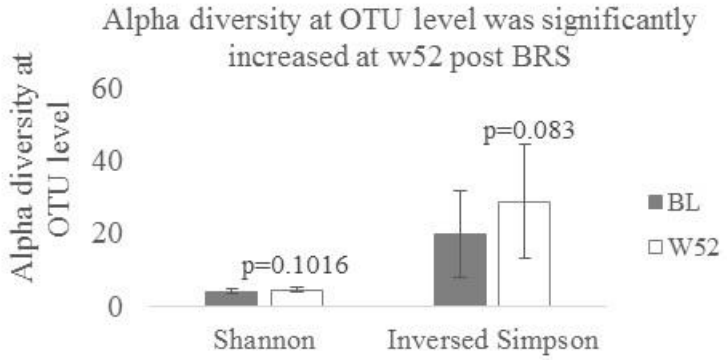

Figure 5.1.4 OTU diversity was significantly increased at week 52 after BRS treatment.

Similarly, we observed that the significant increase of genus diversity at week 52 post LCD treatment, although no significant increase of genus richness was observed. At OTU level, we did not observe a statistically significant increase of richness and diversity, but all the 4 LCD participants whose microbial data were available showed increased OTU richness and diversity.

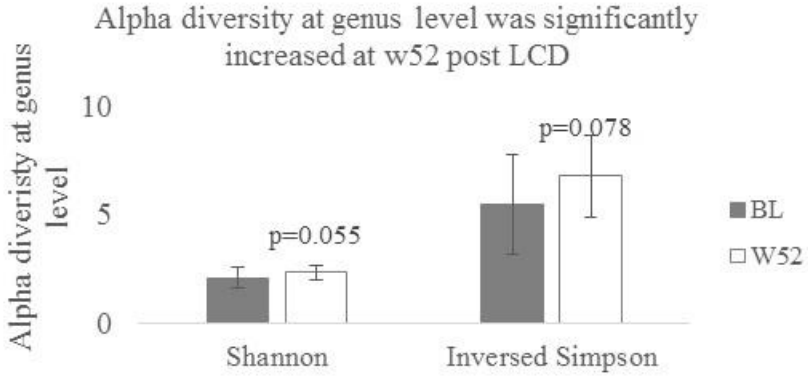

Figure 5.1.5 Genus diversity was significantly increased at week 52 post LCD treatment.

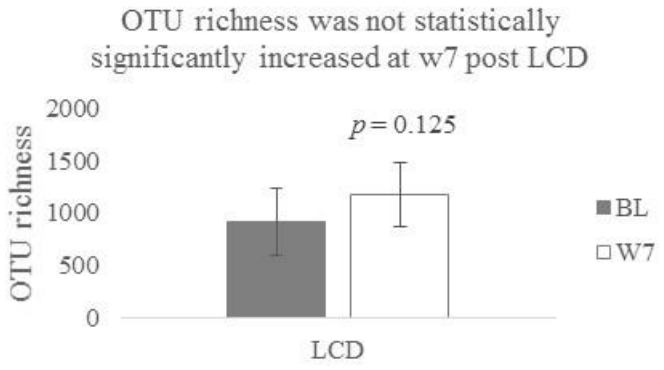

Figure 5.1.6 OTU richness was not statistically significantly increased, but they were all increased in all 4 LCD participants whose microbial data was available.

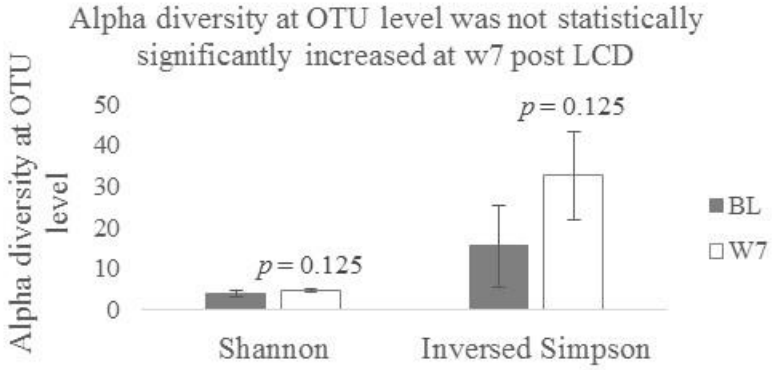

Figure 5.1.7 OTU diversity was not statistically significantly increased, but they were all increased in all 4 LCD participants whose microbial data was available.

Taken together, it indicated that the richness and alpha diversity of the entire microbial community structure were significantly increased after both BRS and LCD treatments, and degree of their increase was higher in the BRS group than the LCD group.

Like all healthy ecosystems, the richness of gut microbiota characterizes the healthy status, and a loss of diversity is linked to several disease statuses (Ott and Schreiber, 2006). Here, our results supported that the increased microbial richness and diversity was linked to the improved obesity condition, and greater increased microbial richness and diversity was linked to greater improved obesity condition in the severely obese subjects. It was reported that fasting treatment increased gut microbial diversity (Remely et al., 2015), and considering that bariatric surgeries induced different degrees of calorie restriction (the direct effect of BRS), so our result confirmed this link and indicated that the calorie restriction induced by BRS could be one of the mechanisms that contributed to the increased microbial diversity. Besides, considering that the main physiological alteration of the patients after BRS was weight loss and better healthiness status (indirect effects of BRS), so the increased microbial diversity could be induced by weight loss or improved health condition. In addition, there could be some other alteration of physiological

alterations initiated by BRS, such as hormone levels, alteration of pH levels, temperature etc, etc that could be contributed to the increased microbial diversity.

5.2 Gut Microbial Distribution and Composition Was Altered at Different Taxonomic Levels

The overall microbial taxonomy represented by the fecal microcosm in vitro was distributed amongst defined phyla, classes, orders, families, genera, and some undefined taxa. Around 99.86% of sequences belong to bacteria and 0.14% sequences belong to Archaea. The phylum was dominated by Firmicutes (70.37%), Bacteroidetes (14.40%), Actinobacteria (7.67%), Proteobacteria (5.51%), Verrucomicrobia (1.49%) and others (0.56%, including Euryarchaeota, Fusobacteria, Acidobacteria, CyanobacteriaChloroplast, Spirochaetes, Synergistetes, Gemmatimonadetes, Nitrospira, Planctomycetes, TM7, Deinococcus-Thermus, Chloroflexi, Thermotogae, Chlorobi, Deferribacteres, Armatimonadetes and unclassified).

The phylum Actinobacteria was significantly reduced, while the phylum Verrucomicrobia was significantly increased at week 52 after BRS treatment (Figure 5.2.3).

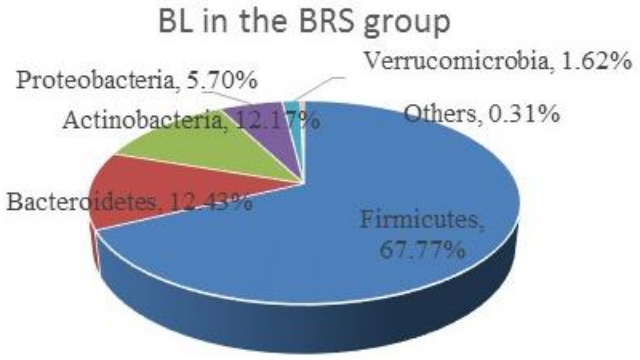

Figure 5.2.1 Phylum distribution at baseline post-BRS treatment.

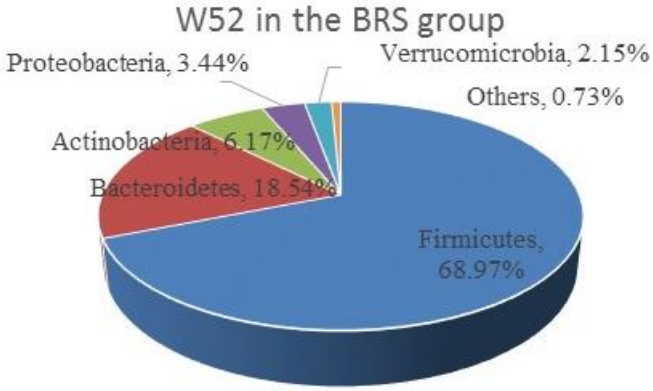

Figure 5.2.2 Phylum distribution at week 52 post-BRS treatment.

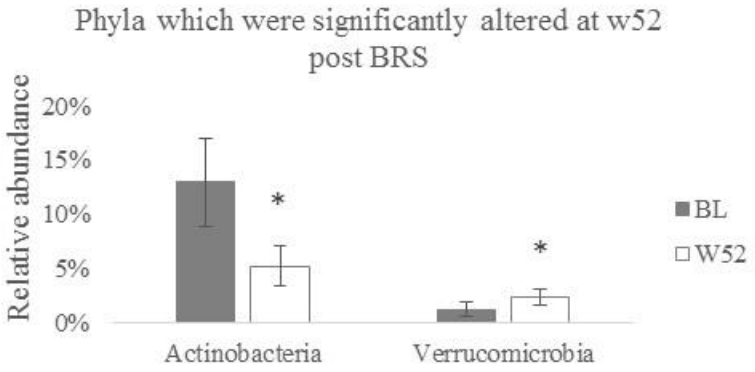

Figure 5.2.3 Phyla Actinobacteria and Verrucomicrobia were significantly altered at week 52 after BRS treatment.

It has been reported that the phylum Actinobacteria increased its relative abundance in the gut of mice fed a high-fat diet (Clarke et al., 2012). Also, it has been reported that it was higher in the gut microbiota belonging to the obese ones in the twins than the lean ones (Turnbaugh et al., 2009). Additionally, it has been reported that it was reduced after RYGB treatment (Graessler et al., 2013).

It has been reported that the obese individuals had a lower relative abundance of Verrucomicrobia (Clarke et al., 2012), and it was increased after RYGB (Liou et al., 2013). It was also reported that it was more abundant in normal-weight and post-gastric bypass individuals than the obese individuals (Zhang et al., 2009).

In addition, we observed that Proteobacteria was significantly increased from baseline mean of 6.3% (std = 14.5%) to week 7 mean of 13.1% (std = 21.5%) post BRS treatment (p = 0.0029) and this observation was consistent with the finding reported by other groups which found that Proteobacteria was enriched after RYGB in the individual's distal gut (Sweeney and Morton, 2014, Tremaroli et al., 2015).

We did not observe significant alteration of the relative abundance of any phyla at week 7 post LCD treatment. However, at week 52 post LCD treatment, we observed that phylum Firmicutes were significantly reduced, while phylum Bacteroidetes was significantly increased (Figure 5.2.6).

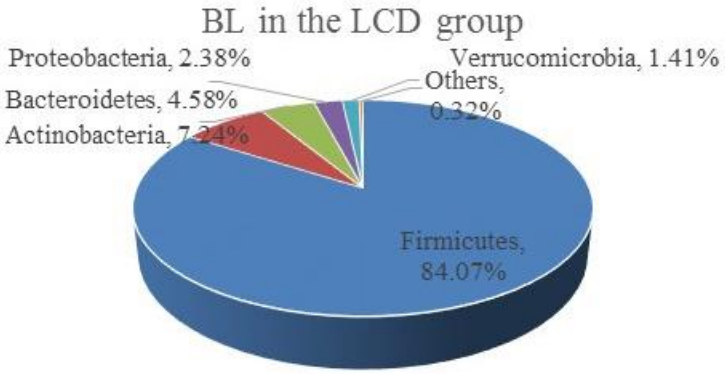

Figure 5.2.4 Phylum distribution at baseline post LCD treatment.

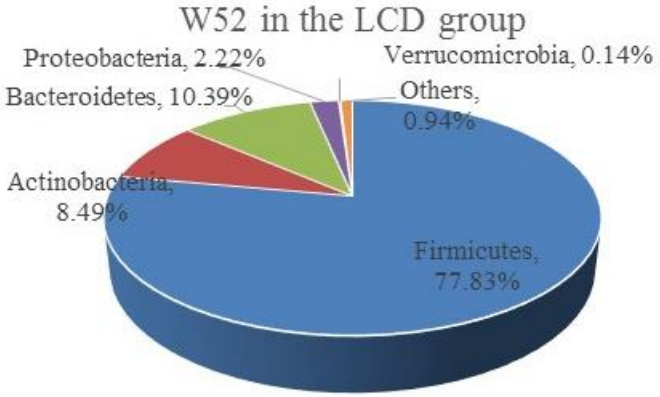

Figure 5.2.5 Phylum distribution at week 52 post LCD treatment.

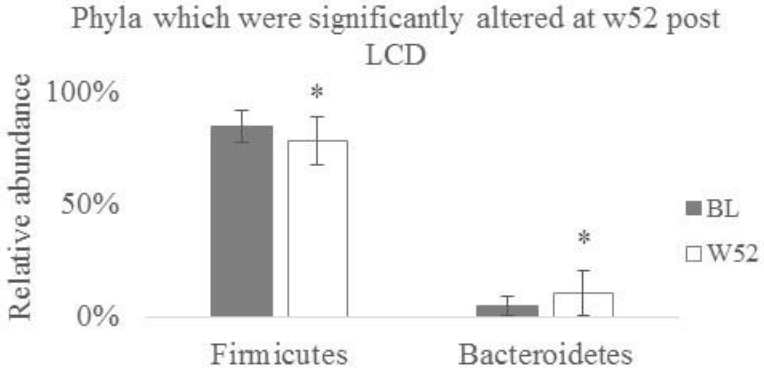

Figure 5.2.6 Phylum Firmicutes and Bacteroidetes were significantly altered at week 52 post LCD treatment.

At class level, Clostridia (60.67%) dominated, followed by Bacteroidia (14.3%), Actinobacteria (7.67%), Bacilli (5.53%), Gammaproteobacteria (4%), Erysipelotrichia (3.17%), Verrucomicrobiae (1.48%), Alphaproteobacteria (1.19%), and others (1.98%, including Negativicutes, Betaproteobacteria, Methanobacteria, Deltaproteobacteria, Fusobacteria, Flavobacteria, Sphingobacteria, Chloroplast, Spirochaetes, Synergistia, Acidobacteria Gp4, Acidobacteria Gp6, Acidobacteria Gp1, Gemmatimonadetes, Nitrospira, Planctomycetacia, Spartobacteria, Acidobacteria Gp7, Deinococci, Acidobacteria Gp3, Bacteroidetes incertae sedis, Subdivision3, Anaerolineae, Epsilonproteobacteria, Thermotogae, Acidobacteria Gp18, Acidobacteria Gp16, Deferribacteres, Holophagae, Ignavibacteria, Cyanobacteria, Acidobacteria Gp10, Acidobacteria Gp17, Methanococci, Zetaproteobacteria and unclassified).

We observed that the class Gammaproteobacteria was significantly increased at week 7 after BRS treatment, and it was consistent with the finding reported by the other group and they also found after RYGB, Gammaproteobacteria was significantly increased (Zhang et al., 2009). Also, the class Actinobacteria was significantly reduced, and Verrucomicrobiae was significantly increased at week 52 after BRS treatment.

Table 5.2.1 Class Gammaproteobacteria was significantly increased at week 7 post-BRS treatment.

BRS	Gammaproteobacteria	
Class	Mean	Std
BL	6.5%	1.51%
W7	1.14%	2.32%
Wilcoxon signed rank (*p*)	0.0273	

Table 5.2.2 Class Actinobacteria was significantly reduced, while Verrucomicrobiae was significantly increased at week 52 after BRS treatment.

BRS	Actinobacteria		Verrucomicrobiae	
Class	Mean	Std	Mean	Std
BL	12.97%	13.54%	1.21%	2.18%
W52	5.21%	6.12%	2.36%	2.35%
Wilcoxon signed rank (*p*)	0.0537		9.77E-04	

We did not a significant alteration of the relative abundance of any classes at week 7 post LCD treatment, but it was detected that at week 52, class Clostridia was significantly reduced and Deltaproteobacteria was significantly increased when comparing with the baseline level. Reduction of clostridia was reported to be correlated with weight loss.

Table 5.2.3 Classes which were significantly altered at week 52 post LCD treatment.

Class	Clostridia		Deltaproteobacteria	
LCD	BL	W52	BL	W52
Mean	76.37%	68.07%	0.06%	0.16%
Std	14.34%	18.15%	0.10%	0.30%
Wilcoxon signed rank (*p*)	0.091		0.0629	

At genus level, *Blautia* dominated (26.20%), followed by *Bacteroides* (11.82%), *Lachnospiracea incertae sedis* (8.89%), *Bifidobacterium* (4.68%), *Dorea* (3.82%), *Roseburia* (3.28%), *EscherichiaShigella* (2.84%), *Streptococcus* (2.51%), *Anaerostipes* (2.47%), *Collinsella* (2.25%), *Faecalibacterium* (2.20%), *Clostridium IV* (1.89%), *Akkermansia* (1.48%), *Alistipes* (1.14%), *Granulicatella* (1.13%), *Gemmiger* (1.12%), *Clostridium XVIII* (1.03%), and others (12.59%, including *Erysipelotrichaceae incertae sedis*, *Clostridium XlVa*, *Ruminococcus*, *Lactobacillus*, *Clostridium sensu stricto*, *Coprococcus*, *Clostridium XI*, *Parabacteroides*, *Prevotella*, *Megasphaera*, *Enterococcus*, *Lactococcus*, *Catenibacterium*, *Eggerthella*, *Pantoea*, *Haemophilus*, *Oscillibacter*, *Sporobacter*, *Dialister*, *Anaerotruncus*, *Turicibacter*, *Eubacterium*, *Mogibacterium*, *Subdoligranulum*, *Methanobrevibacter*, *Butyricicoccus*, *Dysgonomonas*, *Paraprevotella*, *Veillonella*, *Actinomyces*, *Slackia*, *Fusobacterium*, *Peptococcus*, *Flavonifractor*,

Clostridium XlVb, Barnesiella, Phascolarctobacterium, Pediococcus, Acetanaerobacterium, Coprobacillus, Lachnobacterium, Burkholderia, Gordonibacter, Sutterella, Acidaminococcus, Odoribacter, Parasutterella, Lactonifactor, Morganella, Chryseobacterium, Bilophila, Stenotrophomonas, Rothia, Succiniclasticum, Desulfovibrio, Rhodanobacter, Pseudoflavonifractor, Hespellia, Butyricimonas, Acinetobacter, Pseudoflavonifractor, Hespellia, Acinetobacter, Butyricimonas, Olsenella, Leuconostoc, Gemella, Allisonella, Thiobacillus, Clostridium III, Citrobacter, Streptophyta, Bulleidia, Enterorhabdus, Anaerosporobacter, Dyella, Tannerella, Comamonas, Howardella, Nakamurella, Tepidimonas, Holdemania, Anaerofustis, Anaerovorax, Anaerofilum, Peptostreptococcus, Pseudobutyrivibrio, Variovorax, Zoogloea, Acetitomaculum, Papillibacter, Robinsoniella, Bradyrhizobium, Atopobium, Peptoniphilus, Pseudomonas, Treponema, Lysobacter, Brevundimonas, Methyloversatilis, Delftia, Rummeliibacillus, Staphylococcus, Rhizobium, Cloacibacillus, Solobacterium, Corynebacterium, Ethanoligenens, Sphingomonas, Paracoccus, Weissella, Arsenicicoccus, Bosea, Megamonas, Methanosphaera, Acidovorax, Caulobacter, Alcaligenes, Gp6, Gp4, Caulobacter, Alcaligenes, Gp4, Gp6, Azoarcus, Clostridium XII, Anaerococcus, Finegoldia, Gemmatimonas, Methylobacterium, Lactovum, Parvimonas, Alloscardovia, Gp1, Herbaspirillum, Nitrospira, Ralstonia, Aquamicrobium, Mitsuokella, Pseudorhodoferax, Spartobacteria genera incertae sedis, Tsukamurella, Vampirovibrio, Varibaculum, Hydrogenoanaerobacterium, Solirubrobacter, Thauera, Anaerorhabdus, Xanthobacter, Limnobacter, Rudaea, Terrimonas, Gp7, Mycobacterium, Naxibacter, Paludibacter, Porphyromonas, Sphingobacterium, Sphingopyxis, TM7 genera incertae sedis, Vagococcus, Williamsia, Dechloromonas, Ensifer, Ferruginibacter, Flavisolibacter, Moryella, Pseudoxanthomonas, Singulisphaera, Syntrophococcus, Dyadobacter, Gp3, Rhodobacter, Sphingosinicella, Acetivibrio, Aeromonas, Arthrobacter, Cellulosilyticum, Mucilaginibacter, Inquilinus, Arthrobacter, Cellulosilyticum, Inquilinus, Mucilaginibacter, Ohtaekwangia, Pandoraea, Pedomicrobium, Salmonella, Subdivision3 genera incertae sedis, Auritidibacter, Cryptobacterium, Mesorhizobium, Pasteuria, Phenylobacterium, Roseomonas, Sarcina, Skermanella, Sporichthya, Thermus, Acidisoma, Anaeroglobus, Anaeromyxobacter, Aquabacterium, Bacillariophyta, Conexibacter, Devosia, Duganella, Flavobacterium, Janibacter, Labrys, Nocardioides, Petrimonas, Thermotoga, Alkaliphilus, Bacillus, Bellilinea, Blastococcus, Caldithrix, Chelatococcus, Chondromyces, Cupriavidus, Edaphobacter, Ferribacterium, Geothrix, Gp16, Gp18, Hallella, Ignavibacterium, Kaistia, Kofleria, Luteimonas, Micrococcus, Oribacterium, Oxobacter, Pedobacter, Roseateles, Steroidobacter, Thiohalophilus, Achromobacter, Abiotrophia, Steroidobacter, Thiohalophilus, Abiotrophia, Achromobacter, Actinobaculum, Aminobacter, Asticcacaulis, Brucella, Cellulomonas, Deinococcus, Denitratisoma, Desulfobulbus, Fusibacter, Gallicola, Geobacillus, GpIX, Gracilibacter, Hydrocarboniphaga, Luteibacter, Marvinbryantia, Pseudolabrys, Pseudoramibacter, Rhizomicrobium, Rhodococcus, Rhodoplanes, Rhodovulum, Rikenella, Schlegelella, Spirosoma, Streptomyces, Thiohalobacter, Actinomadura, Alicyclobacillus, Amycolatopsis, Ancylobacter, Armatimonadetes gp5, Azonexus, Azospirillum, Beijerinckia, Blastochloris, Brevibacterium,

Catenulispora, *Chitinophaga*, *Cloacibacterium*, *Curvibacter*, *Cystobacter*, *Desulfocapsa*, *Desulfuromonas*, *Dokdonella*, *Dongia*, *Enhydrobacter*, *Gardnerella*, *Gemmata*, *Geobacter*, *Globicatella*, *Gp10*, *Gp17*, *Haliangium*, *Kocuria*, *Hydrogenophaga*, *Gp17*, *Haliangium*, *Hydrogenophaga*, *Kocuria*, *Luteolibacter*, *Mariprofundus*, *Methanococcus*, *Methanothermobacter*, *Methylococcus*, *Methylomonas*, *Methylosarcina*, *Neisseria*, *Novosphingobium*, *Nubsella*, *Oxalicibacterium*, *Parascardovia*, *Parasporobacterium*, Phaeobacter, *Piscicoccus*, *Planctomyces*, *Porphyrobacter*, *Propionivibrio*, *Prosthecobacter*, *Pseudonocardia*, *Rhodoblastus*, *Rhodopseudomonas*, *Saxeibacter*, *Scardovia*, *Sediminibacter*, *Sharpea*, *Stella*, *Syntrophus*, *Terribacillus*, *Terriglobus*, *Truepera*, *Virgisporangium*, and *Zavarzinella*).

Beta-diversity measuring the dissimilarity for every pair of samples were calculated based on the incidence-based Jaccard dissimilarity index and abundance-based Bray-Curtis dissimilarity index. Then the permutational multivariate analysis of variance test (Adonis) detected the significant dissimilarity between the baseline and week 52 genus community after both BRS and LCD treatments. As shown in the two PCA plots, the distance between the baseline and week 52 groups were further than the distances within the baseline and week 52 groups. Also, it showed that most of the significantly altered genera were increased and were the ones associating with better obesity or health condition, such as *Oscillibacter* (Tims et al., 2013, Hu et al., 2015), *Desulfovibrio* (Karlsson et al., 2012), *Subdoligranulum* (Louis et al., 2016) and *Akkermansia* (Everard et al., 2013, Schneeberger et al., 2015), and were increased significantly. The number of the significantly reduced genera was much less and most of them were the ones associating with worse obesity or health conditions, such as *Arsenicicoccus* (rho = 0.4636, p = 0.0298 with GLU; rho = 0.4382, p = 0.0414 with INS; rho = 0.362, p = 0.0978 with TRIG), *Parasutterella* (Zhang et al., 2012, Yeom et al., 2016, Dao et al., 2016) and *Rudaea*. There were a few exceptions, for example, *Bifidobacterium* was significantly reduced; its reduction after gastric bypass surgery was also reported by the other group (Furet et al., 2010) and it was also reported the decreased *Bifidobacterium* species after calorie restriction treatment (Santacruz et al., 2009, Queipo-Ortuno et al., 2013).

Table 5.2.4 Dissimilarity test between the baseline and week 52 genus community in the BRS group.

BRS_genus	Adonis	
BL vs W52	F	*p*
Jaccard	1.346	0.042
Bray-Curtis	0.929	0.448

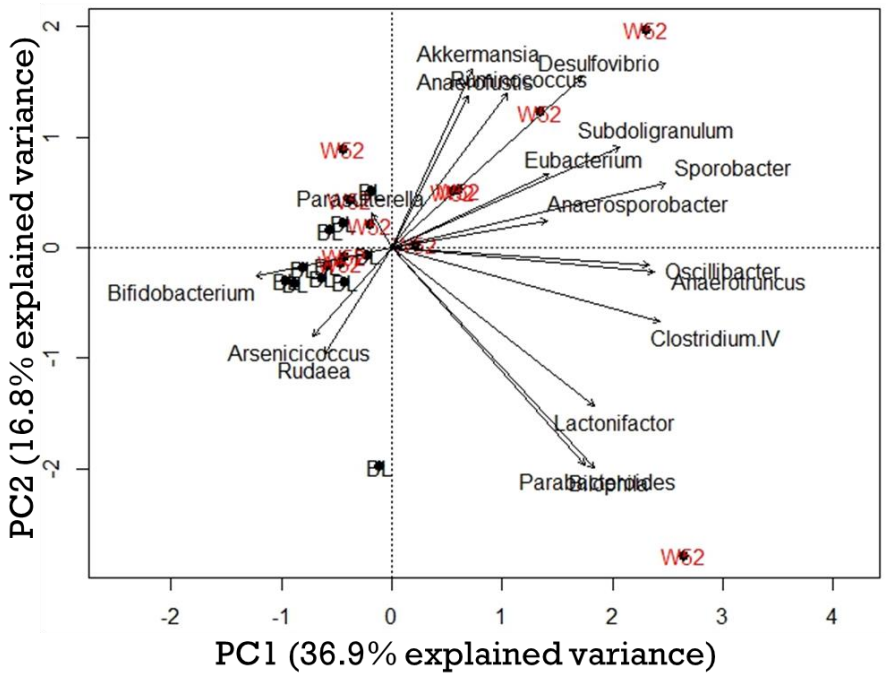

Figure 5.2.7 PCA plots for the genus community at baseline and week 52 in the BRS group.

The similar pattern was shown in the LCD group. The genus community structure at week 52 was significantly different from the genus community structure at week 52 post LCD treatment based on the dissimilarity test. Also, most of the significantly increased genera belong to commensal microbes. For example, the significantly increased genera include *Streptococcus*, wich produce lactate (Pessione, 2012), *Faecalibacterium* (Sokol et al., 2008, Machiels et al., 2014), which produces butyric acid, and *Coprococcus* which produce both butyrate and acetate, and commensal genera *Subdoligranulum* (cor = −0.3667, p = 0.0932 with TRIG; cor = −0.3958, p = 0.0683 with CHOL) and *Bilophila* (rho = −0.4592, p = 0.0316 with LDL), both of which showed significant negative correlations with obesity based on correlation tests.

Table 5.2.5 Dissimilarity test between the genus community at baseline and week 52 post LCD.

LCD_genus	Adonis	
BL vs W52	F	*p*
Jaccard	0.742	0.945
Bray-Curtis	1.735	0.095

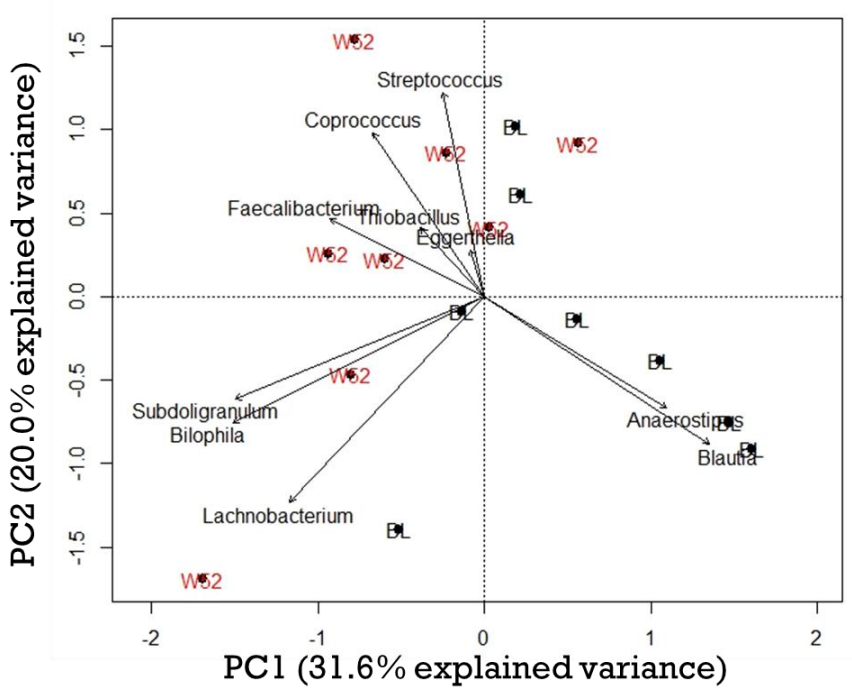

Figure 5.2.8 PCA plots for the genus community at baseline and week 52 in the LCD group.

Taken Together, it indicated that the microbial community structure at different taxonomic levels was significantly altered after both BRS and LCD treatments, and appeared to switch toward a healthier community with a higher relative abundance of beneficial microbial groups and lower relative abundance of harmful microbial groups.

5.3 Gut Microbial Community at Different Taxonomic Levels Were Significantly Correlated with Obesity-related Physiological Variables

We examined the correlation between the entire microbial community structure at different taxonomic levels and obesity-related physiological variables, using the baseline data from the combined BRS and LCD groups, with mantel test based on the Euclidean distance matrix. The result showed that the microbial community at different taxonomic levels was significantly correlated with the obesity-related variables, including subcutaneous fat size, fat mass, glucose, and hormones GLP-1, ADP, and ADPHMW (Table 5.3.1).

In addition, the partial mantel test detected that ADPHMW and subcutaneous fat size were the two main factors that were significantly correlated with the entire microbial community at OTU level (Table5.3.2).

Table 5.3.1 The correlation between the genus community at different taxonomic levels and obesity-related variables in the combined BRS and LCD groups at baseline, based on mantel test.

BRS+LCD_BL Phylum	Mantel r	Mantel *p*
GLP-1	0.50	0.014
ADPHMW	0.46	0.036
GLU	0.22	0.043
SubcutMeanSize	0.28	0.054
ADP	0.39	0.06

BRS+LCD_BL Class	Mantel r	Mantel *p*
ADPHMW	0.40	0.029
ADP	0.36	0.047
SubcutMeanSize	0.25	0.049
GLP-1	0.32	0.069
Fat mass	0.28	0.095

BRS+LCD_BL Order	Mantel r	Mantel *p*
ADPHMW	0.39	0.03
SubcutMeanSize	0.25	0.043
GLP-1	0.32	0.058
ADP	0.35	0.065
Fat mass	0.28	0.083

BRS+LCD_BL Family	Mantel r	Mantel *p*
SubcutMeanSize	0.30	0.026
ADPHMW	0.41	0.039
ADP	0.36	0.054
GLP-1	0.34	0.054

BRS+LCD_BL Genus	Mantel r	Mantel *p*
GLP-1	0.38	0.023
SubcutMeanSize	0.21	0.072
ADPHMW	0.27	0.098

BRS+LCD_BL OTU	Mantel r	Mantel *p*
ADPHMW	0.38	0.004
SubcutMeanSize	0.41	0.021
GLP-1	0.32	0.049
ADP	0.30	0.055
GLU	0.17	0.074

Table 5.3.2 The correlation between the OTU community and obesity-related variables in the combined BRS and LCD groups at baseline, based on mantel test.

OTU ADPHMW	Partial mantel r	Partial mantel *p*
ADP	0.37	0.001
GLU	0.35	0.02
GLP-1	0.33	0.034

OTU SubcutMeanSize	Partial mantel r	Partial mantel *p*
GLU	0.36	0.035
GLP-1	0.32	0.078

Table 5.2.10 The partial mantel test detected that the correlation between the entire microbial community at OTU level and ADPHMW and SubcutMeanSize were still significant when partialling out ADP, GLU, and GLP-1 respectively.

Next, to examine the correlation between microbial connectivity and obesity, we constructed the ecology association network through the random matrix theory-based methods (Deng et al., 2012) using the baseline data in the combined BRS and LCD groups at the genus

level, and it is visualized by the software Cytoscape (Figure 5.3.1). Then the mantel test was used to examine the correlation between the genus connectivity and obesity-related physiological variables, and it detected that the genus connectivity was significantly correlated with fat% and insulin (Table 5.3.3); it further confirmed the significant correlation between the entire microbial community and obesity.

Table 5.3.3 Genus connectivity was significantly correlated with fat% and INS at baseline in the combined BRS and LCD groups.

BRS+LCD_BL	Mantel	
Genus connectivity	r	*p*
Fat%	0.95	0.083
INS	0.98	0.083

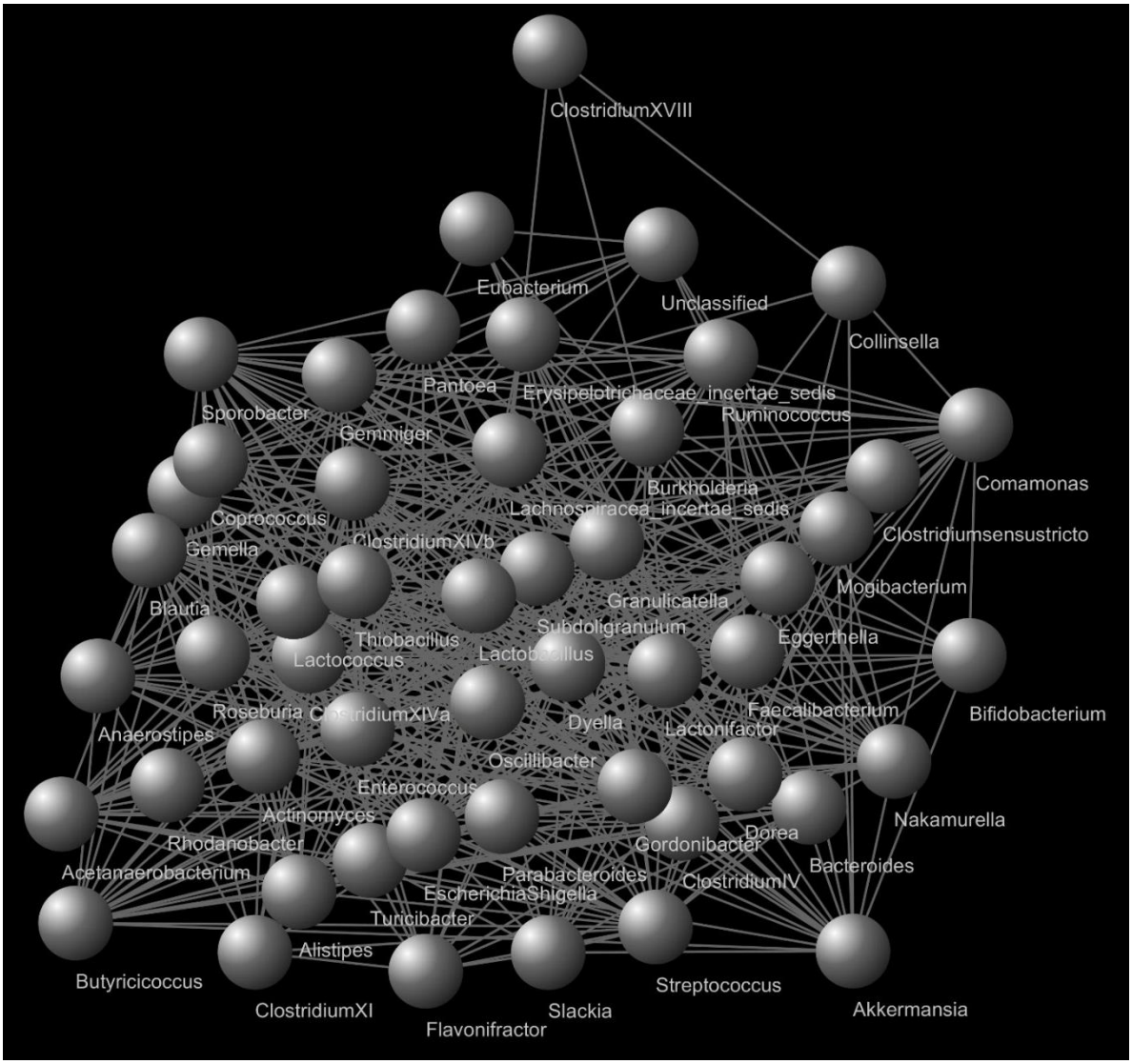

Figure 5.3.1 Ecology association network at genus level visualized by the Cytoscape software.

Taken together, it supported that the entire gut microbial community at different taxonomic levels and microbial connectivity were significantly correlated with obesity, and the hormone ADPHMW might be one of the important players that were involved in their correlation.

5.4 Microbial Functional Gene Community Structure Was Significantly Altered at Week 7 after BRS and LCD Treatments

To test the hypothesis on gene community structure, beta-diversity of the gene community structure before and after treatments were calculated for pairs of samples using Jaccard and Bray-Curtis dissimilarity indices to make the dissimilarity matrix and was then compared by the Adonis test. It showed that, at week 7 post treatments, the gene community structure was significantly altered in both treatment groups, indicating that the two treatments did have a significant effect on the gut microbial gene community structure. Also, the gene community structure of two treatment groups at week 7 also became significantly different, considering that there was no detected significance between these two groups at baseline, indicating that the effect of the alteration of the gut microbial gene community by the BRS and LCD treatments was significantly different. For example, these two treatments may have two totally different effects on the gene community, or two same effects, but the degree of the same effect was significantly different. It suggested that the underlying mechanisms for the change of gut microbial gene community after the two treatments might be significantly different.

Table 5.4.1 Gene community structure was significantly altered at week 7 after BRS and LCD treatments, and at week 7 post treatments, the BRS gene community was significantly different from the LCD group.

Gene community	Adonis		Gene community	Adonis	
BRS_BL vs W7	F	*p*	LCD_BL vs W7	F	*p*
Jaccard	1	0.08	Jaccard	2.66	0.06
Bray-Curtis	1.6	0.07	Bray-Curtis	1.53	0.18

Gene community	Adonis	
BRS vs LCD_W7	F	*p*
Jaccard	3.8	0.04
Bray-Curtis	2.35	0.07

To examine how the gene community was altered at week 7 after both BRS and LCD treatments, we compared the gene richness and diversity but did not find they were significantly altered in both groups. Then we examined the relative abundance of the gene communities under different gene categories and found that many of them were significantly altered at week 7, and this may explain the significantly altered gene community structure.

Next, we examined how the week 7 BRS group was significantly different from the week 7 LCD group, by comparing the richness and alpha diversity of the gene community. As shown in the figure, at week 7 post treatments, the gene richness in the BRS group was significantly higher, with about 2000 more genes on average, compared to the LCD group. The alpha diversity was also significantly higher in the BRS group than in the LCD group as measured by Shannon index and inversed Simpson index. It indicated that no matter what kind of mechanisms contributed to the significant alteration of the gene community structure involved in the BRS and LCD treatments, the BRS treatment had a better effect on gene community structure than the LCD group.

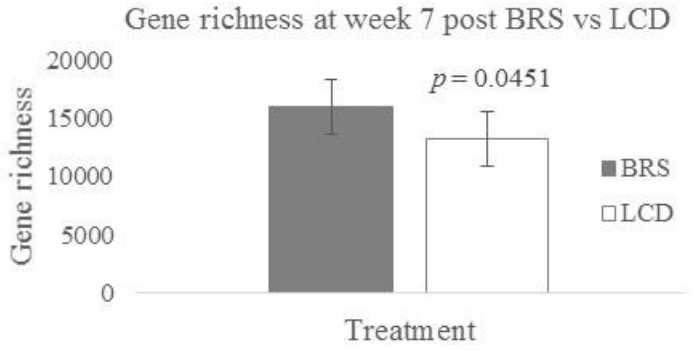

Figure 5.4.1 Gene richness was significantly higher at week 7 in the BRS group than the LCD group.

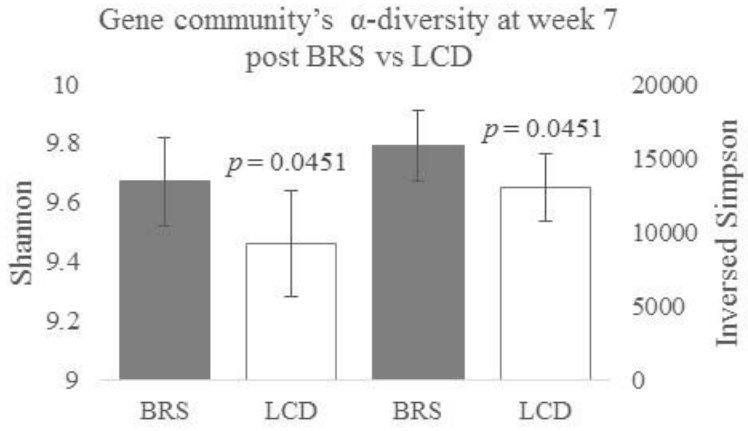

Figure 5.4.2 Gene diversity was significantly higher at week 7 in the BRS group than the LCD group.

The above results indicated that accompanying with significant obesity improvement at week 7 after both BRS and LCD treatments, the microbial functional gene community structure became significantly different from the baseline. Moreover, the functional gene community structure at week 7 was significantly different between the BRS and LCD groups, with significantly higher gene richness and gene diversity in the BRS group.

5.5 Functional Microbial Gene Community Was Significantly Correlated with Obesity-related Physiological Variables

Considering that at week 7 post treatments, the BRS group showed significantly lower levels of GHR and GHRA (Figure 5.5.1). It indicated that the significantly lower GHR and GHRA in the BRS group than the LCD group might be linked to the significantly higher microbial gene richness and diversity in the BRS group than the LCD group). Thus, we examined the correlation between gene richness and diversity, and obesity-related physiological variables by using the baseline data from the combined BRS and LCD groups, with the non-parametric spearman rank correlation test. The result showed that both gene richness and diversity were significantly negatively correlated with hunger hormone ghrelin (GHR) and its active form GHRA (Table 5.5.1 and Table 5.5.2).

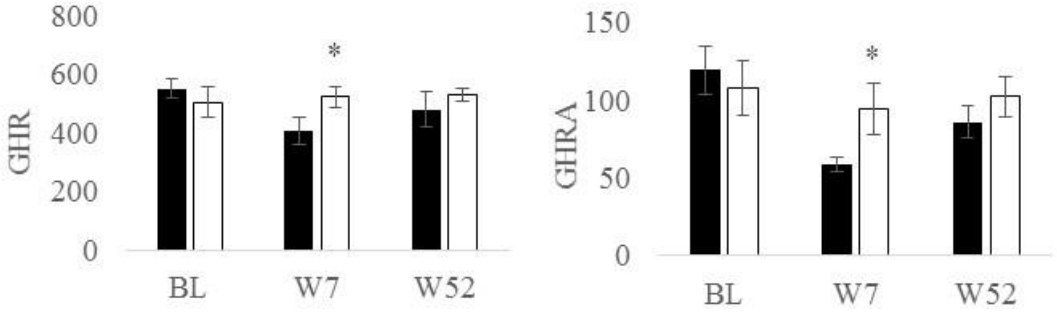

Figure 5.5.1 At week 7 post treatment, GHR and GHRA was significantly lower in the BRS group than the LCD group.

Table 5.5.1 Gene richness was significantly negatively correlated with GHRA and GHR.

Gene richness	Spearman	
BRS+LCD_BL	rho	*p*
GHRA	−0.53	0.04
GHR	−0.41	0.09

Table 5.5.2 Alpha diversity of the functional microbial gene community measured by Shannon index was significantly negatively correlated with GHRA and GHR.

Shannon	Spearman	
BRS+LCD_BL	rho	*p*
GHRA	−0.53	0.04
GHR	−0.41	0.09

Next, the correlation between the entire functional microbial gene community and physiological variables was examined by mantel test, and it showed that the entire functional

microbial gene community was significantly correlated with obesity-related hormones, including ADP, ADPHMW, and GHRA (Table 5.5.3).

Table 5.5.3 The entire microbial gene community was significantly correlated with ADP, ADPHMW, and GHRA.

Gene community	Mantel test	
BRS+LCD_BL	r	*p*
ADP	0.31	0.06
ADPHMW	0.22	0.07
GHRA	0.27	0.09

Next, mantel test was also applied to check the correlations between each gene community under different gene categories and obesity-related physiological variables, and the result showed that over half of them were shown significant correlations with obesity-related physiological variables. These gene categories showing significant correlations with obesity-related physiological variables include the gene categories involved in the metabolism of amino acid, lipid, energy, carbohydrate, glycan, cofactors and vitamins, and antibiotic resistance. We also noticed that the gene communities involved in metabolisms of short-chain fatty acids, such as acetate kinase, propionate kinase, butyrate kinase, L-lactate dehydrogenase, and acetyl-CoA acyltransferase were also significantly correlated with obesity-related variables. These results supported that functional microbial gene communities under over half of the gene categories involved in gut microbial metabolisms were significantly correlated with obesity.

5.6 Conclusions

In summary, accompanying with significant obesity improvement after the BRS and LCD treatments, microbial community structure was significantly altered. First, microbial richness and diversity were significantly increased after both treatments, with the BRS group showing a higher degree of increase of the microbial richness and diversity than the LCD group. Second, microbial distribution and compositions at different taxonomic levels were switched toward a healthier profile with increased beneficial microbial groups and reduced harmful groups. Third, the functional microbial gene community was significantly altered at week 7 after both BRS and LCD treatments, with significantly higher gene richness and gene diversity at week 7 post treatment in the BRS group than the LCD group.

In addition, the entire microbial community structure at different taxonomic levels was significantly correlated with obesity-related variables, and ADPHMW might be an important contributing factor that linked their correlation. Also, over half of the gene categories involved in gut microbial metabolisms were significantly correlated with obesity-related physiological variables, and the entire functional microbial gene community was significantly correlated with obesity-related hormones, including ADP, ADPHMW, and GHRA, with gene richness and gene diversity significantly negatively correlated with GHR and GHRA.

CHAPTER SIX: GENUS *AKKERMANSIA* WAS SIGNIFICANTLY INCREASED AFTER BARIATRIC SURGERIES AND CORRELATED WITH OBESITY

6.1 Abstract

Mechanisms underlying the weight loss effect of bariatric surgery are not fully understood. Recently, several studies suggested that *Akkermansia* may play a role in obesity in mammalian models; however, limited relevant research has been conducted in human subjects. This study aims to investigate the correlation between genus *Akkermansia* and obesity and how *Akkermansia* was involved in obesity improvement after BRS and LCD treatments. We hypothesize that the relative abundance of gut *Akkermansia* is increased after BRS treatment and associated with obesity improvement.

In the bariatric surgery participants, obesity improvement was significantly improved, and the relative abundance of gut *Akkermansia* was significantly increased at week 52 post-BRS. Significant negative correlations were observed between the relative abundance of gut *Akkermansia* and ADPHMW, PYY and fat%. Similar correlations were also seen between changes in the relative abundance of gut *Akkermansia* and changes in several obesity-related physiological variables after BRS. Significant negative correlations were shown between the change of the relative abundance of *Akkermansia* and change of weight, IDXA weight, IDXA fat mass, IDXA lean mass, BMI, 24HourEE, GLU, INS, and GHRA. Significant positive correlations were shown between the change of the relative abundance of gut *Akkermansia* and change of high-dose glucose rate (GDR2/Weight). Change in the relative abundance of *Akkermansia* was also positively correlated with percentage excess weight loss (% EWL), ADP, ADPHMW, GLP-1, and PYY.

The well-known effect of bariatric surgery to reduce body weight was paralleled by an increase in the relative abundance of gut *Akkermansia*. The significant inverse correlation between the relative abundance of gut *Akkermansia* and human obesity indicates that a decrease in weight loss caused by bariatric surgery may increase gut *Akkermansia*'s relative abundance, which may, in turn, further foster weight loss and forms a positive loop contributing to the maintenance of weight loss.

6.2 Introduction

In 2004, the *Akkermansia muciniphila* Muc^T strain was isolated from a human intestinal tract and its physical and genetical information was characterized (Derrien et al., 2004). It was reported that *Akkermansia muciniphila* Muc^T strain is non-motile, Gram-negative, strictly anaerobic, chemo-organotrophic, and mucolytic, and the cells can use mucin as a carbon, nitrogen, and energy source, and release sulfate in a free form from fermenting mucin (Derrien et al., 2004).

In 2011, based on 37 human GI tract metagenome libraries, Mark's group found that the relative abundance of *Akkermansia* (abundance of *Akkermansia's* 16S rDNA divided by the total abundance of 16S rDNA) varied from less than 0.01% to 4%, and 30% of the 37 libraries contained *Akkermansia* species shared greater than 95% similarity of the 16S rRNA gene sequence with *A. muciniphila*, and eight distinct species of the genus *Akkermansia* were discovered. They also found that *A. muciniphila*'s genome contains many mucinase-encoding gene candidates, supporting the proposed mucin-degrading capability of *Akkermansia* (van Passel et al., 2011).

Next, increasing number of studies indicate that *Akkermansia* residing in human GI tract may participate in obesity regulation. In 2013, Patrice's group reported that *A. muciniphila* abundance decreased in both genetically leptin-deficient obese mice and high-fat-fed (HF-fed) mice (Everard et al., 2013), and administration of viable *A. muciniphila* improved metabolic profile of HF-fed mice, including ameliorated diet-induced fasting hyperglycemia by a mechanism related to glucose-6-phosphatase expression shrink in liver, the indication being that there had been a reduction of gluconeogenesis, and reduced the insulin resistance index, increased the levels of adipocyte differentiation and lipid oxidation marker (but not lipogenesis markers), and offset the diminution of the mucus layer (Everard et al., 2013). The involved mechanism might include that *A. muciniphila* administration raised intestinal levels of acylglycerols, including 2-oleoylglylcerol (2-OG), 2-arachidonoylglycerol (2-AG), and 2-palmitoylglycerol (2-PG), which are involved in intestinal and glucose homeostasis, such as inflammation, gut barrier, and gut peptide secretion (Everard et al., 2013).

In 2014, the Bae's group reported that after HFD-fed mice were treated with metformin, the abundance of the mucin-degrading genus *Akkermansia* and the number of mucin-producing goblet cells was significantly increased (Shin et al., 2014). Also, administration of *Akkermansia* to HFD-fed mice without metformin treatment significantly increased glucose tolerance and attenuated adipose tissue inflammation by inducing adipose tissue-resistant CD4 Foxp3 regulatory T cells (Shin et al., 2014).

In 2014, the Roeselers's group reported that *A. muciniphila* and its metabolites propionate, modulate the levels of expression of important regulators of lipolysis, satiety, transcription factor, and cell cycle control, including Fasting-induced adipose factor (Fiaf), G protein-coupled receptor 43 (Gpr43), histone deacetylases (HDACs), and peroxisome proliferator-activated receptor gamma (Pparγ) in the intestinal epithelial organoids of mice (Lukovac et al., 2014). Dao et al. (2016) have also reported that *A. muciniphila* was related to a healthier metabolic status and better clinical outcomes after calorie restriction in overweight or obese adults (Dao et al., 2016).

Based on the above findings, we hypothesize that genus *Akkermansia* might have increased after bariatric surgeries and associated with the substantial and persistent obesity improvement after bariatric surgeries.

6.3 Genus *Akkermansia* Was Associated with Better Health Status

To examine the correlation between *Akkermansia* and obesity-related variables at baseline, we first median split the participants into the group with lower *Akkermansia* abundance and the group with higher *Akkermansia* abundance, and then the non-parametric Wilcoxon rank sum test was used to detect whether the physiological variables in these two group were significantly different, and the result showed that a number of physiological variables (weight, IDXA weight, fat mass, IDXA fat mass, lean mass, 24HourEE and HDL) showed significantly better conditions in the higher *Akkermansia* group than the lower *Akkermansia* group (Figure 6.3.1). The similar pattern was observed when the diabetic participants were not included in the analysis (Figure 6.3.2). These results indicated that the individuals whose GI tract harbored a higher relative abundance of genus *Akkermansia* had lighter obesity conditions, indicated that *Akkermansia* was associated better health condition.

In addition, the non-parametric Spearman and parametric Pearson correlation tests detected that *Akkermansia* was significantly correlated with better conditions of hormones PYY, GLP-1 and ADPHMW (Table 6.3.1). When applying the partial correlation test for checking the correlations between each hormone and *Akkermansia* when partialling out the other two factors,

these three factors still show significant correlations with *Akkermansia*, indicating that their correlations with *Akkermansia* were independent (Table 6.3.2). The similar pattern was observed when the diabetic participants were not included, but fat% replaced ADPHMW (Table 6.3.3). These results further confirmed the significant negative correlation between *Akkermansia* and obesity conditions.

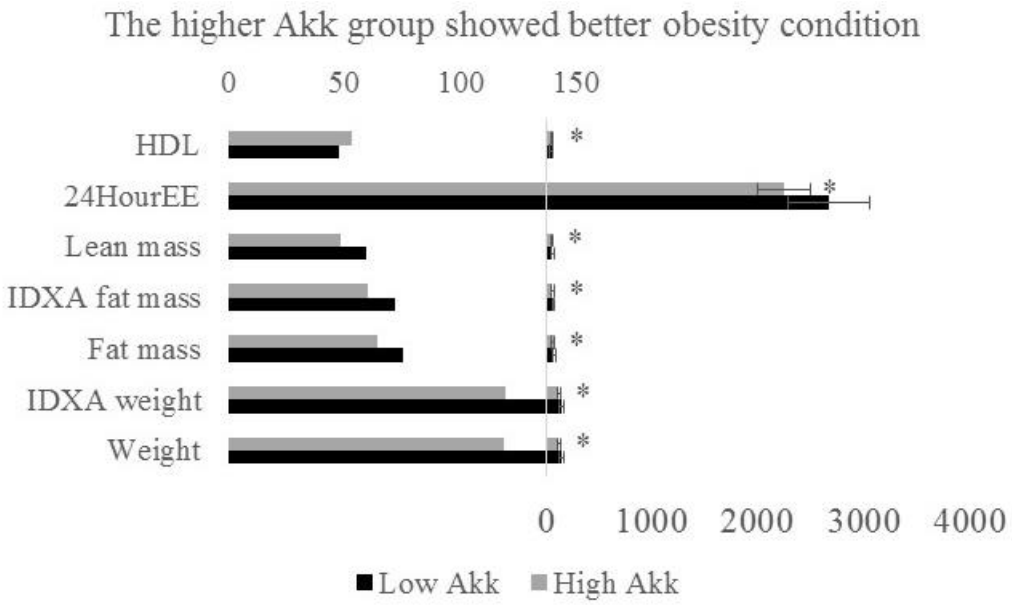

Figure 6.3.1 The higher *Akkermansia* group showed better obesity conditions. Diabetic participants were included in the analysis.

Table 6.3.1 *Akkermansia* at baseline in the combined BRS and LCD group showed significant correlation with obesity-related hormones. Diabetic participants were included in the analysis.

BL_BRS+LCD	Spearman		Pearson	
Akk	rho	*p*	cor	*p*
PYY	0.29	0.278	0.558	0.007
GLP-1	0.191	0.395	0.527	0.012
ADPHMW	0.29	0.236	0.395	0.069

Table 6.3.2 Partial correlation test showed that *Akkermansia* at baseline in the combined BRS and LCD group were significantly correlation with each hormone when controlling the other two hormones. Diabetic participants were included in the analysis.

Partial correlation		ADPHMW	PYY	GLP-1
Spearman	rho	0.3692	0.3797	−0.1237
	p	0.1091	0.0987	0.6032
Pearson	cor	0.5489	0.7077	0.4117
	p	0.0122	0.0005	0.0713

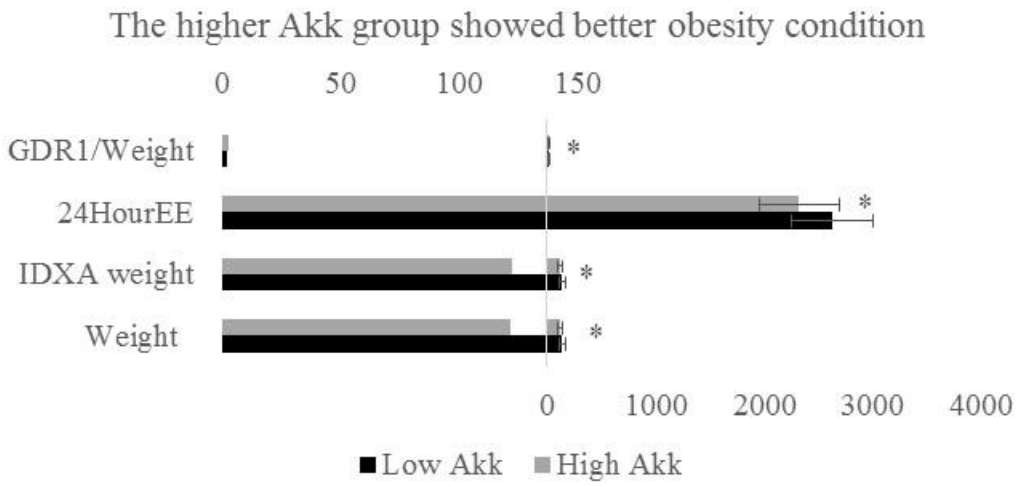

Figure 6.3.2 The higher *Akkermansia* group showed better obesity conditions. Diabetic participants were not included in the analysis.

Table 6.3.3 *Akkermansia* at baseline in the combined BRS and LCD group showed significant correlation with obesity-related hormones. Diabetic participants were not included in the analysis.

BRS+LCD_BL (No DM)	Spearman		Pearson	
Akk	rho	*p*	cor	*p*
Fat%	-0.485	0.048	-0.421	0.092
PYY	0.29	0.202	0.661	0.001
GLP-1	0.031	0.893	0.47	0.032

6.4 Genus *Akkermansia* Was Increased after BRS and Associated with Obesity Improvement

6.4.1 Genus *Akkermansia* Was Significantly Increased after BRS

Considering that the relative abundance of *Akkermansia* was not shown as normally distributed, non-parametric sign test was performed to check whether there was a significant alteration of the relative abundance of *Akkermansia* after BRS treatment. The result showed that the relative abundance of gut *Akkermansia* was significantly enhanced (p = 0.0654) from the baseline level of 1.21% (std = 2.18%) to 2.36% (std = 2.35%) at week 52 after bariatric surgeries. Meantime, we observed that weight was significantly reduced (p = 0.001) from the baseline of 132.45 kg (std = 17.95 kg) to week 52 of 89.12 kg (std = 13.61 kg).

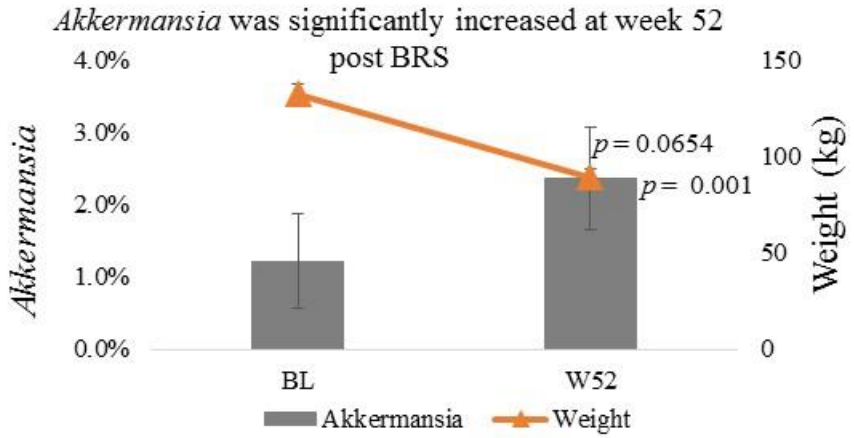

Figure 6.4.1.1 The relative abundance of *Akkermansia* (column plot) was significantly increased, accompanying with the significant weight reduction (line plot) at week 52 post-BRS. The error bars were made based on the standard errors. The sign test was used to calculate the p values.

6.4.2 Increase of *Akkermansia* after BRS Was Significantly Associated with Obesity Improvement

That the coincidence of significant weight loss after BRS and significantly increased relative abundance of *Akkermansia* suggested that there could be correlations between the relative abundance of *Akkermansia* and obesity status. Then, correlation tests were performed to check the correlations between the change of *Akkermansia* (Akk) after BRS and change of obesity-related physiological variables. The results showed that change of Akk at week 7 post-BRS was significantly positively correlated with obesity-related hormones including ADP, ADPHMW, and PYY, while significantly negatively correlated with hormone GHRA (Table 6.4.2.1), indicating the change of Akk at week 7 was associated with improvement of obesity-related hormones. Also, it showed that change of week 52 post-BRS was significantly negatively correlated with change in fasting glucose and insulin levels (Table 6.4.2.2), indicating the increase of Akk at week 52 after BRS was associated with improvement of insulin resistance.

Table 6.4.2.1 Change of *Akkermansia* during baseline and week 7 post-BRS showed significant correlations with the improvement of obesity-related hormones.

BRS_W7−BL	Spearman		Pearson	
Δ Akk	rho	*p*	cor	*p*
Δ ADP	0.38	0.31	0.76	0.02
Δ ADPHMW	0.21	0.59	0.7	0.04
Δ GHRA	−0.68	0.06	−0.51	0.19
Δ PYY	0.61	0.08	0.36	0.35

Table 6.4.2.2 Change of *Akkermansia* during baseline and week 52 post-BRS showed significant correlations with the improvement of GLU and INS.

BRS_W52−BL	Spearman	
Δ Akk	rho	*p*
Δ GLU	−0.57	0.07
Δ INS	−0.55	0.09

After combining all the changes of *Akkermansia* during baseline and week 7, during baseline and week 52, and during week 7 and week 52 post BRS, and then check their correlation with the corresponding change of obesity-related physiological variables, the result showed that the change of the relative abundance of genus *Akkermansia* was significantly negatively correlated with change in the fasting glucose level (Table 6.4.2.3) (the combination was also validated by ANCOVA tests). As shown in the regression plot (Figure 6.4.2.1), the change of *Akkermansia* after BRS was significantly negatively correlated with the change of fasting glucose level; greater increase of the relative abundance of genus *Akkermansia* after BRS, greater reduction of the fasting glucose level. It further confirmed that increase in the relative abundance of *Akkermansia* after BRS was associated with obesity improvement, and it also indicated that obesity-related hormones (ADP, ADPHMW, GHRA, and PYY) might be important factors that linked their association.

Table 6.4.2.3 The correlation between change of *Akkermansia* and change of GLU after BRS treatment.

BRS_W7−BL, W52−BL, W52−W7	Δ Akk	Δ GLU
Spearman	rho	−0.41
	p	0.03
Pearson	cor	−0.45
	p	0.02

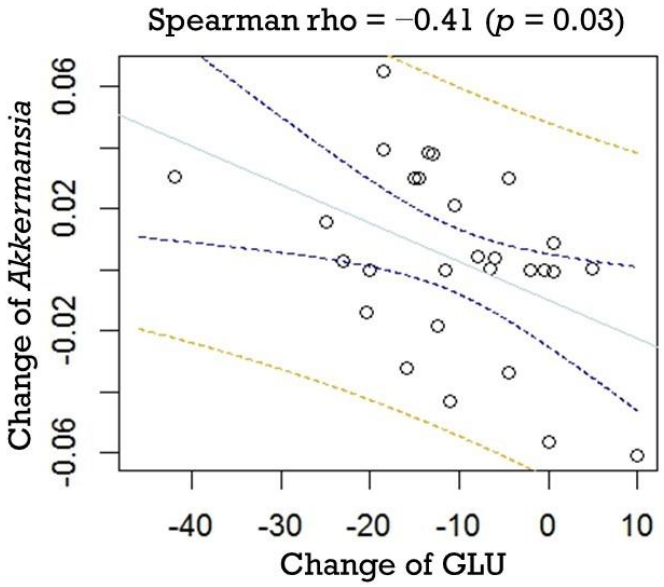

Figure 6.4.2.1 The regression plot showed that a greater increase of *Akkermansia* was associated with a greater reduction of GLU.

6.4.3 Change of *Akkermansia* Was Significantly Negatively Correlated with Change of Obesity Condition

We did not observe significant alteration of the relative abundance of genus *Akkermansia* after the LCD treatment. However, after combining the BRS and LCD groups, the change of *Akkermansia* at week 7 and week 52 still showed significant negative correlation with a change in obesity.

After median splitting the participants based on the change of the relative abundance of genus *Akkermansia*, the group with higher change of the relative abundance of genus *Akkermansia* at week 7 after BRS and LCD treatments showed significantly greater improvement of GLP-1 and PYY levels, than the group with lower change of the relative abundance of *Akkermansia* (Table 6.4.3.1). Also, the change of the relative abundance of genus *Akkermansia* at week 7 after BRS and LCD treatments showed significant positive correlations with a change of GLP-1 and PYY (Table 6.4.3.2), indicating a significant correlation between change of *Akkermansia* and improvement of obesity-related hormones at week 7 after BRS and LCD treatments.

Moreover, the group with a higher change of the relative abundance of genus *Akkermansia* at week 52 after BRS and LCD treatments showed significantly greater improvement of obesity-related physiological variables, including weight, IDXA weight, EWL, BMI, GLU, INS, GDR1/Weight, GDR2/Weight, and TRIG (Table 6.4.3.3). Also, the change of the relative abundance of genus *Akkermansia* at week 52 after BRS and LCD treatments showed significant negative correlations with change of weight, GLU, and INS, and significant positive correlation with change of GDR2/Weight (Table 6.4.3.4), indicating the significant negative correlation between change of *Akkermansia* and change of obesity condition at week 52 post BRS and LCD treatments.

Table 6.4.3.1 The group with a higher change of the relative abundance of genus *Akkermansia* at week 7 after BRS and LCD treatments showed significantly greater improvement of GLP-1 and PYY levels.

BRS & LCD	Low Δ Akk		High Δ Akk		Wilcoxon rank sum
W7−BL	Mean	Std	Mean	Std	*p*
Δ GLP-1	−0.35	0.64	0.37	0.94	0.067
Δ PYY	−21	24	17	31.14	0.032

Table 6.4.3.2 Change of *Akkermansia* during baseline and week 7 in the combined BRS and LCD groups showed significant correlation with a change of GLP-1 and PYY.

BRS & LCD_W7−BL	Spearman	
Δ Akk	rho	*p*
Δ GLP-1	0.55	0.05
Δ PYY	0.59	0.03

Table 6.4.3.3 The group with a higher change of *Akkermansia* during baseline and week 52 in the combined BRS and LCD groups showed significantly better obesity conditions.

BRS & LCD	Low Δ Akk		High Δ Akk		Wilcoxon rank sum
W52−BL	Mean	Std	Mean	Std	*p*
ΔWeight	−15	20	−45	13	0.004
Δ IDXA weight	−16	20	−40	19	0.017
EWL	32	43	69	24	0.055
Δ BMI	−6	7	−16	5	0.012
Δ GLU	−4	6	−18	11	0.004
Δ INS	−1	5	−8	8	0.079
Δ GDR1/Weight	1	2	2	1	0.059
Δ GDR2/Weight	2	3	6	3	0.009
Δ TRIG	−11	40	−61	67	0.079

Table 6.4.3.4 Change of *Akkermansia* at week 52 after BRS and LCD treatments showed significant correlation with a change of obesity condition.

BRS & LCD_W52−BL	Spearman	
Δ Akk	rho	*p*
Δ Weight	−0.49	0.039
Δ GLU	−0.66	0.002
Δ INS	−0.52	0.023
Δ GDR2/Weight	0.45	0.061

Additionally, after combination of the change of the relative abundance of *Akkermansia* during baseline and week 7, during baseline and week 52, and during week 7 and week 52 post BRS and LCD treatments, change of the relative abundance of *Akkermansia* after BRS and LCD treatments showed significant correlations with improvements of obesity-related physiological variables, including weight, BMI, and GLU (the combination was also validated by the ANOVA test). As shown in the regression plot (Figure 6.4.3.1), change of *Akkermansia* after BRS and LCD treatments was significantly negatively correlated with the change of GLU; the greater increase of the relative abundance of genus *Akkermansia*, the greater reduction of GLU after BRS and LCD treatments. It further confirmed the negative correlation between change of *Akkermansia* and change of obesity condition after BRS and LCD treatments.

Table 6.4.3.5 Change of *Akkermansia* after BRS and LCD treatments showed significant correlations with improvements obesity-related physiological variables.

BRS & LCD_W7−BL, W52−W7, W52−BL		Δ Akk	Δ Weight	Δ BMI	Δ GLU
Spearman	rho	−0.2934	−0.3044	−0.3912	
	p	0.0562	0.0472	0.0087	
Pearson	cor	−0.2524	−0.2577	−0.4027	
	p	0.1024	0.0953	0.0067	

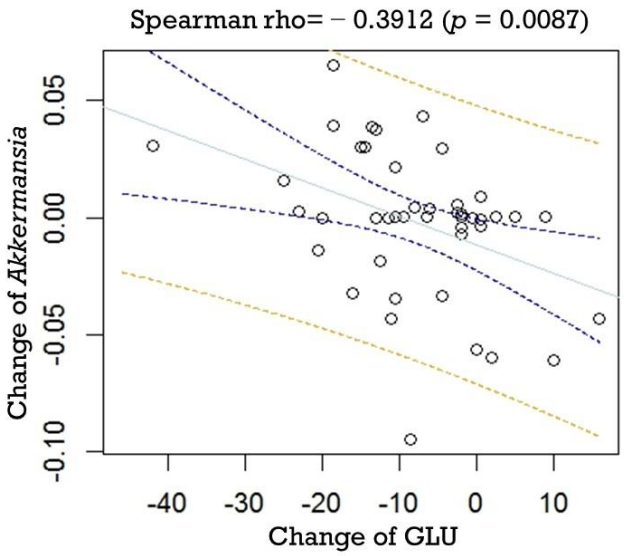

Figure 6.4.3.1 The regression plot showed the significant negative correlation between change in the relative abundance of *Akkermansia* and change of GLU after BRS and LCD treatments.

In addition, no significant difference of the obesity-related physiological variables was observed between the BRS and LCD groups at baseline, but the BRS group showed significantly more improvement of the obesity-related physiological variables, when comparing with the LCD group, including significantly more reduction of weight (p = 8.16E−06), IDXA weight (p = 2.71E−06), fat mass (p = 0.0012), IDXA fat mass (p = 0.0001), IDXA lean mass (p = 0.0194), fat% (p = 0.0001), 24HourEE (p = 0.0011), BMI (p = 8.16E−06), IDXA BMI (p = 2.72E−06), GLU (p = 0.0141), INS (p = 0.0143), TRIG (p = 0.0017), LEP (p = 0.0064) and hsCRP (p = 0.061), and significant more increase of GDR1/Weight (p = 0.0024), GDR2/Weight (p = 0.0011), HDL (p = 0.0087), ADP (p = 0.0926), and ADPHMW (p = 0.0007). Meanwhile, there was no significant difference of the relative abundance of the genus *Akkermansia* between the BRS and LCD group at baseline; however, at week 52 post treatment, the BRS group showed a significantly higher relative abundance of *Akkermansia* than the LCD group (p = 0.0059). Also, the increase of the relative abundance of the genus *Akkermansia* during baseline to week 52 in the BRS group was significantly higher than the LCD group (p = 0.0317). In short, there was no significant obesity difference between BRS and LCD group at baseline, but after treatments, the improvement of obesity and increase of relative abundance of *Akkermansia* after BRS were both significantly higher than the LCD group. It supports that significant increase of the relative abundance of genus *Akkermansia* may be involved in the substantial and persistent weight loss process induced by bariatric surgeries.

6.4.4 Other than *Akkermansia muciniphila*, There Might be Other *Akkermansia* Species Contributing to the Significant Increase of Genus *Akkermansia* after BRS

The Illumina sequencing result detected 42 different OTUs belonging to the genus *Akkermansia* using 97% nucleotide sequence similarity as the clustering threshold. It was further confirmed by using the online software nucleotide baselineAST (Basic Local Alignment Search Tool) (baselineASTN 2.5.0+) (Zhang et al., 2000) to search these 42 OTU sequences (http://blast.ncbi.nlm.nih.gov/Blast.cgi) against the database rRNA_typestrains/prokaryotic_16S_ribosomal_RNA (16S ribosomal RNA (Bacteria and Archaea)) (16S ribosomal RNA sequences from bacteria and archaea; update date: 2016/08/02; number of sequence: 18928)) for identifying them and found that the resulted top hit for all of them are *Akkermansia muciniphila strain ATCC BAA-835* 16S ribosomal RNA gene (Accession NR_074436.1) or *Akkermansia muciniphila strain Muc* 16S ribosomal RNA gene (Accession NR_042817.1), but many of their nucleotide sequence similarity were lower than 97%.

That we detected 42 *Akkermansia* OTUs in total, and most of them were altered to the same direction after BRS, indicating that the increase of genus *Akkermansia* may be also owing to the other *Akkermansia* species, besides the known species *Akkermansia muciniphila*.

6.4.5 Quantitative PCR Results Showed the Similar Patterns as the Above-mentioned Illumina Sequencing Results

The quantitative PCR result showed the similar pattern as Illumina sequencing results. At baseline, the group with a higher abundance of *Akkermansia* had significantly smaller subcutaneous fat size than the group with lower *Akkermansia* abundance (Table 6.4.5.1), and the baseline relative abundance of *Akkermansia* was significantly positively correlated with hormones ADP and ADPHMW (Table 6.4.5.2).

Table 6.4.5.1 The group with a higher abundance of genus *Akkermansia* showed significant smaller subcutaneous fat size than the group with lower *Akkermansia* abundance.

BRS+LCD_BL	SubcutMeanSize		Wilcoxon rank sum (*p*)
Low Akk	1.37	0.32	0.09
High Akk	1.11	0.31	

Table 6.4.5.2 At baseline, the relative abundance of genus *Akkermansia* showed significant positive correlations with ADP and ADPHMW.

BRS+LCD_BL	*Akkermansia*	ADP	ADPHMW
Pearson	cor	0.5	0.53
	p	0.04	0.03

In addition, the qPCR result showed that the relative abundance of genus *Akkermansia* was significantly increased at both week 7 and week 52 post BRS treatment (Figure 6.4.5.1 and Figure

6.4.5.2), and the change of *Akkermansia* after BRS showed significant correlations with the improvement of several obesity-related physiological variables, including weight, IDXA weight, IDXA fat mass, IDXA lean mass, BMI, 24HourEE, GLU, INS and GHRA (Figure 6.4.5.3). These results further confirmed the negative correlation between *Akkermansia* and obesity.

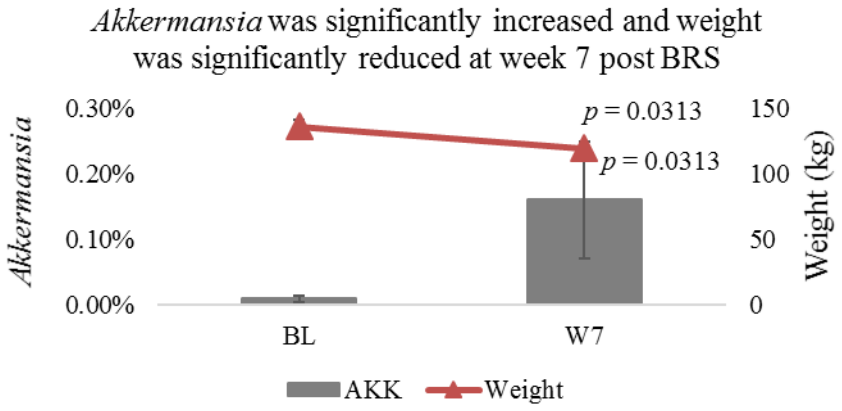

Figure 6.4.5.1 The relative abundance of *Akkermansia* was significantly increased at week 7 after BRS.

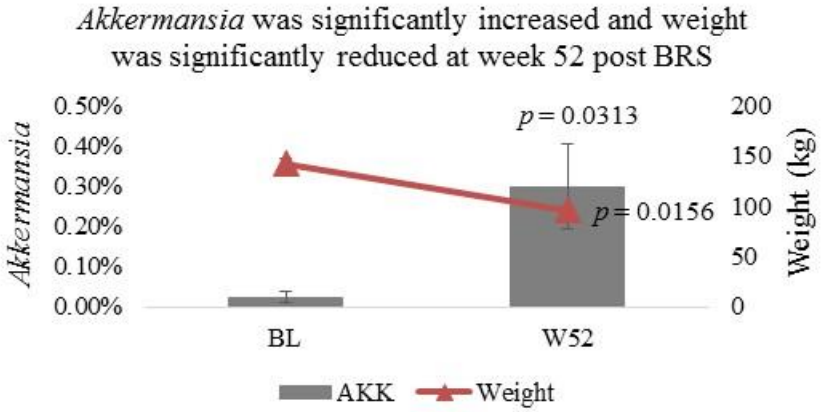

Figure 6.4.5.2 The relative abundance of *Akkermansia* was significantly increased at week 52 after BRS.

Table 6.4.5.3 Change of *Akkermansia* after BRS showed significant negative correlations of change of obesity conditions, including weight, IDXA weight, IDXA fat mass, IDXA lean mass, BMI, 24HourEE, GLU, INS, and GHRA.

BRS	Spearman		Pearson	
Δ Akk	rho	*p*	cor	*p*
Δ Weight	−0.29	0.226	−0.46	0.047
Δ IDXA weight	−0.24	0.329	−0.42	0.077
Δ IDXA fat	−0.13	0.613	−0.42	0.094
Δ IDXA lean	−0.67	0.003	−0.58	0.015
Δ BMI	−0.27	0.26	−0.47	0.042
Δ 24HourEE	−0.38	0.119	−0.41	0.093
Δ GLU	−0.23	0.336	−0.43	0.069
Δ INS	−0.72	5.26E−04	−0.65	0.003
Δ GHRA	−0.73	8.70E−04	−0.78	2.16E−04

6.5 Conclusions

In conclusion, the relative abundance of genus *Akkermansia* was significantly correlated with better health status, and it was significantly increased after the BRS, accompanying with the substantial and long-lasting effect of obesity improvement. Also, alteration of the relative abundance of *Akkermansia* was significantly negatively correlated with alterations of obesity condition, and the obesity-related hormones might be important factors that contribute to their correlation.

It indicates that bariatric surgeries may directly or indirectly cause the increase of the relative abundance of genus *Akkermansia*, which may, in turn, further boost the obesity-improving effect of BRS, forming a positive loop contributing to their persistent effects in alleviating obesity conditions. In addition, the obesity-related hormones might be involved in the correlation between *Akkermansia* and obesity. For example, *Akkermansia* might contribute to the improvement of obesity and insulin resistance after BRS treatment through improving the levels of obesity-related hormones such as ADP, ADPHMW, PYY, and GHRA.

Moreover, based on our observation of several different OTUs in the genus *Akkermansia*, we conclude that except for *Akkermansia muciniphila*, there may exist other *Akkermansia* species contributing to the increase in the relative abundance of genus *Akkermansia* after BRS.

CHAPTER SEVEN: THE AMOUNT AND CONSTITUTION OF SHORT-CHAIN FATTY ACIDS (SCFAS) WERE SIGNIFICANTLY ALTERED AFTER TREATMENTS

7.1 Abstract

Bariatric surgeries have been shown to be efficient in reducing obesity, but the underlying mechanisms have not been completely disclosed. Meanwhile, increasing evidence has shown that human gut microbiota is involved in obesity, and their metabolites, i.e., short-chain fatty acids (SCFAs), might be one of the factors that link their correlation. We hypothesize that the concentration and composition of SCFAs are altered after BRS, and may contribute to its substantial and persistent obesity alleviation effect. Here we used a microFAST™ gas chromatography (GC) to quantitate the concentrations of SCFAs and compare their levels in participants before and after BRS and LCD treatments. The result showed that the total SCFAs was significantly decreased at week 52 after both treatments, and the acetate concentration was significantly reduced at week 7 and week 52 after both BRS and LCD treatments. In addition, after BRS treatment, the percentage of acetate (the ratio of acetate concentration to total SCFAs concentration) was significantly reduced during baseline and week 7, baseline and week 52, and week 7 and week 52, respectively, while the percentage of propionate was significantly increased during week 7 and week 52 and the percentage of butyrate was significantly increased during baseline and week 52. We also identified some butyrate-producing genera and propionate-producing genera which were significantly increased after BRS and LCD treatments. These bacteria may have potential to be developed as probiotics for sustaining weight loss.

7.2 Introduction

SCFAs are saturated aliphatic organic fatty acids with fewer than 6 carbon atoms and they are mainly formed by gut microbial fermentation of carbohydrates, proteins, peptides and amino acids (Gibson et al., 1996). About 95% of SCFAs are composed of acetate (C2), propionate (C3), and butyrate (C4) with a ratio of 3:1:1 (Puddu et al., 2014). They are absorbed by the colonic mucosa and metabolized by the host to provide up to 5-10% of total energy intake in healthy individuals (Du et al., 2010); they contribute to 60-80% of the colon's energy requirement, with butyrate as the primary energy source for colonocytes. The ones that escape metabolism in the colon may enter the hepatic portal blood or be excreted with feces. It was reported that the amount of total SCFAs was significantly higher in obese human subjects than the lean counterparts. The reduced luminal pH by SCFAs may help counteract against pathogenic microbes (Alicia and Mercedes 2013), stimulate mineral absorption through increased mineral solubility (Younes et al., 1996, Coudray et al., 1997), and reduce secondary bile acid formation (Macdonald et al., 1978), which may accumulate as a result of enterohepatic circulation, leading to GI problems, such as the formation of gallstone and colonic cancer (Jason et al. 2006). Also, different SCFAs can have different physiological effects. Acetate is less metabolized in the colon and is easy to be absorbed and transported to the liver (Cook and Sellin, 1998); it is a substrate for lipogenesis and cholesterol synthesis (Wong et al., 2006). Propionate can prevent GI inflammation, lower fatty acid production in liver (Nishina and Freedland, 1990, Demigne et al., 1995) and plasma (Chen et al., 1984, DiCostanzo et al., 1999), and improve insulin resistance (Al-Lahham et al., 2010). Butyrate contributes to about 70% total energy demand of colon and can stimulate the growth of colonic

mucosa. It also showed a preventive and remedial effect in colonic diseases such as colonic ulcerative colitis and colon cancer (Canani et al., 2011), and diet-induced insulin resistance (Gao et al., 2009). In addition, propionate and butyrate can function as signaling molecules to interact with their intestinal receptors in intestinal epithelial cells, inducing the release of gut hormones GLP-1 and PYY, both of which can signal brain the feeling of satiety (Lin et al., 2012, Kuwahara, 2014). Therefore, we hypothesize that the amount and constitution of SCFAs are altered after BRS treatment, with reduced acetate and increased propionate and butyrate, and their alteration may contribute to the efficient obesity alleviation effect by bariatric surgeries.

7.3 Retention Time and Calibration Curve for Each SCFA

The retention time (RT: the time from injection to elution) for each SCFA (acetate, propionate, and butyrate) was obtained from the respective gas chromatogram after injection of the standard solution containing only one type of SCFA into the GC instrument, and the RTs are shown in table 7.3.1. Usually, the compound with a smaller molecular weight elutes out earlier than the compound with a larger molecular weight and thus has a shorter RT. The standard curve for each SCFA was produced based on 6 data sets of known concentrations and their corresponding GC peak areas of the standard solutions for each SCFA, which distributes evenly in the range that covers the measurements of the real samples. GC has different detection specificities for each SCFA, so the selected 6 sets of standard concentrations for each SCFA may not always be the same.

Table 7.3.1 Retention time for each SCFA.

SCFAs	Retention time (seconds)
Acetate	8.6
Propionate	17.5
Butyrate	22.0

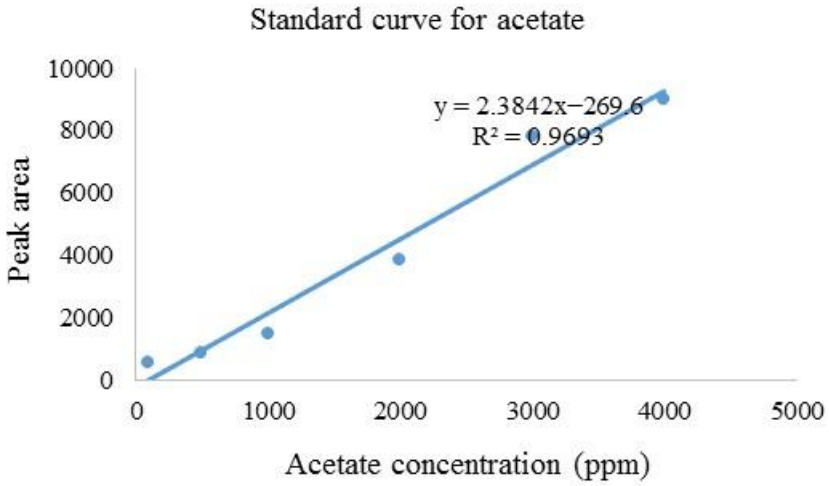

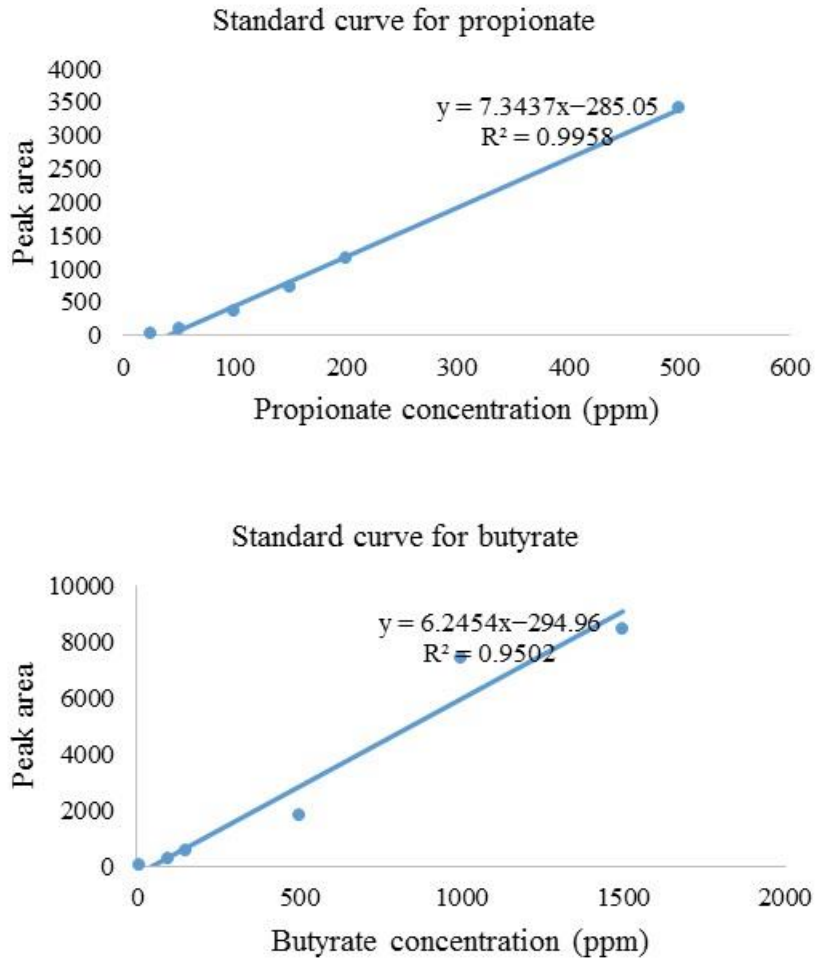

Figure 7.3.1 The calibration curve for each SCFA.

7.4 Concentrations of Total SCFAs and Acetate Were Significantly Reduced after both BRS and LCD Treatments

The total SCFAs amount in the BRS group was significantly reduced at week 52 post treatment (mean = 515.59 ppm, std = 170.21 ppm) when compared with the baseline level (mean = 737.79 ppm, std = 382.98 ppm) (p = 0.1094 by Wilcoxon signed rank test, and p = 0.0724 by paired t-test) (Figure 7.4.1). In addition, the total SCFAs amount was significantly reduced (p = 0.0781 by Wilcoxon signed rank test, and p = 0.0612 by paired t-test) at week 52 in the combined RYGB and SGx group, and it also showed the tendency to decrease at week 7 based on the observation that 6 out of 7 individuals in the combined RYGB and SGx group showed reduced total SCFA at week 7. This observation was similar to the pattern reported previously that total SCFAs tended to decrease 9 years after bariatric surgeries (Tremaroli et al., 2015). Considering that BRS treatment reduced the amount of total food intake, as well as its absorption, and the food is the main source of the gut microbial production of total SCFAs, it is reasonable that after BRS treatment the amount of total SCFAs was significantly reduced. The SCFAs extract extra energy from the indigestible and non-digested food and provide more energy to the host, and thus increase

the harvesting efficiency of the host. It has been reported that the amount of total SCFAs was positively correlated with obesity and was reduced after gastric bypass and gastric band surgeries (Tremaroli et al., 2015).

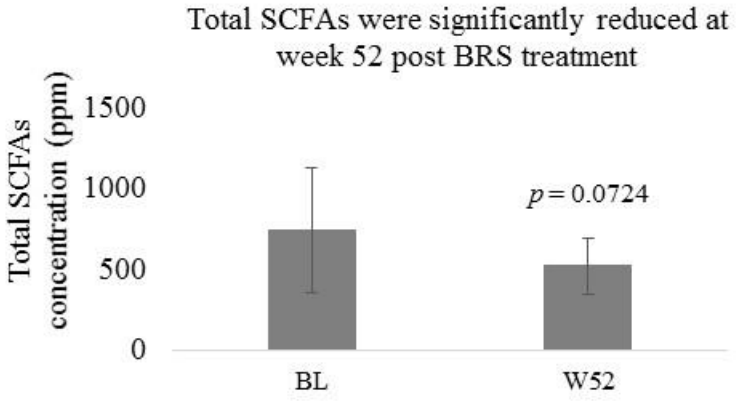

Figure 7.4.1 Total SCFAs concentration was significantly reduced at week 52 post-BRS treatment.

Similarly, there was a significant reduction of total SCFAs at week 52 post LCD treatment (mean = 474.49 ppm, std = 215.42 ppm), when compared with the baseline level (mean = 646.44 ppm, std = 286.82 ppm) (p = 0.0391 by Wilcoxon signed rank test) (Figure 7.4.2). In addition, total SCFAs in the four individuals, whose baseline and week 7 data of total SCFAs were available, were all reduced although the p values calculated by Wilcoxon signed rank and sign test were both 0.125. That the increase cannot be determined as statistically significant could be caused by the small sample size of 4. These results indicated that the LCD treatment might be associated with the reduction of the amount of total SCFAs. Since the LCD treatment reduced the total food intake of the participants and food is the main source of gut microbial production of SCFAs, it is reasonable that the amount of total SCFAs was significantly reduced after the LCD treatment.

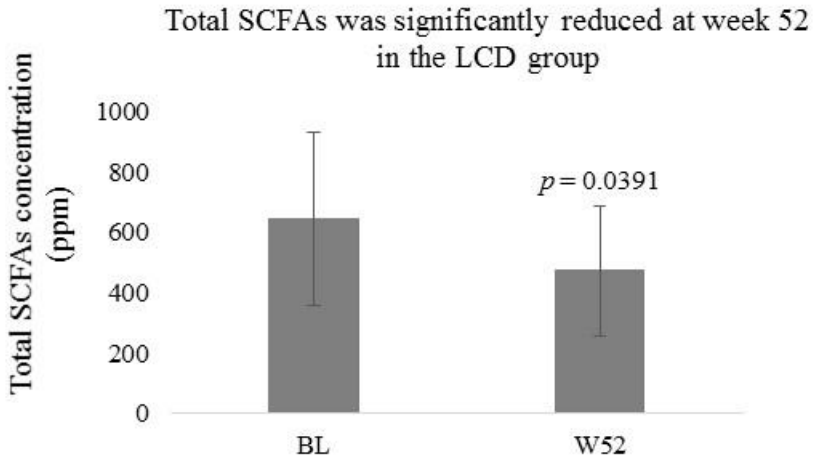

Figure 7.4.2 Total SCFAs concentration was significantly reduced at week 52 post-LCD treatment.

Given that SCFAs can supply more energy to individuals and that obese individuals have a higher total SCFAs amount than the lean group, the significantly reduced total SCFAs after both BRS and LCD treatments might have also contributed to the obesity alleviation.

Moreover, the acetate concentration of the BRS group was significantly reduced at week 7 (mean = 330.12 ppm, std = 235.16 ppm) when compared with the baseline level (mean = 452.56 ppm, std = 305.25 ppm) (p = 0.0703 by sign test) (Figure 7.4.3). The significant reduction was also observed at week 52 (mean = 191.59 ppm, std = 15.36 ppm), when compared with the week 7 level (mean = 248.28 ppm, std = 54.50 ppm) (p = 0.0469 by Wilcoxon signed rank test) (Figure 7.4.3). Significant reduction was observed at week 52 as well (mean = 195.93 ppm, std = 28.52 ppm), when compared with the baseline level (mean = 384.90 ppm, std = 283.94 ppm) (p = 0.0039 by Wilcoxon signed rank test). In summary, the results showed that acetate concentration was significantly reduced from the baseline to week 7, week 7 to week 52, and baseline to week 52 after BRS treatment. The pattern of change of acetate concentration after BRS treatment was similar to the pattern of change of obesity condition, which was significantly reduced during the three periods after BRS treatment. The results indicated that the reduced obesity after BRS might be linked to the reduced acetate concentration.

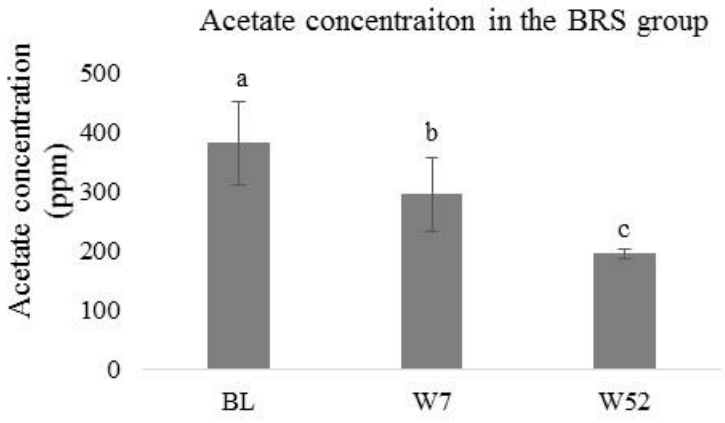

Figure 7.4.3 Acetate concentration was significantly reduced during baseline and week 7, and week 7 and week 52, and baseline and week 52 in the BRS group.

Similar to BRS, LCD significantly reduced the acetate concentration at week 7 (mean = 238.81 ppm, std = 82.87 ppm), in comparison to the baseline level (mean = 312.97 ppm, std = 89.59 ppm) (p = 0.125 by Wilcoxon signed rank test and p = 0.0713 by paired t test), as well as at week 52 (mean = 215.94 ppm, std = 62.40 ppm), when compared with the baseline level (mean = 299.42 ppm, std = 76.17 ppm) (p = 0.0078 by Wilcoxon rank sum test) (Figure 7.4.4). However, we did not observe a significant reduction of acetate concentration during week 7 and week 52 after LCD treatment. The pattern of change of acetate concentration after LCD treatment corresponded to the pattern of change of obesity condition, which was significantly reduced at week 7 and week 52 after LCD treatment, but not during week 7 and week 52, supporting that obesity improvement after LCD treatment might be linked to the reduction of acetate concentration.

Also, the pattern that there was a significant reduction of acetate concentration during week 7 and week 52 in the BRS group, but not in the LCD group, was similar to the pattern that there was a significant reduction of obesity during week 7 and week 52 in the BRS group, but not in the

LCD group, further supporting that the significant improvement of obesity was associated with the significant reduction of acetate concentration after BRS and LCD treatments.

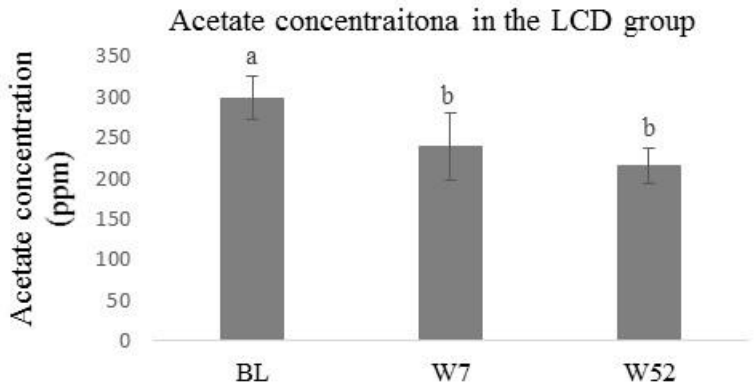

Figure 7.4.4 Acetate concentration was significantly reduced at week 7 and week 52 in the LCD group.

We did not observe a significant alteration of propionate and butyrate concentrations after BRS and LCD treatment. Considering that acetate is the main component of SCFAs and it was significantly reduced while the other two SCFAs were not significantly altered, the observed significant reduction of the total SCFAs after BRS and LCD treatments should be mainly owing to the significant reduction of acetate.

Similarly, considering that both BRS and LCD reduced the amount of the participants' food intake (and their absorption), which is the main source for gut microbial production of acetate, it is reasonable that after both treatments, acetate concentration was significantly reduced; also considering the amount the food intake during week 7 and week 52 post BRS treatment was still limited in comparison to the LCD group, it is reasonable that the concentration of acetate during week 7 and week 52 post BRS was significantly reduced, but not in the LCD group. Compared to other SCFAs, acetate is less metabolized in colon since it can be easily absorbed and transported to liver (Cook and Sellin, 1998), and once it enters the systemic circulation, it can be converted to acetyl-CoA, which is the starting material for fatty acid synthesis (Wong et al., 2006). Besides its involvement in lipogenesis, acetate is also the principal substrate for cholesterol synthesis, so its significant reduction might further contribute to the decreased adiposity post-treatment because of the decreased acetate repertory for lipogenesis. The results suggested one possible pathway that the BRS treatment induced a significant reduction of acetate concentration, which further supported the weight loss and formed a positive loop for persistent weight loss after the treatment.

Propionate and butyrate are more metabolized in the GI tract and provide energy and nutrition to the intestinal cells, and thus maintain their healthiness. If they are significantly increased, they may provide more energy to the patient, and if they are significantly reduced, the healthiness of the GI tract might be compromised. In our study, these two SCFAs were not significantly altered, so they might have helped the maintenance of the healthiness of the GI tract.

7.5 Percentage of Acetate Was Significantly Reduced after BRS treatment

The percentage of acetate was significantly reduced at week 52 post BRS treatment (mean = 53.45%, std = 14.31%), when compared with the baseline level (mean = 40.17%, std = 8.46%)

(p = 0.0547 by Wilcoxon signed rank test) (Figure 7.5.1), and it was also significantly reduced from week 7 (mean = 50.91%, std = 8.96%) to week 52 (mean = 37.54%, std = 12.50%) after BRS treatment (p = 0.0781 by Wilcoxon signed rank test) (Figure 7.5.2).

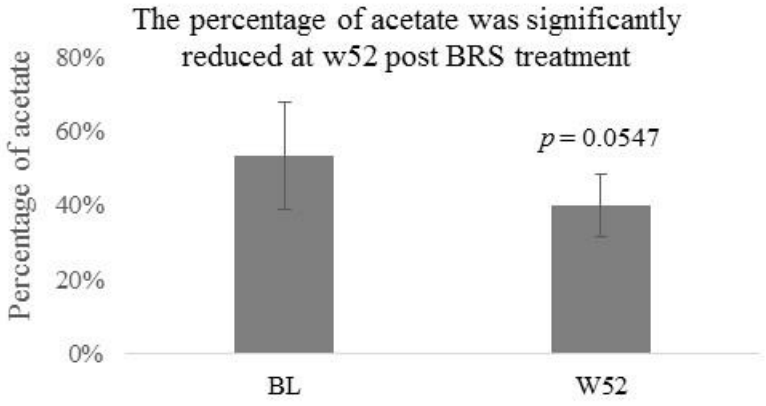

Figure 7.5.1 The percentage of acetate was significantly reduced at week 52 post-BRS treatment.

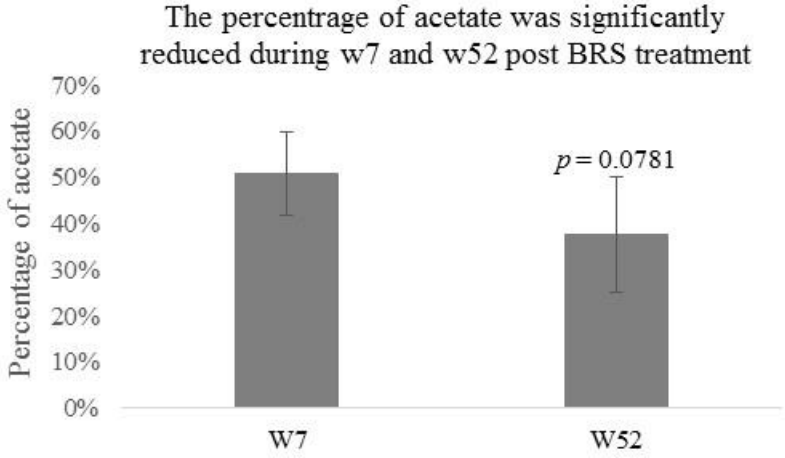

Figure 7.5.2 The percentage of acetate was significantly reduced during week 7 and week 52 post-BRS treatment.

As the above discussion on the reduction of acetate concentration, considering that acetate might not be as good as propionate and butyrate for improving obesity, the significant reduction of the percentage of acetate after BRS treatment might help further weight loss. In addition, the coincidence of the significant reduction of the relative abundance of *Bifidobacteria*, the main fermentation products of which are acetate and lactate, and the significant reduction of the relative proportion of acetate in total SCFAs indicated that one possible underlying mechanism for the weight loss effect of BRS might be that the significant decrease of the relative abundance of acetate-producing bacteria (e.g. *Bifidobacteria*) after BRS results in the significant decrease of the relative proportion of acetate in total SCFAs, which further helps weight loss.

7.6 Percentage of Propionate Was Significantly Increased during Week 7 and Week 52 after BRS treatment

We did not observe significant alteration of propionate concentration after BRS or LCD treatment. However, the percentage of propionate was significantly increased during week 7 (mean = 17.58%, std = 5.58%) and week 52 (mean = 30.25%, std = 13.35%) after BRS treatment (p = 0.0313 by Wilcoxon signed rank test) (Figure 7.6.1). That the coincidence of the significantly increased percentage of propionate and significantly reduced obesity during week 7 and week 52 post-BRS treatment indicated that the efficient and persistent obesity improvement during week 7 and week 52 after BRS treatment might be linked to the significant increase in the percentage of propionate among the total SCFAs.

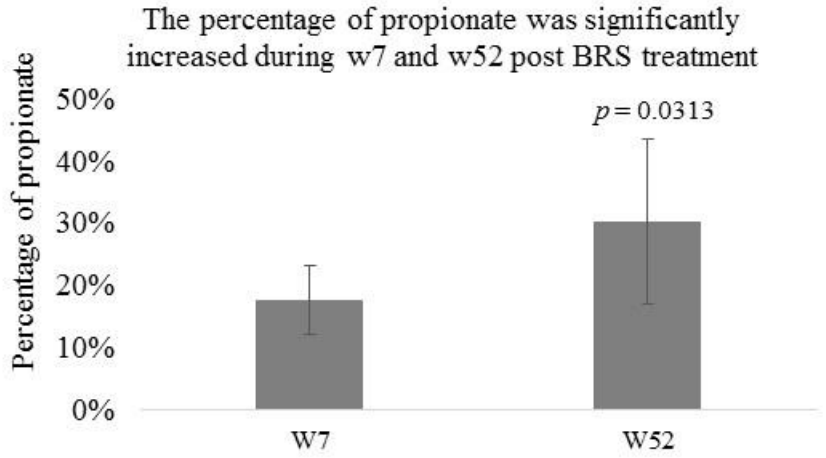

Figure 7.6.1 Propionate percentage was significantly increased during week 7 and week 52 post-BRS treatment.

Propionate has been reported to show protection against diet-induced obesity via inducing the secretion of gastrointestinal hormones that regulate satiety and inhibition of food intake in mice (Lin et al., 2012). It can also inhibit the lipogenesis from acetate in the liver and adipose tissue, which facilitates the weight loss effect of bariatric surgeries (Wolever et al., 1991). In addition, propionate is a substrate for hepatic gluconeogenesis and can inhibit cholesterol synthesis in the liver (Venter et al., 1990, Cheng and Lai, 2000). Therefore, the increased relative proportion of propionate during week 7 and week 52 post-BRS might further help weight loss during this period.

Since genus *Akkermansia* produces propionate and the significant increase in the relative abundance of genus *Akkermansia* at week 52 post-BRS treatment might have contributed to the significant increase in the relative proportion of propionate during week 7 and week 52 after BRS treatment. Thus, the possible mechanism underlying the significant weight loss after BRS might include that the BRS treatment induced significantly increased relative abundance of propionate-producing bacteria (e.g. *Akkermansia*) during week 7 and week 52, resulting in significantly increased the relative proportion of propionate, which might further help weight loss during week 7 and week 52 post BRS treatment.

7.7 Percentage of Butyrate and Relative Abundance of Butyrate-producing Genera Were Significantly Increased after BRS treatment

We did not observe significant alteration of butyrate concentration after BRS or LCD treatment. However, although there was no significant difference of the butyrate concentration between the BRS and LCD group at baseline, the butyrate concentration in the BRS group (mean = 166.74 ppm, std = 63.33 ppm) was significantly higher than the LCD group (mean = 95.80 ppm, std = 45.13 ppm) (p = 0.0582 by Wilcoxon rank sum test) at week 7 post treatments (Figure 7.7.1).

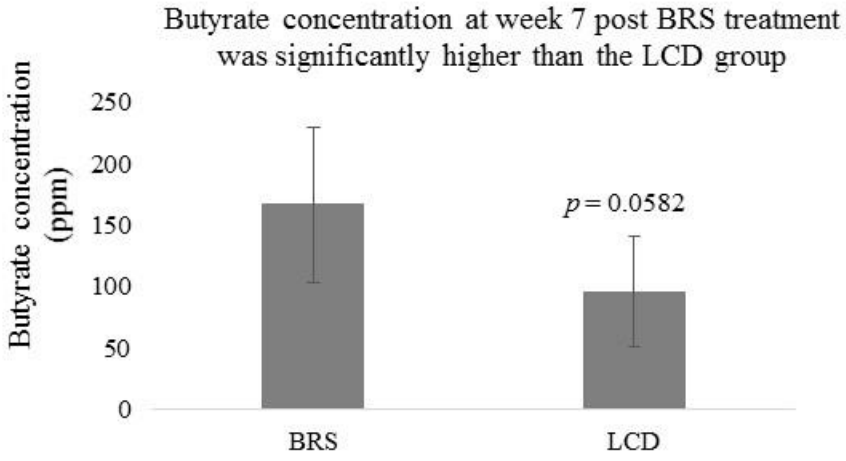

Figure 7.7.1 Butyrate concentration at week 7 post-BRS treatment was significantly higher than that in the LCD group.

Moreover, we observed that the percentage of butyrate was significantly increased at week 52 (mean = 35.79%, std = 5.74%) post BRS treatment when comparing with the baseline level (mean = 28.92%, std = 11.03%) (p = 0.0703 by Wilcoxon signed rank test) (Figure 7.7.2). That the coincidence of significantly increased of butyrate percentage among total SCFAs and significantly reduced obesity at week 52 post-BRS treatment indicated that the significant obesity improvement after BRS might be linked with the significant increase in the percentage of butyrate among the total SCFAs.

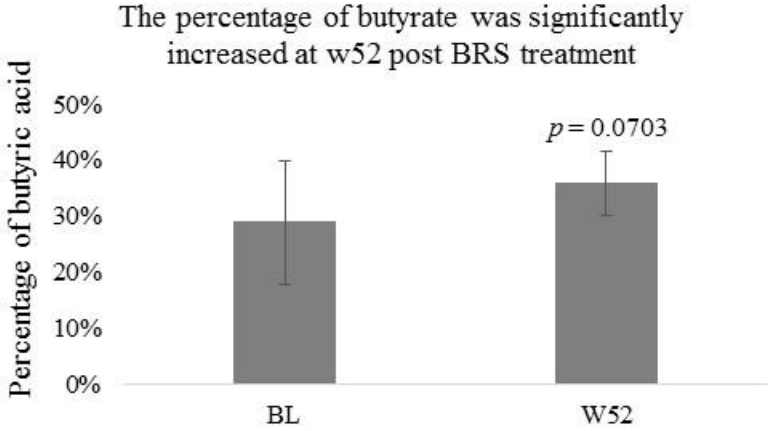

Figure 7.7.2 The percentage of butyrate was significantly increased at week 52 post-BRS treatment.

It was reported that butyrate and propionate, but not acetate, induce gastrointestinal hormones which can signal brain feeling of satiety to reduce food intake (Lin et al. 2012). Butyrate has been reported to improve insulin sensitivity and increase energy expenditure in mice (Gao et al. 2009). In addition, both propionic acid and butyric acid showed protection against diet-induced obesity via induction of gut hormones and inhibition of food intake independent of free fatty acid receptor3 (FFAR3) in mice (Lin et al., 2012).

Moreover, we found that most butyrate-producing genera were significantly increased at week 52 after BRS treatment (Figure 7.7.3), and were significantly negatively correlated with obesity based on non-parametric Spearman correlation test and/or parametric Pearson correlation test using the baseline data from the combined BRS and LCD groups. For example, *Eubacterium* was significantly negatively correlated with GLU (cor = −0.3611, p = 0.0987), LDL (rho = −0.4076, p = 0.0597) and CHOL (rho = −0.5283, p = 0.0115). *Anaerotruncus* was significantly positively correlated with GDR1/Weight (cor = 0.4136, p = 0.0557) and GDR2/Weight (cor = 0.3923, p = 0.071), *Anaerostipes* was significantly correlated with GLU (rho = −0.5123, p = 0.0148) and LEP (rho = 0.4213, p = 0.0508), and *subdoligranulum* was significantly correlated with TRIG (cor = −0.3667, p = 0.0932) and CHOL (cor = −0.3958, p = 0.0683). It indicated that the significant increase in the percentage of butyrate among total SCFAs might result from the significant increase in the relative abundance of these butyrate-producing genera.

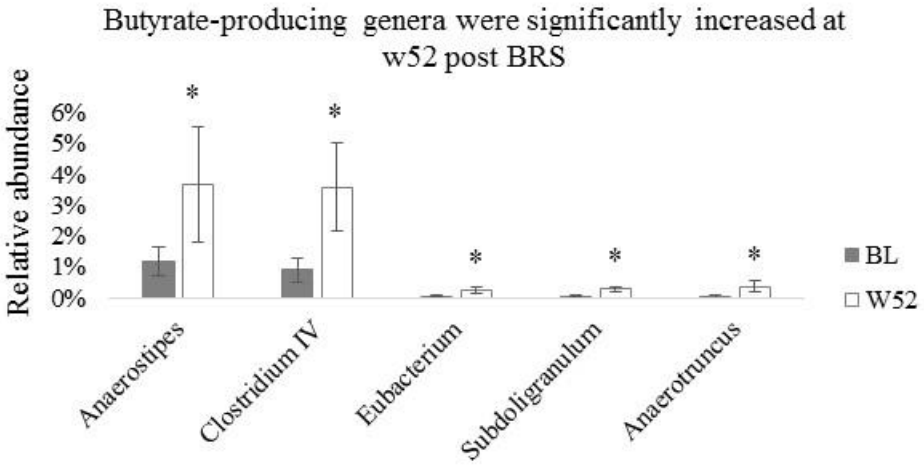

Figure 7.7.3 The relative abundance of butyrate-producing genera were significantly increased after BRS.

7.8 Functional Microbial Gene Communities Involved in Metabolism of SCFAs Were Significantly Correlated with Obesity-related Hormones

Mantel test was used to check the correlations between the gene categories involved in the metabolism of SCFAs, including acetate kinase, acetyl-CoA acyltransferase, propionate kinase, and butyrate kinase, and obesity-related physiological variables, by using the baseline data in the combined BRS and LCD group. The result showed that the SCFA-related gene communities were

significantly correlated with obesity-related hormones, including ADP, ADPHMW, PYY and GHRA (Figure 7.8.1), indicating that obesity-related hormones might be important factors that linked obesity and gut microbiota. The possible underlying mechanism could be like the loop of SCFA-producing microbes----metabolism of SCFAs----obesity-related hormones----obesity. That is, 1) SCFA-producing microbes produce SCFAs; 2) the produced SCFAs induce the alteration of obesity-related hormones; 3) the altered obesity-related hormones alter the obesity condition. In the case of BRS treatment, it is possible that BRS treatment induced the significant alteration of the SCFA profile, including the significant reduction of total SCFAs and acetate concentration, and significant reduction of the percentage of acetate, and significant increase in the percentage of propionate and butyrate, which induced the significant improvement of obesity-related hormones, (especially ADP and ADPHMW, both were significantly increased after BRS treatment), and then the significantly improved hormones (e.g. increased ADP and ADPHMW) contributed to the significant obesity improvement after BRS treatment.

Table 7.8.1 Gene communities under the gene categories involved in the metabolisms of short-chain fatty acids were significantly correlated with obesity-related hormones including ADP, ADPHMW, PYY and GHRA.

BRS & LCD_BL	Acetate kinase	ADP	ADPHMW
Mantel test	r	0.26	0.23
	p	0.08	0.08

BRS & LCD_BL	Acetyl-CoA acyltransferase	ADP	ADPHMW
Mantel test	r	0.65	0.57
	p	0.05	0.05

BRS & LCD_BL	Propionate kinase	PYY	ADPHMW
Mantel test	r	0.1	0.1
	p	0.05	0.08

BRS & LCD_BL	Butyrate kinase	PYY	GHRA
Mantel test	r	0.25	0.2
	p	0.06	0.06

7.9 Conclusions

In summary, accompanied with significant obesity improvement by BRS and LCD treatments, the concentrations of total SCFAs was significantly reduced at week 52 post both BRS and LCD treatments. Acetate concentration was significantly reduced at week 7 and week 52 after BRS and LCD treatments, and it was also significantly reduced during week 7 and week 52 after BRS treatment.

After BRS treatment, the relative proportion of acetate in total SCFAs was significantly decreased during baseline and week 52, and during week 7 and week 52, while that of propionate was significantly increased during week 7 and week 52 and that of butyrate was significantly

increased during baseline and week 52. This phenomenon was not observed in the LCD group. In addition, after BRS treatment, the relative abundance of butyrate-producing genera was significantly enhanced.

Moreover, the gene communities involved in the metabolism of SCFAs were significantly correlated with obesity-related hormones, including ADP, ADPHMW, PYY and GHRA.

CHAPTER EIGHT: DISCUSSIONS

Microbial richness and diversity were significantly increased after both treatments. Like all healthy ecosystems, a higher diversity of gut microbiota structure characterizes the healthy status, and a loss of diversity is linked to disease status. The microbial increased richness and diversity may indicate that the microbial community structure and the host's health status become healthier after the treatments. It was reported that fasting induces an increase of microbial diversity (Remely et al., 2015). It is likely that the reduction of calorie intake after both BRS and LCD treatments lowered the food sources of the originally dominating microbial groups, making the abundance of each microbial component became evener. Also, the significant improvement of obesity after these two weight-loss treatments might have improved the patients' entire physiological conditions, especially the gastrointestinal physiological conditions, and the improved physiological variables may allow the growth of more different types of microbes. A healthy ecosystem usually has mild conditions that allow various types of organisms to live in the system, while the extreme environmental conditions (e.g. pH, temperature, etc.) usually only allow the growth of specific microbial groups. As we have observed, more types of genera were significantly increased, and only a few genera were significantly reduced. This indicates that the total richness of the genera was increased, which was in agreement with the statistical tests. In addition, the significantly improved physiological conditions after bariatric surgeries may support the growth of the beneficial microbes more than the growth of the harmful microbes. As we observed, most of the significantly increased genera were commensal microbes. The degree of the increase of the microbial richness and diversity was greater in the BRS group than in the LCD group, and this pattern was consistent with the greater obesity improvement occurred in the BRS group, further confirming that higher microbial richness and diversity was correlated with better health conditions.

The distribution and composition of the microbial community at different taxonomic levels were switched toward a healthier profile with more beneficial microbes and less harmful microbes. For example, it has been reported that the phylum Actinobacteria was increased in the high-fat-fed mice and it was higher in the obese ones in the twins than the lean ones (Turnbaugh et al., 2009), and it was reduced after RYGB. The relative abundance of Actinobacteria was also significantly reduced after BRS in our research. Also, it has been reported that obese individuals had lower relative abundance of phylum Verrucomicrobia (Clarke et al., 2012) and it was increased after RYGB (Liou et al., 2013), and it was also more abundant in normal-weight and post-RYGB individuals than the obese individuals (Zhang et al., 2009). The phylum Verrucomicrobia was significantly increased at week 52 after BRS treatment in our study. We did not observe significant alterations of other phyla at week 52 after BRS, indicating that, when compared with the baseline level, the week 52 microbial community was switched to a healthier profile with significantly increased beneficial phylum Verrucomicrobia and significantly reduced harmful phylum Actinobacteria after BRS. Phylum Firmicutes dominates the gut microbiota in most human populations and has been found to associate with obesity. After each meal, its abundance increases more than the abundance of other phyla. The increased availability of incoming food may increase the abundance of this phylum and lead to more energy intake and adipose formation in the host. High-calorie food is also related to the increased Firmicutes abundance, and it was reported that Firmicutes was significantly reduced in individuals after RYGB (Zhang et al., 2009). The Firmicutes/Bacteroidetes ratio is greater in obese than normal people (Abdallah Ismail et al., 2011). In addition, the significantly reduced phylum Firmicutes and significantly increased Bacteroidetes

at week 52 post LCD treatment indicated that at the phylum level the microbial community became healthier after the LCD treatment. The gut microbiota structure became healthier after both treatments, but the pattern was not totally the same, indicating that the involved mechanism in the BRS and LCD groups might be different. Their changing pattern was not totally the same at other taxonomic levels, either. For example, at the genus level, the community structure at week 52 post both treatments became significantly different than the baseline level; however, the only a few genera were significantly altered in both treatments. Additionally, it seems that the degree of the change of the gut microbiota toward a healthier profile was higher in the BRS group than the LCD group. For example, nearly all the known butyrate-producing genera were significantly increased and showed significantly negative correlation with obesity, and the propionate-producing genus, *Akkermansia*, was also significantly increased.

Microbial functional gene community was significantly altered at week 7 after both treatments, but not at week 52 post treatments, while the change of the host's physiological conditions (especially the GI tract's physiological condition) was more substantial at week 7 for both BRS and LCD groups and the obesity improvement was more significant at week 52 post both treatments. These observations suggest that the microbial functional gene community might be mostly correlated with the change of the GI tract's physiological condition. The entire microbial functional gene community contains the gene categories (143 in total in this research) involved in all kinds of metabolic processes, and not all of the 143 gene categories are significantly involved in obesity condition. Thus, the significant alteration of the GI tract's environmental conditions at week 7 and week 52 after BRS was associated with the significantly altered entire gene community. The relative abundance of some gene categories and gene communities under different gene categories were significantly altered at week 7 and week 52 post treatments and they may have correlated with the significant alteration of obesity conditions after the treatments. After week 52, the physiological condition was not as extreme as at week 7 and this may explain why the significant alteration of the entire gene community structure was observed. Having no significant alteration of the entire gene community might also display the resilience of human microbiota.

Total SCFAs and acetate were significantly reduced after both treatments. It has been reported that total SCFAs were positively correlated with obesity possibly because they can provide more energy. The significantly reduced SCFAs after the two weight-loss treatments might have reduced the amount of the total energy that the host can obtain and thus help their weight loss. As mentioned previously, the acetate was the main component of the total SCFAs and it was harmful to obesity, so its significant reduction might have contributed to the significant reduction of total SCFAs and benefited the weight loss process, considering that no significant alteration of the concentrations of the propionate and butyrate was observed.

The significantly reduced proportion of acetate and significantly increased proportion of propionate and butyrate after bariatric surgeries indicate that the SCFA profile after bariatric surgeries becomes healthier for obesity, considering that in general acetate is harmful to obesity, while propionate and butyrate are beneficial to health status. This shifted profile of the SCFAs was not observed in the LCD group, and it may have contributed to the more substantial obesity improvement after BRS treatment compared to the LCD group.

That the relative abundance of most butyrate-producing genera was significantly increased after BRS may explain the source of the significantly increased proportion of the butyrate. *Akkermansia* is one of the propionate-producing genera and the significant increase of its relative abundance may explain the source of the significantly increased proportion of the propionate. Also, the significant reduction of the relative abundance of the genus *Bifidobacteria*, the main

fermentation products of which are acetate and lactate, may explain the significant reduction in the proportion of the acetate after the bariatric surgeries.

The gene communities relevant to the metabolisms of short-chain fatty acids were significantly correlated with obesity-related hormones (ADP, ADPHW, PYY and GHRA), indicating the possible pathway that links SCFAs and obesity. That is, the SCFAs might induce the alteration of obesity-related hormones, which further exert their functions in regulating adiposity. For example, it has been reported that butyrate can stimulate the gene expression of adiponectin, which is associated with AMPK (Adiponectin-induced AMP-activated protein kinase or Adenosine monophosphate-activated protein) that monitors the energy status of the cell and stimulates fatty acid oxidation.

The degree of the change in gut microbiota community was higher in the BRS group than in the LCD group, including the greater degree of the increase of microbial richness and diversity and beneficial microbes, such as genus *Akkermansia* and butyrate-producing genera, and the greater gene richness and diversity, and the healthier profile of their metabolites SCFAs that include greater degree of acetate reduction and better SCFA composition (significantly reduced proportion of acetate and increased proportions of propionate and butyrate). Considering that the degree of the obesity improvement effect of BRS was also greater than the LCD group, the difference in the degree of the change of the gut microbial community structure and the profile of their metabolites, SCFAs, may either be caused by the different mechanisms that drive the change of the gut microbial community, or by use of the same/similar mechanism with different degrees of change, or by a mix of the two.

In addition, the microbial community structure at different taxonomic levels and the microbial connectivity showed significant correlations with obesity, and it seemed that ADPHMW was an important factor involved in their correlation. Moreover, over half of the gene communities under different types of gene categories showed significant correlations with obesity-related variables and the entire gene community was significantly correlated with obesity-related hormones (ADP, ADPHMW, and GHRA), with gene richness and diversity significantly negatively correlated with GHR and GHRA. The gene communities relating to the metabolism of SCFAs also showed significant correlations with obesity-related hormones, including ADP, ADPHMW, PYY and GHRA). These findings together suggest that the obesity-related hormones may be the factors involved in the link between gut microbiota and obesity. Studies have reported the involvement of GLP-1, PYY, and GHR, but very few have evidenced the link between gut microbiota and obesity via ADP or ADPHMW.

CHAPTER NINE: CONCLUSIONS

After bariatric surgeries and low-calorie diet treatment, the gut microbial community structure and function were significantly altered. The changes included significantly increased microbial diversity, altered microbial distribution and composition toward a healthier profile with significantly increased commensal microbes (for example, the genus *Akkermansia* and the butyrate-producing genera) and reduced harmful microbes, altered microbial functional gene community, and the altered amount and composition of the gut microbial metabolites SCFAs, with significantly reduced concentrations of total short-chain fatty acids and acetate.

The degree of the change in the gut microbiota community after BRS was higher compared with the LCD group, including the greater degree of the increase of microbial richness and diversity, greater degree of the increase of the relative abundance of beneficial microbes, such as genus *Akkermansia* and butyrate-producing genera, greater gene richness and diversity, and healthier profiles of their metabolites SCFAs, including greater degree of acetate reduction, better SCFA composition (significantly reduced proportion of acetate and significantly increased proportions of propionate and butyrate). Also, the reduction of the acetate concentration after BRS was more efficient and persistent compared with the LCD treatment, and the significant reduction of the proportion of acetate was observed during baseline to week 7, week 7 to week 52 and baseline to week 52 after BRS treatment, but not in the LCD group. The significant increase of the proportion of propionate was only observed during week 7 to week 52 after BRS treatment, and not in the LCD group, and the significant increase of the proportion of butyrate was only observed at week 52 after BRS treatment, and not in the LCD group. These results indicated that the BRS treatment had better effects in improving the gut microbial community's healthiness, including the microbial richness and diversity, microbial functional gene richness and diversity, and the amount and composition of the microbial metabolites than the LCD group. This corresponded to the more significant obesity and health improvement effects of the BRS treatment when compared to the LCD treatment. The difference in the degree of the change of the gut microbial community structure and the profile of their metabolites, SCFAs, may either be caused by the different mechanisms that drive the change of the gut microbial community, or by the same/similar mechanism with different degrees of change, or by a mix of the two.

Our results supported that the increased microbial richness and diversity was linked to the improved obesity condition, and the greater increased microbial richness and diversity was linked to the greater improved obesity condition in the severely obese subjects. The distribution and composition of microbial community were switched toward a healthier profile with a significantly lower relative abundance of phylum Actinobacteria, and significantly higher relative abundance of phylum Verrucomicrobia at week 52 post-BRS treatment, and significantly lower relative abundance of the phylum Firmicutes, and a significant increase of phylum Bacteroidetes after low-calorie diet treatment. Microbial functional gene community structure was significantly altered at week 7, accompanying with the more significant alteration of the GI tract's physiological conditions.

In addition, based on the baseline data combined from the both BRS and LCD groups, we found that the entire microbial communities at different taxonomical levels were significantly correlated with obesity-related physiological variables, and the hormone ADPHMW and might be an important factor that links the significant correlation between the entire microbial community and obesity, at OTU level. Also, the microbial connectivity also showed significant correlations with obesity, suggesting that microbes with higher connectivity were significantly correlated with

obesity, supporting the significant correlation between the topology of the microbial association network and obesity and further confirming the significant correlation between the microbial community structure and obesity. The relative abundance of many genera (or other taxonomic microbial groups) also showed significant correlations with obesity-related physiological variables, further supporting the involvement of gut microbes in the obesity condition. Moreover, over half of the gene communities under different gene categories showed significant correlations with obesity-related physiological variables, further confirming the significant correlation between microbial community and obesity, and supporting the involvement of microbial genes in the host's obesity conditions. In addition, the entire gene community was significantly correlated with obesity-related hormones, ADP, ADPHMW, and GHRA, and the richness and diversity of the entire gene community were significantly negatively correlated with GHR and GHRA, suggesting these obesity-related hormones might be the factors that linked the significant correlation between gut microbiota and obesity.

Additionally, this research discovered that the *Akkermansia*'s relative abundance was significantly increased after bariatric surgeries, and there was a significant reverse nexus between human gut *Akkermansia*'s relative abundance and obesity condition. It indicates that bariatric surgeries may directly or indirectly increase gut *Akkermansia*'s relative abundance, which may, in turn, further boost the obesity-alleviating effect of bariatric surgeries, forming a positive loop that contributes to their persistent effects in improving obesity conditions. *Akkermansia* may have the potential to serve as a physiological indicator of obesity status and be developed as a supplement for the prevention and/or treatment of obesity and obesity-related complexities.

REFERENCES

ABBOTT, C. R., MONTEIRO, M., SMALL, C. J., SAJEDI, A., SMITH, K. L., PARKINSON, J. R., GHATEI, M. A. & baselineOOM, S. R. 2005. The inhibitory effects of peripheral administration of peptide YY(3-36) and glucagon-like peptide-1 on food intake are attenuated by ablation of the vagal-brainstem-hypothalamic pathway. *Brain Res,* 1044**,** 127-31.

ABDALLAH ISMAIL, N., RAGAB, S. H., ABD ELBAKY, A., SHOEIB, A. R., ALHOSARY, Y. & FEKRY, D. 2011. Frequency of Firmicutes and Bacteroidetes in gut microbiota in obese and normal weight Egyptian children and adults. *Arch Med Sci,* 7**,** 501-7.

AHN, S. J., COSTA, J. & EMANUEL, J. R. 1996. PicoGreen quantitation of DNA: effective evaluation of samples pre- or post-PCR. *Nucleic Acids Res,* 24**,** 2623-5.

AL-LAHHAM, S. H., PEPPELENBOSCH, M. P., ROELOFSEN, H., VONK, R. J. & VENEMA, K. 2010. Biological effects of propionic acid in humans; metabolism, potential applications and underlying mechanisms. *Biochim Biophys Acta,* 1801**,** 1175-83.

ANDERSON, M. J. 2001. A new method for non-parametric multivariate analysis of variance. *Austral Ecology,* 26**,** 32-46.

ANDREW, C. G., HANNA, W., LOOK, D., MCLEAN, A. P. & CHRISTOU, N. V. 2006. Early results after laparoscopic Roux-en-Y gastric bypass: effect of the learning curve. *Can J Surg,* 49**,** 417-21.

ARRIETA, M. C. & FINLAY, B. B. 2012. The commensal microbiota drives immune homeostasis. *Front Immunol,* 3**,** 33.

BACKHED, F., DING, H., WANG, T., HOOPER, L. V., KOH, G. Y., NAGY, A., SEMENKOVICH, C. F. & GORDON, J. I. 2004. The gut microbiota as an environmental factor that regulates fat storage. *Proceedings of the National Academy of Sciences of the United States of America,* 101**,** 15718-15723.

BAE, H. S., HOU, A. X., MARTIN, R. J., ZHOU, J. & KEENAN, M. J. 2009. Molecular Characterization of Gut Micro-flora of Mice Fed Dietary Resistant Starch. *Faseb Journal,* 23.

BEAUMONT, W. 1977. Nutrition Classics. Experiments and observations on the gastric juice and the physiology of digestion. By William Beaumont. Plattsburgh. Printed by F. P. Allen. 1833. *Nutr Rev,* 35**,** 144-5.

BECCUTI, G. & PANNAIN, S. 2011. Sleep and obesity. *Curr Opin Clin Nutr Metab Care,* 14**,** 402-12.

BECK, C. & SCHLÖGL, F. 1993. *Thermodynamics of chaotic systems: an introduction.* , Cambridge University Press.

BEGON, M. T., C. R., HARPER, J. L. 2006. *Ecology: From individuals to ecosystems. (4th ed.),* Blackwell.

BEHARY, P. & MIRAS, A. D. 2015. Food preferences and underlying mechanisms after bariatric surgery. *Proc Nutr Soc,* 74**,** 419-25.

BELACHEW, M., LEGRAND, M. J., DEFECHEREUX, T. H., BURTHERET, M. P. & JACQUET, N. 1994. Laparoscopic adjustable silicone gastric banding in the treatment of morbid obesity. A preliminary report. *Surg Endosc,* 8**,** 1354-6.

BIAGINI, J. & KARAM, L. 2008. Ten years experience with laparoscopic adjustable gastric banding. *Obes Surg,* 18**,** 573-7.

BINLADEN, J., GILBERT, M. T. P., BOLLBACK, J. P., PANITZ, F., BENDIXEN, C., NIELSEN, R. & WILLERSLEV, E. 2007. The Use of Coded PCR Primers Enables High-Throughput Sequencing of Multiple Homolog Amplification Products by 454 Parallel Sequencing. *Plos One,* 2.

BJORKHOLM, B., BOK, C. M., LUNDIN, A., RAFTER, J., HIBBERD, M. L. & PETTERSSON, S. 2009. Intestinal microbiota regulate xenobiotic metabolism in the liver. *PLoS One,* 4**,** e6958.

BORG, C. M., LE ROUX, C. W., GHATEI, M. A., baselineOOM, S. R., PATEL, A. G. & AYLWIN, S. J. 2006. Progressive rise in gut hormone levels after Roux-en-Y gastric bypass suggests gut adaptation and explains altered satiety. *Br J Surg,* 93**,** 210-5.

BOTTIGLIERI, T. 1996. Folate, vitamin B12, and neuropsychiatric disorders. *Nutr Rev,* 54**,** 382-90.

BOUCHER, F., HANDRIGAN, G. A., MACKROUS, I. & HUE, O. 2015. Childhood obesity affects postural control and aiming performance during an upper limb movement. *Gait Posture,* 42**,** 116-21.

BRETHAUER, S. A., AMINIAN, A., ROMERO-TALAMAS, H., BATAYYAH, E., MACKEY, J., KENNEDY, L., KASHYAP, S. R., KIRWAN, J. P., ROGULA, T., KROH, M., CHAND, B. & SCHAUER, P. R. 2013. Can diabetes be surgically cured? Long-term metabolic effects of bariatric surgery in obese patients with type 2 diabetes mellitus. *Ann Surg,* 258**,** 628-36; discussion 636-7.

BUCHWALD, H., ESTOK, R., FAHRBACH, K., BANEL, D., JENSEN, M. D., PORIES, W. J., BANTLE, J. P. & SLEDGE, I. 2009. Weight and type 2 diabetes after bariatric surgery: systematic review and meta-analysis. *Am J Med,* 122**,** 248-256 e5.

BUCKERIDGE, K. M., BANERJEE, S., SICILIANO, S. D. & GROGAN, P. 2013. The seasonal pattern of soil microbial community structure in mesic low arctic tundra. *Soil Biology & Biochemistry,* 65**,** 338-347.

BUETER, M., MIRAS, A. D., CHICHGER, H., FENSKE, W., GHATEI, M. A., baselineOOM, S. R., UNWIN, R. J., LUTZ, T. A., SPECTOR, A. C. & LE ROUX, C. W. 2011. Alterations of sucrose preference after Roux-en-Y gastric bypass. *Physiol Behav,* 104**,** 709-21.

CAESAR, R., FAK, F. & BACKHED, F. 2010. Effects of gut microbiota on obesity and atherosclerosis via modulation of inflammation and lipid metabolism. *J Intern Med,* 268**,** 320-8.

CANANI, R. B., COSTANZO, M. D., LEONE, L., PEDATA, M., MELI, R. & CALIGNANO, A. 2011. Potential beneficial effects of butyrate in intestinal and extraintestinal diseases. *World J Gastroenterol,* 17**,** 1519-28.

CANNON, W. B. & WASHBURN, A. L. 1993. An explanation of hunger. 1911. *Obes Res,* 1**,** 494-500.

CAPORASO, J. G., LAUBER, C. L., COSTELLO, E. K., BERG-LYONS, D., GONZALEZ, A., STOMBAUGH, J., KNIGHTS, D., GAJER, P., RAVEL, J., FIERER, N., GORDON, J. I. & KNIGHT, R. 2011. Moving pictures of the human microbiome. *Genome Biol,* 12**,** R50.

CHANG, Y., RYU, S., SUH, B. S., YUN, K. E., KIM, C. W. & CHO, S. I. 2012. Impact of BMI on the incidence of metabolic abnormalities in metabolically healthy men. *Int J Obes (Lond),* 36**,** 1187-94.

CHEN, J. & HUANG, X. F. 2015. High fat diet-induced obesity increases the formation of colon polyps induced by azoxymethane in mice. *Ann Transl Med,* 3**,** 79.

CHEN, Q., ZHUANG, H. & LIU, Y. 2012. The association between obesity factor and esophageal caner. *J Gastrointest Oncol,* 3**,** 226-31.

CHEN, W. J., ANDERSON, J. W. & JENNINGS, D. 1984. Propionate may mediate the hypocholesterolemic effects of certain soluble plant fibers in cholesterol-fed rats. *Proc Soc Exp Biol Med,* 175**,** 215-8.

CHENG, H. H. & LAI, M. H. 2000. Fermentation of resistant rice starch produces propionate reducing serum and hepatic cholesterol in rats. *J Nutr,* 130**,** 1991-5.

CHENNA, R., SUGAWARA, H., KOIKE, T., LOPEZ, R., GIBSON, T. J., HIGGINS, D. G. & THOMPSON, J. D. 2003. Multiple sequence alignment with the Clustal series of programs. *Nucleic Acids Res,* 31**,** 3497-500.

CLARKE, K. R. 1993. Nonparametric Multivariate Analyses of Changes in Community Structure. *Australian Journal of Ecology,* 18**,** 117-143.

CLARKE, S. F., MURPHY, E. F., NILAWEERA, K., ROSS, P. R., SHANAHAN, F., O'TOOLE, P. W. & COTTER, P. D. 2012. The gut microbiota and its relationship to diet and obesity: new insights. *Gut Microbes,* 3**,** 186-202.

CLEMENT, K., VAISSE, C., LAHLOU, N., CABROL, S., PELLOUX, V., CASSUTO, D., GOURMELEN, M., DINA, C., CHAMBAZ, J., LACORTE, J. M., BASDEVANT, A., BOUGNERES, P., LEBOUC, Y., FROGUEL, P. & GUY-GRAND, B. 1998. A mutation in the human leptin receptor gene causes obesity and pituitary dysfunction. *Nature,* 392**,** 398-401.

COLLADO, M. C., ISOLAURI, E., LAITINEN, K. & SALMINEN, S. 2010. Effect of mother's weight on infant's microbiota acquisition, composition, and activity during early infancy: a prospective follow-up study initiated in early pregnancy. *Am J Clin Nutr,* 92**,** 1023-30.

CONSORTIUM, T. H. 2012. Structure, function and diversity of the healthy human microbiome. *Nature* 486**,** 207-214.

COOK, S. I. & SELLIN, J. H. 1998. Review article: short chain fatty acids in health and disease. *Aliment Pharmacol Ther,* 12**,** 499-507.

COUDRAY, C., BELLANGER, J., CASTIGLIA-DELAVAUD, C., REMESY, C., VERMOREL, M. & RAYSSIGNUIER, Y. 1997. Effect of soluble or partly soluble dietary fibres supplementation on absorption and balance of calcium, magnesium, iron and zinc in healthy young men. *Eur J Clin Nutr,* 51**,** 375-80.

CRYAN, J. F. & DINAN, T. G. 2012. Mind-altering microorganisms: the impact of the gut microbiota on brain and behaviour. *Nat Rev Neurosci,* 13**,** 701-12.

CUMMINGS, J. H. & MACFARLANE, G. T. 1997. Role of intestinal bacteria in nutrient metabolism. *JPEN J Parenter Enteral Nutr,* 21**,** 357-65.

DAMMS-MACHADO, A. & MITRA, S. 2015. Effects of surgical and dietary weight loss therapy for obesity on gut microbiota composition and nutrient absorption. 2015**,** 806248.

DAO, M. C., EVERARD, A., ARON-WISNEWSKY, J., SOKOLOVSKA, N., PRIFTI, E., VERGER, E. O., KAYSER, B. D., LEVENEZ, F., CHILLOUX, J., HOYLES, L., CONSORTIUM, M. I.-O., DUMAS, M. E., RIZKALLA, S. W., DORE, J., CANI, P. D. & CLEMENT, K. 2016. Akkermansia muciniphila and improved metabolic health during a dietary intervention in obesity: relationship with gut microbiome richness and ecology. *Gut,* 65**,** 426-36.

DARAKI, V., GEORGIOU, V., PAPAVASILIOU, S., CHALKIADAKI, G., KARAHALIOU, M., KOINAKI, S., SARRI, K., VASSILAKI, M., KOGEVINAS, M. & CHATZI, L. 2015. Metabolic profile in early pregnancy is associated with offspring adiposity at 4 years of age: the Rhea pregnancy cohort Crete, Greece. *PLoS One,* 10**,** e0126327.

DE LA SERRE, C. B., ELLIS, C. L., LEE, J., HARTMAN, A. L., RUTLEDGE, J. C. & RAYBOULD, H. E. 2010. Propensity to high-fat diet-induced obesity in rats is associated with changes in the gut microbiota and gut inflammation. *American Journal of Physiology-Gastrointestinal and Liver Physiology,* 299**,** G440-G448.

DELGADO, J., BARRANCO, P. & QUIRCE, S. 2008. Obesity and asthma. *J Investig Allergol Clin Immunol,* 18**,** 420-5.

DEMIGNE, C., MORAND, C., LEVRAT, M. A., BESSON, C., MOUNDRAS, C. & REMESY, C. 1995. Effect of propionate on fatty acid and cholesterol synthesis and on acetate metabolism in isolated rat hepatocytes. *Br J Nutr,* 74**,** 209-19.

DENG, Y., JIANG, Y. H., YANG, Y., HE, Z., LUO, F. & ZHOU, J. 2012. Molecular ecological network analyses. *BMC Bioinformatics,* 13**,** 113.

DENG, Y., Z. **HE,** J. D. VAN NOSTRAND, AND J. ZHOU 2008. Design and analysis of mismatch probes for long oligonucleotide microarrays. *BMC Genomics,* 9**,** 491.

DERRIEN, M., VAUGHAN, E. E., PLUGGE, C. M. & DE VOS, W. M. 2004. Akkermansia muciniphila gen. nov., sp nov., a human intestinal mucin-degrading bacterium. *International Journal of Systematic and Evolutionary Microbiology,* 54**,** 1469-1476.

DIBAISE, J. K., ZHANG, H., CROWELL, M. D., KRAJMALNIK-BROWN, R., DECKER, G. A. & RITTMANN, B. E. 2008. Gut microbiota and its possible relationship with obesity. *Mayo Clin Proc,* 83**,** 460-9.

DICOSTANZO, A., WILLIAMS, J. E. & KEISLER, D. H. 1999. Effects of short- or long-term infusions of acetate or propionate on luteinizing hormone, insulin, and metabolite concentrations in beef heifers. *J Anim Sci,* 77**,** 3050-6.

DIMITRIADIS, E., DASKALAKIS, M., KAMPA, M., PEPPE, A., PAPADAKIS, J. A. & MELISSAS, J. 2013. Alterations in gut hormones after laparoscopic sleeve gastrectomy: a prospective clinical and laboratory investigational study. *Ann Surg,* 257**,** 647-54.

DING, S., CHI, M. M., SCULL, B. P., RIGBY, R., SCHWERBROCK, N. M., MAGNESS, S., JOBIN, C. & LUND, P. K. 2010. High-fat diet: bacteria interactions promote intestinal inflammation which precedes and correlates with obesity and insulin resistance in mouse. *PLoS One,* 5**,** e12191.

DIRKSEN, C., DAMGAARD, M., BOJSEN-MOLLER, K. N., JORGENSEN, N. B., KIELGAST, U., JACOBSEN, S. H., NAVER, L. S., WORM, D., HOLST, J. J., MADSBAD, S., HANSEN, D. L. & MADSEN, J. L. 2013. Fast pouch emptying, delayed small intestinal transit, and exaggerated gut hormone responses after Roux-en-Y gastric bypass. *Neurogastroenterol Motil,* 25**,** 346-e255.

DIXON, A. F., DIXON, J. B. & O'BRIEN, P. E. 2005. Laparoscopic adjustable gastric banding induces prolonged satiety: a randomized blind crossover study. *J Clin Endocrinol Metab,* 90**,** 813-9.

DIXON, J. B., O'BRIEN, P. E., PLAYFAIR, J., CHAPMAN, L., SCHACHTER, L. M., SKINNER, S., PROIETTO, J., BAILEY, M. & ANDERSON, M. 2008. Adjustable gastric banding and conventional therapy for type 2 diabetes: a randomized controlled trial. *JAMA,* 299**,** 316-23.

DOBBINS, M., DECORBY, K. & CHOI, B. C. 2013. The Association between Obesity and Cancer Risk: A Meta-Analysis of Observational Studies from 1985 to 2011. *ISRN Prev Med,* 2013**,** 680536.

DORE, J., SIMREN, M., BUTTLE, L. & GUARNER, F. 2013. Hot topics in gut microbiota. *United European Gastroenterology Journal,* 1**,** 311-318.

DU, H. D., VAN DER A, D. L., BOSHUIZEN, H. C., FOROUHI, N. G., WAREHAM, N. J., HALKJAER, J., TJONNELAND, A., OVERVAD, K., JAKOBSEN, M. U., BOEING, H., BUIJSSE, B., MASALA, G., PALLI, D., SORENSEN, T. I. A., SARIS, W. H. M. & FESKENS, E. J. M. 2010. Dietary fiber and subsequent changes in body weight and waist circumference in European men and women. *American Journal of Clinical Nutrition,* 91**,** 329-336.

DWASS, M. 1957. Modified Randomization Tests for Nonparametric Hypotheses. *Annals of Mathematical Statistics,* 28**,** 181-187.

ECKBURG, P. B., BIK, E. M., BERNSTEIN, C. N., PURDOM, E., DETHLEFSEN, L., SARGENT, M., GILL, S. R., NELSON, K. E. & RELMAN, D. A. 2005. Diversity of the human intestinal microbial flora. *Science,* 308**,** 1635-8.

ECKEL, R. H., KAHN, S. E., FERRANNINI, E., GOLDFINE, A. B., NATHAN, D. M., SCHWARTZ, M. W., SMITH, R. J., SMITH, S. R., ENDOCRINE, S., AMERICAN DIABETES, A. & EUROPEAN ASSOCIATION FOR THE STUDY OF, D. 2011. Obesity and type 2 diabetes: what can be unified and what needs to be individualized? *Diabetes Care,* 34**,** 1424-30.

EKNOYAN, G. 2006. A history of obesity, or how what was good became ugly and then bad. *Adv Chronic Kidney Dis,* 13**,** 421-7.

ESTEBAN VARELA, J. & NGUYEN, N. T. 2015. Laparoscopic sleeve gastrectomy leads the U.S. utilization of bariatric surgery at academic medical centers. *Surg Obes Relat Dis,* 11**,** 987-90.

EVERARD, A., BELZER, C., GEURTS, L., OUWERKERK, J. P., DRUART, C., BINDELS, L. B., GUIOT, Y., DERRIEN, M., MUCCIOLI, G. G., DELZENNE, N. M., DE VOS, W. M. & CANI, P. D. 2013. Cross-talk between Akkermansia muciniphila and intestinal epithelium controls diet-induced obesity. *Proceedings of the National Academy of Sciences of the United States of America,* 110**,** 9066-9071.

EVERARD, A., LAZAREVIC, V., DERRIEN, M., GIRARD, M., MUCCIOLI, G. G., NEYRINCK, A. M., POSSEMIERS, S., VAN HOLLE, A., FRANCOIS, P., DE VOS, W. M., DELZENNE, N. M., SCHRENZEL, J. & CANI, P. D. 2011. Responses of gut microbiota and glucose and lipid metabolism to prebiotics in genetic obese and diet-induced leptin-resistant mice. *Diabetes,* 60**,** 2775-86.

EVERARD, A., MATAMOROS, S., GEURTS, L., DELZENNE, N. M. & CANI, P. D. 2014. Saccharomyces boulardii administration changes gut microbiota and reduces hepatic steatosis, low-grade inflammation, and fat mass in obese and type 2 diabetic db/db mice. *MBio,* 5**,** e01011-14.

FABBRINI, E., SULLIVAN, S. & KLEIN, S. 2010. Obesity and nonalcoholic fatty liver disease: biochemical, metabolic, and clinical implications. *Hepatology,* 51**,** 679-89.

FABRICATORE, A. & WADDEN, T. 2003. Psychosocial status varies by treatment preference among obese women. *Obesity Research,* 11**,** A111-A111.

FALKEN, Y., HELLSTROM, P. M., HOLST, J. J. & NASLUND, E. 2011. Changes in glucose homeostasis after Roux-en-Y gastric bypass surgery for obesity at day three, two months, and one year after surgery: role of gut peptides. *J Clin Endocrinol Metab,* 96**,** 2227-35.

FAY, M. P. & PROSCHAN, M. A. 2010. Wilcoxon-Mann-Whitney or t-test? On assumptions for hypothesis tests and multiple interpretations of decision rules. *Stat Surv,* 4**,** 1-39.

FEZEU, L. K., BATTY, G. D., GALE, C. R., KIVIMAKI, M., HERCBERG, S. & CZERNICHOW, S. 2015. Is the Relationship between Common Mental Disorder and Adiposity Bidirectional? Prospective Analyses of a UK General Population-Based Study. *PLoS One,* 10**,** e0119970.

FOSTER, G. D., WADDEN, T. A., PETERSON, F. J., LETIZIA, K. A., BARTLETT, S. J. & CONILL, A. M. 1992. A controlled comparison of three very-low-calorie diets: effects on weight, body composition, and symptoms. *Am J Clin Nutr,* 55**,** 811-7.

FRANK, D. N., ST AMAND, A. L., FELDMAN, R. A., BOEDEKER, E. C., HARPAZ, N. & PACE, N. R. 2007. Molecular-phylogenetic characterization of microbial community imbalances in human inflammatory bowel diseases. *Proc Natl Acad Sci U S A,* 104**,** 13780-5.

FRANKS, P. W. & LING, C. 2010. Epigenetics and obesity: the devil is in the details. *BMC Med,* 8**,** 88.

FRIED, M. & PESKOVA, M. 1995. New Approach in Surgical Treatment of Morbid Obesity: Laparoscopic Gastric Banding. *Obes Surg,* 5**,** 74-76.

FROST, J. 2015. *Choosing Between a Nonparametric Test and a Parametric Test* [Online]. 2016 Minitab Inc. [Accessed August 31st 2016].

FRUHBECK, G., DIEZ CABALLERO, A. & GIL, M. J. 2004. Fundus functionality and ghrelin concentrations after bariatric surgery. *N Engl J Med,* 350**,** 308-9.

FURET, J. P., KONG, L. C., TAP, J., POITOU, C., BASDEVANT, A., BOUILLOT, J. L., MARIAT, D., CORTHIER, G., DORE, J., HENEGAR, C., RIZKALLA, S. & CLEMENT, K. 2010. Differential adaptation of human gut microbiota to bariatric surgery-induced weight loss: links with metabolic and low-grade inflammation markers. *Diabetes,* 59**,** 3049-57.

GAO, H., YANG, Z. K., GENTRY, T. J., WU, L., SCHADT, C. W. & ZHOU, J. 2007. Microarray-based analysis of microbial community RNAs by whole-community RNA amplification. *Appl Environ Microbiol,* 73**,** 563-71.

GAO, Z., YIN, J., ZHANG, J., WARD, R. E., MARTIN, R. J., LEFEVRE, M., CEFALU, W. T. & YE, J. 2009. Butyrate improves insulin sensitivity and increases energy expenditure in mice. *Diabetes,* 58**,** 1509-17.

GEVERS, D., KNIGHT, R., PETROSINO, J. F., HUANG, K., MCGUIRE, A. L., BIRREN, B. W., NELSON, K. E., WHITE, O., METHE, B. A. & HUTTENHOWER, C. 2012. The Human Microbiome Project: a community resource for the healthy human microbiome. *PLoS Biol,* 10**,** e1001377.

GIBSON, G. R., WILLEMS, A., READING, S. & COLLINS, M. D. 1996. Fermentation of non-digestible oligosaccharides by human colonic bacteria. *Proc Nutr Soc,* 55**,** 899-912.

GOGEBAKAN, O., OSTERHOFF, M. A., SCHULER, R., PIVOVAROVA, O., KRUSE, M., SELTMANN, A. C., MOSIG, A. S., RUDOVICH, N., NAUCK, M. & PFEIFFER, A. F. 2015. GIP increases adipose tissue expression and blood levels of MCP-1 in humans and links high energy diets to inflammation: a randomised trial. *Diabetologia,* 58**,** 1759-68.

GONNELLI, S., CAFFARELLI, C. & NUTI, R. 2014. Obesity and fracture risk. *Clin Cases Miner Bone Metab,* 11**,** 9-14.

GORE, J. L., PHAM, P. T., DANOVITCH, G. M., WILKINSON, A. H., ROSENTHAL, J. T., LIPSHUTZ, G. S. & SINGER, J. S. 2006. Obesity and outcome following renal transplantation. *Am J Transplant,* 6**,** 357-63.

GRAESSLER, J., QIN, Y., ZHONG, H., ZHANG, J., LICINIO, J., WONG, M. L., XU, A., CHAVAKIS, T., BORNSTEIN, A. B., EHRHART-BORNSTEIN, M., LAMOUNIER-ZEPTER, V., LOHMANN, T., WOLF, T. & BORNSTEIN, S. R. 2013. Metagenomic sequencing of the human gut microbiome before and after bariatric surgery in obese patients with type 2 diabetes: correlation with inflammatory and metabolic parameters. *Pharmacogenomics J,* 13**,** 514-22.

GREENWAY, F., O'NEIL, C. E., STEWART, L., ROOD, J., KEENAN, M. & MARTIN, R. 2007. Fourteen weeks of treatment with Viscofiber increased fasting levels of glucagon-like peptide-1 and peptide-YY. *J Med Food,* 10**,** 720-4.

GREENWAY, F. L., RAUM, W. J. & ATKINSON, R. L. 1994. Higher calorie content preserves myocardial electrical activity during very-low-calorie dieting. *Obes Res,* 2**,** 95-9.

GUARNER, F. & MALAGELADA, J. R. 2003. Gut flora in health and disease. *Lancet,* 361**,** 512-519.

GUO, X., XIA, X., TANG, R., ZHOU, J., ZHAO, H. & WANG, K. 2008. Development of a real-time PCR method for Firmicutes and Bacteroidetes in faeces and its application to quantify intestinal population of obese and lean pigs. *Lett Appl Microbiol,* 47**,** 367-73.

GUSTAFSON, B. & SMITH, U. 2015. Regulation of white adipogenesis and its relation to ectopic fat accumulation and cardiovascular risk. *Atherosclerosis,* 241**,** 27-35.

HAMADY, M., WALKER, J. J., HARRIS, J. K., GOLD, N. J. & KNIGHT, R. 2008. Error-correcting barcoded primers for pyrosequencing hundreds of samples in multiplex. *Nat Methods,* 5**,** 235-7.

HASLAM, D. W. & JAMES, W. P. T. 2005. Obesity. *Lancet,* 366**,** 1197-1209.

HASLER, G., BUYSSE, D. J., KLAGHOFER, R., GAMMA, A., AJDACIC, V., EICH, D., ROSSLER, W. & ANGST, J. 2004. The association between short sleep duration and obesity in young adults: a 13-year prospective study. *Sleep,* 27**,** 661-6.

HE, Z., WU, L., LI, X., FIELDS, M. W. & ZHOU, J. 2005. Empirical establishment of oligonucleotide probe design criteria. *Appl Environ Microbiol,* 71**,** 3753-60.

HE, Z. & ZHOU, J. 2008. Empirical evaluation of a new method for calculating signal-to-noise ratio for microarray data analysis. *Appl Environ Microbiol,* 74**,** 2957-66.

HEATHER, J. M. & CHAIN, B. 2016. The sequence of sequencers: The history of sequencing DNA. *Genomics,* 107**,** 1-8.

HILL, M. J. 1997. Intestinal flora and endogenous vitamin synthesis. *Eur J Cancer Prev,* 6 Suppl 1**,** S43-5.

HILL, M. O. 1973. Diversity and Evenness: A Unifying Notation and Its Consequences. *Ecology,* 54**,** 427-432.

HSU, C. Y., MCCULLOCH, C. E., IRIBARREN, C., DARBINIAN, J. & GO, A. S. 2006. Body mass index and risk for end-stage renal disease. *Ann Intern Med,* 144**,** 21-8.

HU, H. J., PARK, S. G., JANG, H. B., CHOI, M. K., PARK, K. H., KANG, J. H., PARK, S. I., LEE, H. J. & CHO, S. H. 2015. Obesity Alters the Microbial Community Profile in Korean Adolescents. *PLoS One,* 10**,** e0134333.

JACCARD, P. 1901. Distribution de la flore alpine dans le bassin des Dranses et dans quelques régions voisines. *Bulletin de la Société Vaudoise des Sciences Naturelles.* **,** 241-272.

JACOBSEN, S. H., OLESEN, S. C., DIRKSEN, C., JORGENSEN, N. B., BOJSEN-MOLLER, K. N., KIELGAST, U., WORM, D., ALMDAL, T., NAVER, L. S., HVOLRIS, L. E., REHFELD, J. F., WULFF, B. S., CLAUSEN, T. R., HANSEN, D. L., HOLST, J. J. & MADSBAD, S. 2012. Changes in gastrointestinal hormone responses, insulin sensitivity, and beta-cell function within 2 weeks after gastric bypass in non-diabetic subjects. *Obes Surg,* 22**,** 1084-96.

JANDA, J. M. & ABBOTT, S. L. 2007. 16S rRNA gene sequencing for bacterial identification in the diagnostic laboratory: pluses, perils, and pitfalls. *J Clin Microbiol,* 45**,** 2761-4.

JORGENSEN, N. B., DIRKSEN, C., BOJSEN-MOLLER, K. N., JACOBSEN, S. H., WORM, D., HANSEN, D. L., KRISTIANSEN, V. B., NAVER, L., MADSBAD, S. & HOLST, J. J. 2013. Exaggerated glucagon-like peptide 1 response is important for improved beta-cell

function and glucose tolerance after Roux-en-Y gastric bypass in patients with type 2 diabetes. *Diabetes,* 62**,** 3044-52.

JORGENSEN, N. B., JACOBSEN, S. H., DIRKSEN, C., BOJSEN-MOLLER, K. N., NAVER, L., HVOLRIS, L., CLAUSEN, T. R., WULFF, B. S., WORM, D., LINDQVIST HANSEN, D., MADSBAD, S. & HOLST, J. J. 2012. Acute and long-term effects of Roux-en-Y gastric bypass on glucose metabolism in subjects with Type 2 diabetes and normal glucose tolerance. *Am J Physiol Endocrinol Metab,* 303**,** E122-31.

JORM, A. F., KORTEN, A. E., CHRISTENSEN, H., JACOMB, P. A., RODGERS, B. & PARSLOW, R. A. 2003. Association of obesity with anxiety, depression and emotional well-being: a community survey. *Aust N Z J Public Health,* 27**,** 434-40.

JOSHU, C. E., MONDUL, A. M., MENKE, A., MEINHOLD, C., HAN, M., HUMPHREYS, E. B., FREEDLAND, S. J., WALSH, P. C. & PLATZ, E. A. 2011. Weight gain is associated with an increased risk of prostate cancer recurrence after prostatectomy in the PSA era. *Cancer Prev Res (Phila),* 4**,** 544-51.

JOST, L. 2006. Entropy and diversity. *Oikos,* 113**,** 363-375.

JOVANOVIC-PETERSON, L. & PETERSON, C. M. 1996. Vitamin and mineral deficiencies which may predispose to glucose intolerance of pregnancy. *J Am Coll Nutr,* 15**,** 14-20.

KAAKS, R., LUKANOVA, A. & KURZER, M. S. 2002. Obesity, endogenous hormones, and endometrial cancer risk: a synthetic review. *Cancer Epidemiol Biomarkers Prev,* 11**,** 1531-43.

KAHN, B. B. & FLIER, J. S. 2000. Obesity and insulin resistance. *Journal of Clinical Investigation,* 106**,** 473-481.

KAHN, S. E., HULL, R. L. & UTZSCHNEIDER, K. M. 2006. Mechanisms linking obesity to insulin resistance and type 2 diabetes. *Nature,* 444**,** 840-6.

KAMADA, N., CHEN, G. Y., INOHARA, N. & NUNEZ, G. 2013. Control of pathogens and pathobionts by the gut microbiota. *Nat Immunol,* 14**,** 685-90.

KARLSSON, C. L., ONNERFALT, J., XU, J., MOLIN, G., AHRNE, S. & THORNGREN-JERNECK, K. 2012. The microbiota of the gut in preschool children with normal and excessive body weight. *Obesity (Silver Spring),* 20**,** 2257-61.

KEENAN, M. J., ZHOU, J., MCCUTCHEON, K. L., RAGGIO, A. M., BATEMAN, H. G., TODD, E., JONES, C. K., TULLEY, R. T., MELTON, S., MARTIN, R. J. & HEGSTED, M. 2006. Effects of resistant starch, a non-digestible fermentable fiber, on reducing body fat. *Obesity (Silver Spring),* 14**,** 1523-34.

KERSHAW, E. E. & FLIER, J. S. 2004. Adipose tissue as an endocrine organ. *J Clin Endocrinol Metab,* 89**,** 2548-56.

KIM, H. N., KIM, S. H., EUN, Y. M. & SONG, S. W. 2015. Obesity with metabolic abnormality is associated with the presence of carotid atherosclerosis in Korean men: a cross-sectional study. *Diabetology & Metabolic Syndrome,* 7.

KIM, S., PARKS, C. G., DEROO, L. A., CHEN, H., TAYLOR, J. A., CAWTHON, R. M. & SANDLER, D. P. 2009. Obesity and weight gain in adulthood and telomere length. *Cancer Epidemiol Biomarkers Prev,* 18**,** 816-20.

KING, H., ABDULLAEV, B., DJUMAEVA, S., NIKITIN, V., ASHWORTH, L. & DOBO, M. G. 1998. Glucose intolerance and associated factors in the Fergana Valley, Uzbekistan. *Diabet Med,* 15**,** 1052-62.

KISHIMOTO, R., TAMADA, K., LIU, X., OKUBO, H., ISE, S., OHTA, H., RUF, S., NAKATANI, J., KOHNO, N., SPITZ, F. & TAKUMI, T. 2015. Model mice for 15q11-13 duplication syndrome exhibit late-onset obesity and altered lipid metabolism. *Hum Mol Genet,* 24**,** 4559-72.

KNUTSON, K. L. 2012. Does inadequate sleep play a role in vulnerability to obesity? *Am J Hum Biol,* 24**,** 361-71.

KORNER, J., INABNET, W., CONWELL, I. M., TAVERAS, C., DAUD, A., OLIVERO-RIVERA, L., RESTUCCIA, N. L. & BESSLER, M. 2006. Differential effects of gastric bypass and banding on circulating gut hormone and leptin levels. *Obesity (Silver Spring),* 14**,** 1553-61.

KROTKIEWSKI, M. 1984. Effect of guar gum on body-weight, hunger ratings and metabolism in obese subjects. *Br J Nutr,* 52**,** 97-105.

KUWAHARA, A. 2014. Contributions of colonic short-chain Fatty Acid receptors in energy homeostasis. *Front Endocrinol (Lausanne),* 5**,** 144.

LAFERRERE, B., HESHKA, S., WANG, K., KHAN, Y., MCGINTY, J., TEIXEIRA, J., HART, A. B. & OLIVAN, B. 2007. Incretin levels and effect are markedly enhanced 1 month after Roux-en-Y gastric bypass surgery in obese patients with type 2 diabetes. *Diabetes Care,* 30**,** 1709-16.

LE ROUX, C. W., AYLWIN, S. J., BATTERHAM, R. L., BORG, C. M., COYLE, F., PRASAD, V., SHUREY, S., GHATEI, M. A., PATEL, A. G. & baselineOOM, S. R. 2006. Gut hormone profiles following bariatric surgery favor an anorectic state, facilitate weight loss, and improve metabolic parameters. *Ann Surg,* 243**,** 108-14.

LEbaselineANC, J. G., LAINO, J. E., DEL VALLE, M. J., VANNINI, V., VAN SINDEREN, D., TARANTO, M. P., DE VALDEZ, G. F., DE GIORI, G. S. & SESMA, F. 2011. B-Group vitamin production by lactic acid bacteria - current knowledge and potential applications. *Journal of Applied Microbiology,* 111**,** 1297-1309.

LEDERBERG, J. & MCCRAY, A. T. 2001. 'Ome sweet 'omics - A genealogical treasury of words. *Scientist,* 15**,** 8-8.

LEE, J., LEE, J. Y., LEE, J. H., JUNG, S. M., SUH, Y. S., KOH, J. H., KWOK, S. K., JU, J. H., PARK, K. S. & PARK, S. H. 2015. Visceral fat obesity is highly associated with primary gout in a metabolically obese but normal weighted population: a case control study. *Arthritis Res Ther,* 17**,** 79.

LEE, K. I., CHIANG, C. W., LIN, H. C., ZHAO, J. F., LI, C. T., SHYUE, S. K. & LEE, T. S. 2016. Maternal exposure to di-(2-ethylhexyl) phthalate exposure deregulates blood pressure, adiposity, cholesterol metabolism and social interaction in mouse offspring. *Arch Toxicol,* 90**,** 1211-24.

LEY, R. E., BACKHED, F., TURNBAUGH, P., LOZUPONE, C. A., KNIGHT, R. D. & GORDON, J. I. 2005. Obesity alters gut microbial ecology. *Proc Natl Acad Sci U S A,* 102**,** 11070-5.

LEY, R. E., TURNBAUGH, P. J., KLEIN, S. & GORDON, J. I. 2006. Microbial ecology: human gut microbes associated with obesity. *Nature,* 444**,** 1022-3.

LIEBICH, J., SCHADT, C. W., CHONG, S. C., HE, Z., RHEE, S. K. & ZHOU, J. 2006. Improvement of oligonucleotide probe design criteria for functional gene microarrays in environmental applications. *Appl Environ Microbiol,* 72**,** 1688-91.

LIN, H. V., FRASSETTO, A., KOWALIK, E. J., JR., NAWROCKI, A. R., LU, M. M., KOSINSKI, J. R., HUBERT, J. A., SZETO, D., YAO, X., FORREST, G. & MARSH, D. J. 2012. Butyrate and propionate protect against diet-induced obesity and regulate gut hormones via free fatty acid receptor 3-independent mechanisms. *PLoS One,* 7**,** e35240.

LIOU, A. P., PAZIUK, M., LUEVANO, J. M., MACHINENI, S., TURNBAUGH, P. J. & KAPLAN, L. M. 2013. Conserved Shifts in the Gut Microbiota Due to Gastric Bypass Reduce Host Weight and Adiposity. *Science Translational Medicine,* 5.

LIU, J., ZHANG, A. & LI, L. 2012. Sleep duration and overweight/obesity in children: review and implications for pediatric nursing. *J Spec Pediatr Nurs,* 17**,** 193-204.

LONROTH, H., DALENBACK, J., HAGLIND, E. & LUNDELL, L. 1996. Laparoscopic gastric bypass. Another option in bariatric surgery. *Surg Endosc,* 10**,** 636-8.

LOUIS, S., TAPPU, R. M., DAMMS-MACHADO, A., HUSON, D. H. & BISCHOFF, S. C. 2016. Characterization of the Gut Microbial Community of Obese Patients Following a Weight-Loss Intervention Using Whole Metagenome Shotgun Sequencing. *Plos One,* 11.

LUKOVAC, S., BELZER, C., PELLIS, L., KEIJSER, B. J., DE VOS, W. M., MONTIJN, R. C. & ROESELERS, G. 2014. Differential modulation by Akkermansia muciniphila and Faecalibacterium prausnitzii of host peripheral lipid metabolism and histone acetylation in mouse gut organoids. *MBio,* 5.

MACDONALD, I. A., SINGH, G., MAHONY, D. E. & MEIER, C. E. 1978. Effect of pH on bile salt degradation by mixed fecal cultures. *Steroids,* 32**,** 245-56.

MACHIELS, K., JOOSSENS, M., SABINO, J., DE PRETER, V., ARIJS, I., EECKHAUT, V., BALLET, V., CLAES, K., VAN IMMERSEEL, F., VERBEKE, K., FERRANTE, M., VERHAEGEN, J., RUTGEERTS, P. & VERMEIRE, S. 2014. A decrease of the butyrate-producing species Roseburia hominis and Faecalibacterium prausnitzii defines dysbiosis in patients with ulcerative colitis. *Gut,* 63**,** 1275-83.

MANN, H. B. & WHITNEY, D. R. 1947. On a Test of Whether One of 2 Random Variables Is Stochastically Larger Than the Other. *Annals of Mathematical Statistics,* 18**,** 50-60.

MARLENE, R., SIMONE, D., BERIT, H., JUTTA, Z., EVA, A., HELMUT, B. & ALEXANDER, H. 2013. Abundance and diversity of microbiota in type 2 diabetes and obesity. *Journal of Diabetes & Metabolism,* 2013.

MECHANICK, J. I., KUSHNER, R. F., SUGERMAN, H. J., GONZALEZ-CAMPOY, J. M., COLLAZO-CLAVELL, M. L., GUVEN, S., SPITZ, A. F., APOVIAN, C. M., LIVINGSTON, E. H., BROLIN, R., SARWER, D. B., ANDERSON, W. A. & DIXON, J. 2008. American Association of Clinical Endocrinologists, The Obesity Society, and American Society for Metabolic & Bariatric Surgery Medical Guidelines for Clinical Practice for the perioperative nutritional, metabolic, and nonsurgical support of the bariatric surgery patient. *Surg Obes Relat Dis,* 4**,** S109-84.

MEEK, C. L., LEWIS, H. B., REIMANN, F., GRIBbaselineE, F. M. & PARK, A. J. 2016. The effect of bariatric surgery on gastrointestinal and pancreatic peptide hormones. *Peptides,* 77**,** 28-37.

MERRITT, R. J., HACK, S. L., KALSCH, M. & OLSON, D. 1986. Corticosteroid therapy-induced obesity in children. *Clin Pediatr (Phila),* 25**,** 149-52.

MESSIER, S. P. 2009. Obesity and Osteoarthritis: Disease Genesis and Nonpharmacologic Weight Management. *Medical Clinics of North America,* 93**,** 145-+.

MIRAS, A. D. & LE ROUX, C. W. 2013. Mechanisms underlying weight loss after bariatric surgery. *Nat Rev Gastroenterol Hepatol,* 10**,** 575-84.

MISSION, J. F., MARSHALL, N. E. & CAUGHEY, A. B. 2015. Pregnancy risks associated with obesity. *Obstet Gynecol Clin North Am,* 42**,** 335-53.

MORPURGO, G., FIORETTI, B. & CATACUZZENO, L. 2012. The increased incidence of malignant melanoma in obese individuals is due to impaired melanogenesis and melanocyte DNA repair. *Med Hypotheses,* 78**,** 533-5.

MORTON, G. J., CUMMINGS, D. E., BASKIN, D. G., BARSH, G. S. & SCHWARTZ, M. W. 2006. Central nervous system control of food intake and body weight. *Nature,* 443**,** 289-95.

MUSSO, G., GAMBINO, R. & CASSADER, M. 2011. Interactions between gut microbiota and host metabolism predisposing to obesity and diabetes. *Annu Rev Med,* 62**,** 361-80.

NAKAMURA, K., FUSTER, J. J. & WALSH, K. 2014. Adipokines: a link between obesity and cardiovascular disease. *J Cardiol,* 63**,** 250-9.

NAWROCKI, E. P. & EDDY, S. R. 2007. Query-dependent banding (QDB) for faster RNA similarity searches. *PLoS Comput Biol,* 3**,** e56.

NICHOLS, T. E. & HOLMES, A. P. 2002. Nonparametric permutation tests for functional neuroimaging: a primer with examples. *Hum Brain Mapp,* 15**,** 1-25.

NICHOLSON, J. K., HOLMES, E., KINROSS, J., BURCELIN, R., GIBSON, G., JIA, W. & PETTERSSON, S. 2012. Host-gut microbiota metabolic interactions. *Science,* 336**,** 1262-7.

NISHINA, P. M. & FREEDLAND, R. A. 1990. Effects of propionate on lipid biosynthesis in isolated rat hepatocytes. *J Nutr,* 120**,** 668-73.

O'BRIEN, P. E. & DIXON, J. B. 2003. Lap-band: outcomes and results. *J Laparoendosc Adv Surg Tech A,* 13**,** 265-70.

O'BRIEN, P. E., DIXON, J. B., LAURIE, C., SKINNER, S., PROIETTO, J., MCNEIL, J., STRAUSS, B., MARKS, S., SCHACHTER, L., CHAPMAN, L. & ANDERSON, M. 2006. Treatment of mild to moderate obesity with laparoscopic adjustable gastric banding or an intensive medical program: a randomized trial. *Ann Intern Med,* 144**,** 625-33.

OGDEN, C. L., CARROLL, M. D., KIT, B. K. & FLEGAL, K. M. 2014. Prevalence of childhood and adult obesity in the United States, 2011-2012. *JAMA,* 311**,** 806-14.

OGDEN, C. L., YANOVSKI, S. Z., CARROLL, M. D. & FLEGAL, K. M. 2007. The epidemiology of obesity. *Gastroenterology,* 132**,** 2087-102.

OGNA, A., FORNI OGNA, V., BOCHUD, M., GUESSOUS, I., PACCAUD, F., BURNIER, M. & WUERZNER, G. 2016. Association between obesity and glomerular hyperfiltration: the confounding effect of smoking and sodium and protein intakes. *Eur J Nutr,* 55**,** 1089-97.

OTT, S. J. & SCHREIBER, S. 2006. Reduced microbial diversity in inflammatory bowel diseases. *Gut,* 55**,** 1207.

OVREAS, L., FORNEY, L., DAAE, F. L. & TORSVIK, V. 1997. Distribution of bacterioplankton in meromictic Lake Saelenvannet, as determined by denaturing gradient gel electrophoresis of PCR-amplified gene fragments coding for 16S rRNA. *Appl Environ Microbiol,* 63**,** 3367-73.

PAOLINI, B. M., LAURIENTI, P. J., SIMPSON, S. L., BURDETTE, J. H., LYDAY, R. G. & REJESKI, W. J. 2015. Global integration of the hot-state brain network of appetite predicts short term weight loss in older adult. *Front Aging Neurosci,* 7**,** 70.

PASQUALI, R., PATTON, L. & GAMBINERI, A. 2007. Obesity and infertility. *Curr Opin Endocrinol Diabetes Obes,* 14**,** 482-7.

PESSIONE, E. 2012. Lactic acid bacteria contribution to gut microbiota complexity: lights and shadows. *Front Cell Infect Microbiol,* 2**,** 86.

PETROV, D., LUQUE, M., PEDROS, I., ETTCHETO, M., ABAD, S., PALLAS, M., VERDAGUER, E., AULADELL, C., FOLCH, J. & CAMINS, A. 2016. Evaluation of the Role of JNK1 in the Hippocampus in an Experimental Model of Familial Alzheimer's Disease. *Mol Neurobiol,* 53**,** 6183-6193.

PORIES, W. J., SWANSON, M. S., MACDONALD, K. G., LONG, S. B., MORRIS, P. G., BROWN, B. M., BARAKAT, H. A., DERAMON, R. A., ISRAEL, G., DOLEZAL, J. M. & ET AL. 1995. Who would have thought it? An operation proves to be the most effective therapy for adult-onset diabetes mellitus. *Ann Surg,* 222**,** 339-50; discussion 350-2.

PRINGLE, T. H., SCOBIE, I. N., MURRAY, R. G., KESSON, C. M. & MACCUISH, A. C. 1983. Prolongation of the QT interval during therapeutic starvation: a substrate for malignant arrhythmias. *Int J Obes,* 7**,** 253-61.

PUDDU, A., SANGUINETI, R., MONTECUCCO, F. & VIVIANI, G. L. 2014. Evidence for the gut microbiota short-chain fatty acids as key pathophysiological molecules improving diabetes. *Mediators Inflamm,* 2014**,** 162021.

QUEIPO-ORTUNO, M. I., SEOANE, L. M., MURRI, M., PARDO, M., GOMEZ-ZUMAQUERO, J. M., CARDONA, F., CASANUEVA, F. & TINAHONES, F. J. 2013. Gut microbiota composition in male rat models under different nutritional status and physical activity and its association with serum leptin and ghrelin levels. *PLoS One,* 8**,** e65465.

REMELY, M., HIPPE, B., GERETSCHLAEGER, I., STEGMAYER, S., HOEFINGER, I. & HASLBERGER, A. 2015. Increased gut microbiota diversity and abundance of Faecalibacterium prausnitzii and Akkermansia after fasting: a pilot study. *Wien Klin Wochenschr,* 127**,** 394-8.

RHEE, S. K., LIU, X., WU, L., CHONG, S. C., WAN, X. & ZHOU, J. 2004. Detection of genes involved in biodegradation and biotransformation in microbial communities by using 50-mer oligonucleotide microarrays. *Appl Environ Microbiol,* 70**,** 4303-17.

RIZZO, G. S. & SEN, S. 2015. Maternal obesity and immune dysregulation in mother and infant: A review of the evidence. *Paediatr Respir Rev,* 16**,** 251-7.

RUBINO, F. 2006. Bariatric surgery: effects on glucose homeostasis. *Curr Opin Clin Nutr Metab Care,* 9**,** 497-507.

RUTTERS, F., GERVER, W. J., NIEUWENHUIZEN, A. G., VERHOEF, S. P. & WESTERTERP-PLANTENGA, M. S. 2010. Sleep duration and body-weight development during puberty in a Dutch children cohort. *Int J Obes (Lond),* 34**,** 1508-14.

S. PATRICIA, S. J., VANDERBERG; ITAMAR, GLAZER; NOEL, BOEMARE 2009. *Insect Pathogens: Molecular Approaches and Techniques,* CAB International.

SAM, S. 2007. Obesity and Polycystic Ovary Syndrome. *Obes Manag,* 3**,** 69-73.

SANTACRUZ, A., MARCOS, A., WARNBERG, J., MARTI, A., MARTIN-MATILLAS, M., CAMPOY, C., MORENO, L. A., VEIGA, O., REDONDO-FIGUERO, C., GARAGORRI, J. M., AZCONA, C., DELGADO, M., GARCIA-FUENTES, M., COLLADO, M. C., SANZ, Y. & GROUP, E. S. 2009. Interplay between weight loss and gut microbiota composition in overweight adolescents. *Obesity (Silver Spring),* 17**,** 1906-15.

SANZ, Y., SANTACRUZ, A. & GAUFFIN, P. 2010. Gut microbiota in obesity and metabolic disorders. *Proc Nutr Soc,* 69**,** 434-41.

SAYIN, S. I., WAHLSTROM, A., FELIN, J., JANTTI, S., MARSCHALL, H. U., BAMBERG, K., ANGELIN, B., HYOTYLAINEN, T., ORESIC, M. & BACKHED, F. 2013. Gut microbiota regulates bile acid metabolism by reducing the levels of tauro-beta-muricholic acid, a naturally occurring FXR antagonist. *Cell Metab,* 17**,** 225-35.

SCHNEEBERGER, M., EVERARD, A., GOMEZ-VALADES, A. G., MATAMOROS, S., RAMIREZ, S., DELZENNE, N. M., GOMIS, R., CLARET, M. & CANI, P. D. 2015. Akkermansia muciniphila inversely correlates with the onset of inflammation, altered adipose tissue metabolism and metabolic disorders during obesity in mice. *Sci Rep,* 5**,** 16643.

SCHWARTZ, A. R., PATIL, S. P., LAFFAN, A. M., POLOTSKY, V., SCHNEIDER, H. & SMITH, P. L. 2008. Obesity and obstructive sleep apnea: pathogenic mechanisms and therapeutic approaches. *Proc Am Thorac Soc,* 5**,** 185-92.

SEARS, C. L. 2005. A dynamic partnership: Celebrating our gut flora. *Anaerobe,* 11**,** 247-251.

SEKIROV, I., RUSSELL, S. L., ANTUNES, L. C. & FINLAY, B. B. 2010. Gut microbiota in health and disease. *Physiol Rev,* 90**,** 859-904.

SHIN, N. R., LEE, J. C., LEE, H. Y., KIM, M. S., WHON, T. W., LEE, M. S. & BAE, J. W. 2014. An increase in the Akkermansia spp. population induced by metformin treatment improves glucose homeostasis in diet-induced obese mice. *Gut,* 63**,** 727-735.

SHIRI, R., KARPPINEN, J., LEINO-ARJAS, P., SOLOVIEVA, S. & VIIKARI-JUNTURA, E. 2010. The Association Between Obesity and Low Back Pain: A Meta-Analysis. *American Journal of Epidemiology,* 171**,** 135-154.

SICKLE, J. V. 1997. Using mean similarity dendrograms to evaluate classifications. *J. Agric. Biol. Environ. Stat.* **,** 370–388.

SOKOL, H., PIGNEUR, B., WATTERLOT, L., LAKHDARI, O., BERMUDEZ-HUMARAN, L. G., GRATADOUX, J. J., baselineUGEON, S., BRIDONNEAU, C., FURET, J. P., CORTHIER, G., GRANGETTE, C., VASQUEZ, N., POCHART, P., TRUGNAN, G., THOMAS, G., baselineOTTIERE, H. M., DORE, J., MARTEAU, P., SEKSIK, P. & LANGELLA, P. 2008. Faecalibacterium prausnitzii is an anti-inflammatory commensal bacterium identified by gut microbiota analysis of Crohn disease patients. *Proc Natl Acad Sci U S A,* 105**,** 16731-6.

SOURS, H. E., FRATTALI, V. P., BRAND, C. D., FELDMAN, R. A., FORBES, A. L., SWANSON, R. C. & PARIS, A. L. 1981. Sudden death associated with very low calorie weight reduction regimens. *Am J Clin Nutr,* 34**,** 453-61.

SPIEGEL, K., TASALI, E., PENEV, P. & VAN CAUTER, E. 2004. Brief communication: Sleep curtailment in healthy young men is associated with decreased leptin levels, elevated ghrelin levels, and increased hunger and appetite. *Ann Intern Med,* 141**,** 846-50.

SRIVASTAVA, T. 2006. Nondiabetic consequences of obesity on kidney. *Pediatr Nephrol,* 21**,** 463-70.

STEELE, C. A., CUTHBERTSON, D. J., MACFARLANE, I. A., JAVADPOUR, M., DAS, K. S., GILKES, C., WILDING, J. P. & DAOUSI, C. 2013. Hypothalamic obesity: prevalence, associations and longitudinal trends in weight in a specialist adult neuroendocrine clinic. *Eur J Endocrinol,* 168**,** 501-7.

STOECKLI, R., CHANDA, R., LANGER, I. & KELLER, U. 2004. Changes of body weight and plasma ghrelin levels after gastric banding and gastric bypass. *Obes Res,* 12**,** 346-50.

STONE, B. G., ANSEL, H. J., PETERSON, F. J. & GEBHARD, R. L. 1992. Gallbladder emptying stimuli in obese and normal-weight subjects. *Hepatology,* 15**,** 795-8.

STUDENT 1908. The Probable Error of a Mean. *Biometrika,* 6 1–25.

SUCHNER, U., SENFTLEBEN, U., ECKART, T., SCHOLZ, M. R., BECK, K., MURR, R., ENZENBACH, R. & PETER, K. 1996. Enteral versus parenteral nutrition: Effects on gastrointestinal function and metabolism. *Nutrition,* 12**,** 13-22.

SUN, J. W., ZHAO, L. G., YANG, Y., MA, X., WANG, Y. Y. & XIANG, Y. B. 2015. Obesity and risk of bladder cancer: a dose-response meta-analysis of 15 cohort studies. *PLoS One,* 10**,** e0119313.

SWEENEY, T. E. & MORTON, J. M. 2014. Metabolic surgery: action via hormonal milieu changes, changes in bile acids or gut microbiota? A summary of the literature. *Best Pract Res Clin Gastroenterol,* 28**,** 727-40.

TADROSS, J. A. & LE ROUX, C. W. 2009. The mechanisms of weight loss after bariatric surgery. *Int J Obes (Lond),* 33 Suppl 1**,** S28-32.

TICE, J. A., KARLINER, L., WALSH, J., PETERSEN, A. J. & FELDMAN, M. D. 2008. Gastric banding or bypass? A systematic review comparing the two most popular bariatric procedures. *Am J Med,* 121**,** 885-93.

TIMS, S., DEROM, C., JONKERS, D. M., VLIETINCK, R., SARIS, W. H., KLEEREBEZEM, M., DE VOS, W. M. & ZOETENDAL, E. G. 2013. Microbiota conservation and BMI signatures in adult monozygotic twins. *ISME J,* 7**,** 707-17.

TIQUIA, S. M., WU, L. Y., CHONG, S. C., PASSOVETS, S., XU, D., XU, Y. & ZHOU, J. Z. 2004. Evaluation of 50-mer oligonucleotide arrays for detecting microbial populations in environmental samples. *Biotechniques,* 36**,** 664-+.

TODENDI, P. F., POSSUELO, L. G., KLINGER, E. I., REUTER, C. P., BURGOS, M. S., MOURA, D. J., FIEGENBAUM, M. & VALIM, A. R. 2016. Low-grade inflammation markers in children and adolescents: Influence of anthropometric characteristics and CRP and IL6 polymorphisms. *Cytokine,* 88**,** 177-183.

TREMAROLI, V. & BACKHED, F. 2012. Functional interactions between the gut microbiota and host metabolism. *Nature,* 489**,** 242-249.

TREMAROLI, V., KARLSSON, F., WERLING, M., STAHLMAN, M., KOVATCHEVA-DATCHARY, P., OLBERS, T., FANDRIKS, L., LE ROUX, C. W., NIELSEN, J. & BACKHED, F. 2015. Roux-en-Y Gastric Bypass and Vertical Banded Gastroplasty Induce Long-Term Changes on the Human Gut Microbiome Contributing to Fat Mass Regulation. *Cell Metab,* 22**,** 228-38.

TU, Q., HE, Z., LI, Y., CHEN, Y., DENG, Y., LIN, L., HEMME, C. L., YUAN, T., VAN NOSTRAND, J. D., WU, L., ZHOU, X., SHI, W., LI, L., XU, J. & ZHOU, J. 2014. Development of HuMiChip for functional profiling of human microbiomes. *PLoS One,* 9**,** e90546.

TU, Q., LI, J., SHI, Z., CHEN, Y., LIN, L., LI, J., WANG, H., YAN, J., ZHOU, Q., LI, X., LI, L., ZHOU, J. & HE, Z. 2016. HuMiChip2 for strain level identification and functional profiling of human microbiomes. *Appl Microbiol Biotechnol*.

TUOMISTO, H. 2010. A consistent terminology for quantifying species diversity? Yes, it does exist. *Oecologia,* 164**,** 853-860.

TURNBAUGH, P. J., HAMADY, M., YATSUNENKO, T., CANTAREL, B. L., DUNCAN, A., LEY, R. E., SOGIN, M. L., JONES, W. J., ROE, B. A., AFFOURTIT, J. P., EGHOLM, M., HENRISSAT, B., HEATH, A. C., KNIGHT, R. & GORDON, J. I. 2009. A core gut microbiome in obese and lean twins. *Nature,* 457**,** 480-4.

TURNBAUGH, P. J., LEY, R. E., MAHOWALD, M. A., MAGRINI, V., MARDIS, E. R. & GORDON, J. I. 2006. An obesity-associated gut microbiome with increased capacity for energy harvest. *Nature,* 444**,** 1027-31.

UMEDA, L. M., SILVA, E. A., CARNEIRO, G., ARASAKI, C. H., GELONEZE, B. & ZANELLA, M. T. 2011. Early improvement in glycemic control after bariatric surgery and its relationships with insulin, GLP-1, and glucagon secretion in type 2 diabetic patients. *Obes Surg,* 21**,** 896-901.

VAISSE, C., CLEMENT, K., GUY-GRAND, B. & FROGUEL, P. 1998. A frameshift mutation in human MC4R is associated with a dominant form of obesity. *Nat Genet,* 20**,** 113-4.

VAN CAUTER, E. & KNUTSON, K. L. 2008. Sleep and the epidemic of obesity in children and adults. *Eur J Endocrinol,* 159 Suppl 1**,** S59-66.

VAN PASSEL, M. W., KANT, R., ZOETENDAL, E. G., PLUGGE, C. M., DERRIEN, M., MALFATTI, S. A., CHAIN, P. S., WOYKE, T., PALVA, A., DE VOS, W. M. & SMIDT, H. 2011. The genome of Akkermansia muciniphila, a dedicated intestinal mucin degrader, and its use in exploring intestinal metagenomes. *PLoS One,* 6**,** e16876.

VENTER, C. S., VORSTER, H. H. & CUMMINGS, J. H. 1990. Effects of dietary propionate on carbohydrate and lipid metabolism in healthy volunteers. *Am J Gastroenterol,* 85**,** 549-53.

VERBYLA, D. L. & LITVAITIS, J. A. 1989. Resampling Methods for Evaluating Classification Accuracy of Wildlife Habitat Models. *Environmental Management,* 13**,** 783-787.

VERTES, V., GENUTH, S. M. & HAZELTON, I. M. 1977. Supplemented fasting as a large-scale outpatient program. *JAMA,* 238**,** 2151-3.

VIEIRA, A. A., MICHELS, M., FLORENTINO, D., NASCIMENTO, D. Z., REZIN, G. T., LEFFA, D. D., FORTUNATO, J. J., DAL-PIZZOL, F., BARICHELLO, T., QUEVEDO, J. & PETRONILHO, F. 2015. Obesity promotes oxidative stress and exacerbates sepsis-induced brain damage. *Curr Neurovasc Res,* 12**,** 147-54.

WANG, H., MAITRA, A. & WANG, H. 2015. Obesity, Intrapancreatic Fatty Infiltration, and Pancreatic Cancer. *Clin Cancer Res,* 21**,** 3369-71.

WANG, Q., GARRITY, G. M., TIEDJE, J. M. & COLE, J. R. 2007. Naive Bayesian classifier for rapid assignment of rRNA sequences into the new bacterial taxonomy. *Appl Environ Microbiol,* 73**,** 5261-7.

WEINSIER, R. L. & ULLMANN, D. O. 1993. Gallstone formation and weight loss. *Obes Res,* 1**,** 51-6.

WHITLEY, E. & BALL, J. 2002. Statistics review 6: Nonparametric methods. *Crit Care,* 6**,** 509-13.

WILCOXON, F. 1946. Individual comparisons of grouped data by ranking methods. *J Econ Entomol,* 39**,** 269.

WILMSHURST, P. & CRAWLEY, J. C. 1980. The measurement of gastric transit time in obese subjects using 24Na and the effects of energy content and guar gum on gastric emptying and satiety. *Br J Nutr,* 44**,** 1-6.

WILSON, K. M. & CHO, E. 2016. Obesity and Kidney Cancer. *Recent Results Cancer Res,* 208**,** 81-93.

WILSON, M. 2005. *Microbial inhabitants of humans. Their ecology and role in health and disease.*

WISEN, O. & HELLSTROM, P. M. 1995. Gastrointestinal motility in obesity. *J Intern Med,* 237**,** 411-8.

WOLEVER, T. M., SPADAFORA, P. & ESHUIS, H. 1991. Interaction between colonic acetate and propionate in humans. *Am J Clin Nutr,* 53**,** 681-7.

WONG, J. M., DE SOUZA, R., KENDALL, C. W., EMAM, A. & JENKINS, D. J. 2006. Colonic health: fermentation and short chain fatty acids. *J Clin Gastroenterol,* 40**,** 235-43.

WU, L., LIU, X., SCHADT, C. W. & ZHOU, J. 2006. Microarray-based analysis of subnanogram quantities of microbial community DNAs by using whole-community genome amplification. *Appl Environ Microbiol,* 72**,** 4931-41.

WU, L., THOMPSON, D. K., LI, G., HURT, R. A., TIEDJE, J. M. & ZHOU, J. 2001. Development and evaluation of functional gene arrays for detection of selected genes in the environment. *Appl Environ Microbiol,* 67**,** 5780-90.

WU, L. Y., THOMPSON, D. K., LIU, X. D., FIELDS, M. W., BAGWELL, C. E., TIEDJE, J. M. & ZHOU, J. Z. 2004. Development and evaluation of microarray-based whole-genome hybridization for detection of microorganisms within the context of environmental applications. *Environmental Science & Technology,* 38**,** 6775-6782.

XU, G., JI, C., SONG, G., ZHAO, C., SHI, C., SONG, L., CHEN, L., YANG, L., HUANG, F., PANG, L., ZHANG, N., ZHAO, Y. & GUO, X. 2015. MiR-26b modulates insulin sensitivity in adipocytes by interrupting the PTEN/PI3K/AKT pathway. *Int J Obes (Lond),* 39**,** 1523-30.

YE, J., COULOURIS, G., ZARETSKAYA, I., CUTCUTACHE, I., ROZEN, S. & MADDEN, T. L. 2012. Primer-baselineAST: a tool to design target-specific primers for polymerase chain reaction. *BMC Bioinformatics,* 13**,** 134.

YEOM, Y., KIM, B. S., KIM, S. J. & KIM, Y. 2016. Sasa quelpaertensis leaf extract regulates microbial dysbiosis by modulating the composition and diversity of the microbiota in dextran sulfate sodium-induced colitis mice. *BMC Complement Altern Med,* 16**,** 481.

YOUNES, H., DEMIGNE, C. & REMESY, C. 1996. Acidic fermentation in the caecum increases absorption of calcium and magnesium in the large intestine of the rat. *Br J Nutr,* 75**,** 301-14.

ZAR, J. H. 1998. *Biostatistical Analysis. New Jersey: Prentice Hall International, INC.* .

ZHANG, C., ZHANG, M., PANG, X., ZHAO, Y., WANG, L. & ZHAO, L. 2012. Structural resilience of the gut microbiota in adult mice under high-fat dietary perturbations. *ISME J,* 6**,** 1848-57.

ZHANG, H., DIBAISE, J. K., ZUCCOLO, A., KUDRNA, D., BRAIDOTTI, M., YU, Y., PARAMESWARAN, P., CROWELL, M. D., WING, R., RITTMANN, B. E. & KRAJMALNIK-BROWN, R. 2009. Human gut microbiota in obesity and after gastric bypass. *Proc Natl Acad Sci U S A,* 106**,** 2365-70.

ZHANG, X., ZHAO, Y., XU, J., XUE, Z., ZHANG, M., PANG, X., ZHANG, X. & ZHAO, L. 2015. Modulation of gut microbiota by berberine and metformin during the treatment of high-fat diet-induced obesity in rats. *Sci Rep,* 5**,** 14405.

ZHANG, Z., SCHWARTZ, S., WAGNER, L. & MILLER, W. 2000. A greedy algorithm for aligning DNA sequences. *Journal of Computational Biology,* 7**,** 203-214.

ZHOU, J., KANG, S., SCHADT, C. W. & GARTEN, C. T., JR. 2008a. Spatial scaling of functional gene diversity across various microbial taxa. *Proc Natl Acad Sci U S A,* 105**,** 7768-73.

ZHOU, J., MARTIN, R. J., TULLEY, R. T., RAGGIO, A. M., MCCUTCHEON, K. L., SHEN, L., DANNA, S. C., TRIPATHY, S., HEGSTED, M. & KEENAN, M. J. 2008b. Dietary resistant starch upregulates total GLP-1 and PYY in a sustained day-long manner through fermentation in rodents. *Am J Physiol Endocrinol Metab,* 295**,** E1160-6.

ZHOU, J., WU, L., DENG, Y., ZHI, X., JIANG, Y. H., TU, Q., XIE, J., VAN NOSTRAND, J. D., HE, Z. & YANG, Y. 2011. Reproducibility and quantitation of amplicon sequencing-based detection. *ISME J,* 5**,** 1303-13.

ZHOU, X. C., WU, L. Y. & ZHOU, J. Z. 2004. Fabrication of DNA microarrays on nanoengineered polymeric ultrathin film prepared by self-assembly of polyelectrolyte multilayers. *Langmuir,* 20**,** 8877-8885.

.

VITA

Rui Zhang was born in Jingjiang City, Jiangsu Province of the People's Republic of China. She studied pharmacy at North China Coal Medical University in Tangshan, China, during September of 1999 and July of 2003, and graduated with a Bachelor of Science degree. After graduation, she worked in Yangzhou Pharmaceutical Company during 2003 and 2004. She started her graduate study majoring in pharmaceutical sciences in Huazhong University of Science and Technology in Wuhan, China, in September 2005 and graduated with a Master of Science degree in July 2008. In 2010, Rui Zhang started her graduate study majoring in biological sciences at Louisiana State University and graduated with a degree of Master of Science in December 2012. Rui Zhang started her study on human gut microbial ecology in the Department of Environmental Sciences at Louisiana State University in the spring of 2013 and expects to graduate in May 2017.